

ผลของอนุภาคเงินขนาดนาโนเมตรและเฮกซะวาเลนต์โครเมียมต่อหน้าที่อสุจิ
และการพัฒนาตัวอ่อน



วิทยานิพนธ์นี้เป็นส่วนหนึ่งของการศึกษาตามหลักสูตรปริญญาวิทยาศาสตรดุษฎีบัณฑิต
สาขาวิชาเทคโนโลยีชีวภาพ
มหาวิทยาลัยเทคโนโลยีสุรนารี
ปีการศึกษา 2558

**EFFECTS OF SILVER NANOPARTICLES AND
HEXAVALENT CHROMIUM ON SPERM FUNCTIONS
AND EMBRYO DEVELOPMENT**

Ton Yoisungnern



**A Thesis Submitted in Partial Fulfillment of the Requirements for the
Degree of Doctor of Philosophy in Biotechnology
Suranaree University of Technology
Academic Year 2015**

**EFFECTS OF SILVER NANOPARTICLES AND HEXAVALENT
CHROMIUM ON SPERM FUNCTIONS AND EMBRYO
DEVELOPMENT**

Suranaree University of Technology has approved this thesis submitted in partial fulfillment of the requirements for the Degree of Doctor of Philosophy.

Thesis Examining Committee

(Assoc. Prof. Dr. Montarop Yamabhai)

Chairperson

(Assoc. Prof. Dr. Rangsun Parnpai)

Member (Thesis Advisor)

(Prof. Dr. Jin-Hoi Kim)

Member

(Assoc. Prof. Dr. Apichat Boontawan)

Member

(Dr. Chuti Laowtammathron)

Member

(Prof. Dr. Sukit Limpijumnong)

Vice Rector for Academic Affairs
and Innovation

(Asst. Prof. Dr. Suwayd Ningsanond)

Dean of Institute of Agricultural Technology

ต้น ย่อยสูงเนิน : ผลของอนุภาคเงินขนาดนาโนเมตร และเฮกซะวาเลนต์โครเมียมต่อ
หน้าที่ต่าง ๆ ของอสุจิ และการพัฒนาตัวอ่อน (EFFECTS OF SILVER
NANOPARTICLES AND HEXAVALENT CHROMIUM ON SPERMATOZOA
FUNCTIONS AND EMBRYO DEVELOPMENT) อาจารย์ที่ปรึกษา : รองศาสตราจารย์
ดร.รังสรรค์ พาลพ่าย, 155 หน้า.

อนุภาคนาโน (NPs) และโลหะหนักที่ใช้เป็นอุปกรณ์ทางการแพทย์ หรืออุตสาหกรรมอื่น
อาจเป็นสาเหตุที่ก่อให้เกิดอันตรายในสุขภาพของมนุษย์ โดยเฉพาะอย่างยิ่ง ผลกระทบต่อระบบ
สืบพันธุ์ ที่สำคัญการทดลองในห้องปฏิบัติการที่บ่งชี้ถึงผลกระทบของอนุภาคเงิน (AgNPs) และ
เฮกซะวาเลนต์โครเมียม [Cr (VI)] ต่อหน้าที่ต่างๆของอสุจิ และการเจริญเติบโตของตัวอ่อนยังขาด
ข้อมูลที่ชัดเจน ดังนั้นการศึกษานี้จึงได้ทดสอบ AgNPs และ Cr (VI) ต่อตัวอสุจิของหนูเม้าส์ เพื่อ
ศึกษาผลกระทบที่เป็นพิษของ AgNPs ต่อหน้าที่ต่าง ๆ ของอสุจิ ตลอดจนการพัฒนาตัวอ่อน ซึ่ง
ประกอบด้วยปฏิกิริยาอะโครโซม (acrosome reaction) ความสามารถในการปฏิสนธิของอสุจิ ใน
ระหว่างการทำเด็กหลอดแก้ว (IVF) หรืออิกซี่ (ICSI) การพัฒนาตัวอ่อน การเพิ่มจำนวนเซลล์ของ
ตัวอ่อนระยะบลาสโตซิส และการแสดงออกของยีนที่จำเพาะต่อมวลเซลล์ชั้นใน (ICM) และเซลล์
trophectoderm (TE) ของตัวอ่อนในระยะบลาสโตซิส ผลที่ได้จากการทดลองครั้งนี้พบว่า AgNPs
สามารถเข้าสู่เซลล์อสุจิ ซึ่งส่งผลกระทบต่าง ๆ ต่อตัวอสุจิ อาทิเช่น ความผิดปกติทางสัณฐานวิทยา
ลดการมีชีวิตของอสุจิ เพิ่มความเครียดออกซิเดชัน (oxidative stress) และตัวอ่อนระยะบลาสโตซิส
มีพัฒนาการล่าช้า ซึ่งอาจใช้เป็นแบบจำลองการทดสอบความปลอดภัย และการใช้ของอุปกรณ์ทาง
การแพทย์ที่มีองค์ประกอบของ AgNPs ได้

ในส่วนผลกระทบของ Cr (VI) ต่อหน้าที่ต่างๆของอสุจิ และความสามารถในการปฏิสนธิ
ในห้องปฏิบัติการ ตลอดจนการพัฒนาตัวอ่อน พบว่า Cr (VI) ลดการมีชีวิตของอสุจิ และปฏิกิริยา
อะโครโซมซึ่งสอดคล้องกับความเข้มข้นที่เพิ่มขึ้น นอกจากนี้อสุจิที่ถูกทดสอบด้วย Cr (VI) เป็น
สาเหตุที่ทำให้ลดอัตราความสามารถในการปฏิสนธิ ตัวอ่อนมีพัฒนาการล่าช้า และลดการแสดง
ออกของยีนที่เกี่ยวข้องกับ ตัวอ่อนระยะบลาสโตซิส ซึ่งสามารถใช้เป็นข้อมูลเชิงลึกที่บ่งบอกถึง
ผลกระทบจากการใช้ Cr (VI) ต่อการทำงานของอสุจิในสัตว์เลี้ยงลูกด้วยนม

สาขาวิชาเทคโนโลยีชีวภาพ
ปีการศึกษา 2558

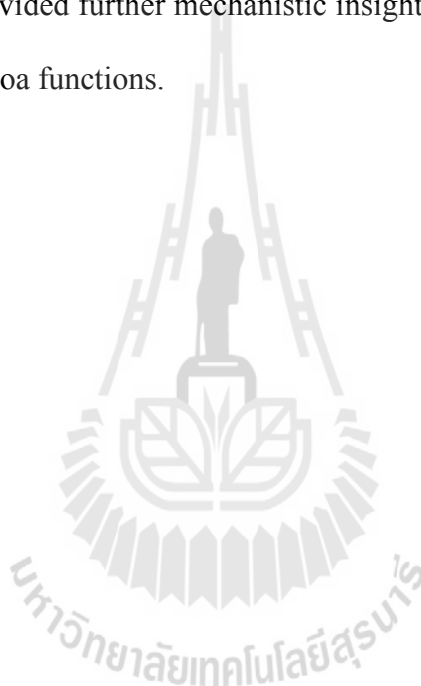
ลายมือชื่อนักศึกษา _____
ลายมือชื่ออาจารย์ที่ปรึกษา _____

TON YOISUNGNERN : EFFECTS OF SILVER NANOPARTICLES AND
HEXAVALENT CHROMIUM ON SPERMATOZOA FUNCTIONS AND
EMBRYO DEVELOPMENT. THESIS ADVISOR : ASSOC. PROF.
RANGSUN PARNPAI, Ph.D., 155 PP.

SILVER NANOPARTICLES/HEXAVALENT CHROMIUM/SPERMATOZOA/
FERTILIZATION/ EMBRYO DEVELOPMENT

Due to the widespread use of nanomaterials and heavy metals in medical and industrial applications which can cause pollution, the question as to whether nanoparticles (NPs) or heavy metals can cause harmful disturbances in human health, especially on the reproductive system, remains a matter of concern. More importantly, *in vitro* studies related to the effects of silver nanoparticles (AgNPs) and hexavalent chromium (Cr (VI)) on spermatozoa functions and embryo development are not yet clearly understood. Thus, we treated AgNPs and Cr (VI) into mouse spermatozoa and then determined the cytotoxic effects of AgNPs on spermatozoa functions including acrosome reaction, fertilization capacity during *in vitro* fertilization (IVF) or intracytoplasmic sperm injection (ICSI), embryonic development, cell proliferation in inner cell mass (ICM)- and trophectoderm cell (TE) of blastocyst stage, and ICM and TE specific genes expression in blastocysts. The results suggested that AgNPs could internalize into sperm cells and resulted in various effects such as spermatozoa morphological abnormalities, reduced viability, induced oxidative stress, and delayed blastocyst formation. Thus, these results may be used as a model for testing the safety and applicability of medical devices using AgNPs.

In the second experiment, the effects of Cr (VI) on spermatozoa functions and spermatozoa fertilizing ability during IVF as well as subsequent development of embryos were investigated. The results showed that Cr (VI)-exposed spermatozoa decreased spermatozoa viability and acrosome reaction with increasing dose. Furthermore, Cr (VI)-treated spermatozoa caused a significant reduction in IVF success, delayed blastocyst formation, and down-regulated blastocyst-related genes. This *in vitro* study provided further mechanistic insights into the effects of Cr (VI) on mammalian spermatozoa functions.



School of Biotechnology

Academic Year 2015

Student's Signature _____

Advisor's Signature _____

ACKNOWLEDGEMENTS

This work was supported by the Royal Golden Jubilee (RGJ) Ph.D. Program of Thailand Research Fund and the part of the work that was done at Department of Animal Biotechnology, College of Animal Bioscience and Biotechnology/Animal Resources Research Center, Konkuk University, Seoul, South Korea.

I would like first to express my deepest gratitude and my sincerest appreciation to my Ph.D. supervisor, Assoc. Prof. Dr. Rangsun Parnpai, for his kind, excellent supervisor and guidance thoughtful the period of the study and provided me a good scholarship that led me to the valuable experiences throughout the entire Ph.D. study. I would have been lost without him.

I would also like to express my deeply-felt thank to my co-advisor, Prof. Dr. Jin-Hoi Kim, for his enthusiasm, inspiration, and great efforts to provide me for the clear and simple explanations on my thesis work during in Korea.

I would also like to thank my committee members, Assoc. Prof. Dr. Montarop Yamabhai, Assoc. Prof. Dr. Apichat Boontawan, and Dr. Chuti Laowtammathron, for their valuable comments and partial corrections of this thesis.

I wish to acknowledge to all the members in Professor Kim's lab for discussions, technical support and recommendations: Dr. Yun-Jung Choi, Dr. Joydeep Das, Dr. Deng-Nam Kwon, Jae Woong Han, Min-Hee Kang, Eunzu Kim, and Dasom Kim at Department of Animal Biotechnology, College of Animal Bioscience and Biotechnology/Animal Resources Research Center.

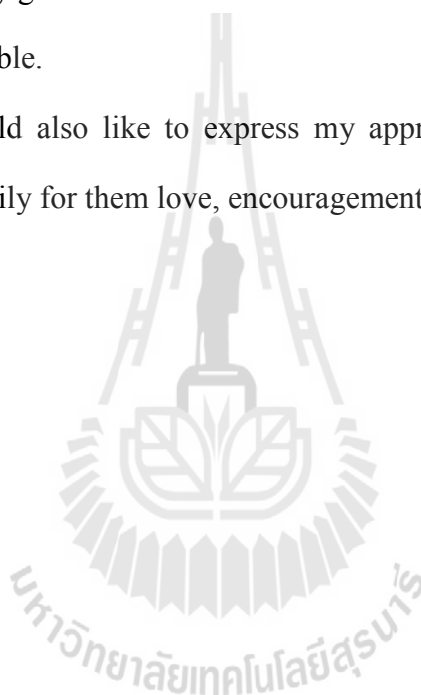
I would like to thank the member of Embryo Technology and Stem Cell Research Center, Suranaree University of Technology, including Kanokwan

Srirattana, Sumeth Imsoonthornruksa, Anawat Sangmalee, Kittiphong Putkhao, Aniruth Aree-Uea, Nucharin Sripunya, Kwanrudee Keawmungkun, Wanwisa Phewsoi, Kanchana Punyawai, and Ashit Kumar Paul for their beneficial advice to improve my skill. Special thanks are extended to every mouse that donates the ovary and sperm for this study. Without them this work would not success.

Most importantly, I would like to thank my family for giving me the opportunity to push my graduate studies and for their love and support. Without them, my life would impossible.

Finally, I would also like to express my appreciation to Miss Natthaphorn Nutamarn and her family for them love, encouragement and support within everything during my study.

Ton Yoisungnern



CONTENTS

| | Page |
|-----------------------------------|-------------|
| ABSTRACT IN THAI..... | I |
| ABSTRACT IN ENGLISH | II |
| ACKNOWLEDGEMENTS..... | IV |
| CONTENTS..... | VI |
| LIST OF TABLES..... | IX |
| LIST OF FIGURES | X |
| LIST OF ABBREVIATIONS..... | XII |
| CHAPTER | |
| I INTRODUCTION..... | 1 |
| 1.1 Background..... | 1 |
| 1.2 Research objectives..... | 4 |
| 1.3 Research hypotheses | 4 |
| 1.4 Scope of this study | 5 |
| 1.5 References | 5 |
| II LITERATURE REVIEWS..... | 12 |
| 2.1 Nanoparticles..... | 12 |
| 2.2 Silver nanoparticles..... | 13 |
| 2.3 Mouse spermatozoa..... | 27 |
| 2.4 Fertilization | 33 |

CONTENTS (Continued)

| | Page |
|--|-------------|
| 2.5 Mouse embryo development..... | 33 |
| 2.6 TE and ICM formation..... | 34 |
| 2.7 Cytotoxic of AgNPs on biology fields..... | 34 |
| 2.8 Chromium | 41 |
| - Hexavalent chromium..... | 41 |
| 2.9 Why use mouse as a model?..... | 50 |
| 2.10 References..... | 50 |
| III INTERNALIZATION OF SILVER NANOPARTICLES IN TO | |
| MOUSE SPERMATOZOA RESULT IN POOR OOCYTE | |
| FERTILIZATION AND COMPROMISED EMBRYO | |
| DEVELOPMENT..... | |
| 3.1 Abstract..... | 74 |
| 3.2 Introduction..... | 75 |
| 3.3 Materials and methods..... | 78 |
| 3.4 Results..... | 88 |
| 3.5 Discussions..... | 111 |
| 3.6 Conclusion..... | 116 |
| 3.7 References..... | 116 |

CONTENTS (Continued)

| | Page |
|---|------|
| IV EFFECT OF HEXAVALENT CHROMIUM-TREATED SPERM ON <i>IN VITRO</i> FERTILIZATION AND EMBRYO DEVELOPMENT | 127 |
| 4.1 Abstract | 127 |
| 4.2 Introduction | 128 |
| 4.3 Materials and methods | 129 |
| 4.4 Results | 135 |
| 4.5 Discussions | 142 |
| 4.6 Conclusion | 144 |
| 4.7 References | 145 |
| V CONCLUSION | 150 |
| APPENDIX | 151 |
| BIOGRAPHY | 155 |

LIST OF TABLES

| Table | Page |
|--|------|
| 2.1 Cytotoxic of AgNPs on biology fields..... | 35 |
| 2.2 Hexavalent chromium cytotoxicity..... | 44 |
| 3.1 Primers sets used for real-time qRT-PCR..... | 87 |
| 3.2 Developmental competence of mouse oocytes fertilized <i>in vitro</i> after culture 96 h after insemination..... | 105 |
| 3.3 Developmental competence of mouse embryos derived from ICSI with dead AgNP-exposed sperm with different morphology after culture for 96 h..... | 109 |
| 4.1 Primers and conditions used for real-time qRT-PCR..... | 134 |
| 4.2 Developmental competence of mouse oocytes 96 h after IVF..... | 139 |
| 4.3 TE and ICM cell counts in blastocysts at 96 h after IVC via oct4 and cdx2 expression analysis..... | 140 |

LIST OF FIGURES

| Figure | Page |
|---|------|
| 2.1 AgNPs derived from TEM picture..... | 14 |
| 2.2 Mechanism of AgNPs cytotoxicity..... | 20 |
| 2.3 Mechanism of oxidative stress on cellular damage | 22 |
| 2.4 Representation of AgNPs induces apoptosis | 24 |
| 2.5 Mechanism of AgNPs cause DNA damage..... | 26 |
| 2.6 Interaction of nanoparticles with proteins: relation to bioreactivity of the nanoparticles..... | 27 |
| 2.7 Spermatozoa (mouse) cross-sections of tail (EM) and diagram..... | 28 |
| 2.8 Working model of the sequence of events involved in preparation of spermatozoa for the capacitation..... | 30 |
| 2.9 Schematic diagram of acrosome reaction in mammals | 31 |
| 2.10 The glycoproteins of the inner acrosomal membrane are labeled specific monoclonal antibody (anti-CD46)..... | 32 |
| 2.11 Role of cellular response, repair and recovery mechanisms..... | 43 |
| 3.1 The characterization of AgNPs | 89 |
| 3.2 SEM and TEM analysis of AgNP-treated sperms | 91 |
| 3.3 Localization of AgNPs in sperm cells by SEM. Sperm cells were co-cultured with or without AgNPs (1, 10 and 50g/mL) for 3 h | 92 |
| 3.4 Localization of AgNPs in sperm cells by TEM..... | 93 |
| 3.5 Mitochondrial damage and ROS analysis in AgNP-treated sperm cells..... | 95 |

LIST OF FIGURES (Continued)

| Figure | Page |
|--|------|
| 3.6 Localization of AgNPs in sperm cells by TEM..... | 96 |
| 3.7 Abnormal sperm morphology analysis after treatment with different concentrations of AgNPs | 98 |
| 3.8 Sperm mortality and acrosome reaction analysis | 99 |
| 3.9 Analysis of dead and live sperm cells in non-capacitation medium after AgNP exposure..... | 101 |
| 3.10 Acrosome pattern analysis according to CD46 immunofluorescent staining in sperm cells cultured in non-capacitation medium after incubation with different dosage of AgNPs | 102 |
| 3.11 Acrosome reaction analysis in sperm cells cultured in non-capacitation medium using flow cytometry | 103 |
| 3.12 Quality analysis of blastocyst stage embryos developed <i>in vitro</i> after IVF with AgNP-treated sperm cells | 106 |
| 3.13 Quality analysis of blastocyst stage embryos developed <i>in vitro</i> after ICSI with AgNP-treated sperm cells with normal or abnormal morphology | 110 |
| 4.1 Sperm viability under Cr(VI) exposure | 136 |
| 4.2 Acrosome reaction analysis by using CD46 immunofluorescence staining and flow cytometry | 137 |
| 4.3 Blastocyst quality analysis..... | 141 |

LIST OF ABBREVIATIONS

| | | |
|---------------|---|--|
| μg | = | Microgram |
| μL | = | Microliter |
| ACTB | = | Actin beta |
| Ag^+ | = | Silver ion |
| AgNPs | = | Silver nanoparticles |
| BSA | = | Bovine serum albumin |
| CDX2 | = | Caudal type homeobox 2 |
| CP | = | Capacitation |
| Cr | = | Chromium |
| Cr (VI) | = | Hexavalent chromium |
| DCFH-DA | = | 2',7'-dichlorodihydrofluorescein diacetate |
| DLS | = | Dynamic light scattering |
| ICM | = | Inner cell mass |
| ICSI | = | Intracytoplasmic sperm injection |
| IVC | = | <i>In vitro</i> culture |
| IVF | = | <i>In vitro</i> fertilization |
| Cytb | = | Cytochrome b |
| DEPC | = | Diethylpyrocarbonate |
| EDS | = | Energy Dispersive Spectroscopy |
| EOMES | = | Eomesodermin |
| FACS | = | Flow cytometric analysis |

LIST OF ABBREVIATIONS (Continued)

| | | |
|---------|---|--|
| GPx | = | Glutathione peroxidase |
| GST | = | Glutathione S-transferase |
| GSH | = | Glutathione |
| hCG | = | Human chorionic gonadotropin |
| h | = | Hour |
| IAM | = | Inner acrosomal membrane |
| KLF4 | = | Kruppel-like factor 4 |
| KRT8 | = | Keratin 8 |
| mL | = | Microliter |
| mtDNA | = | Mitochondrial DNA |
| NAC | = | <i>N</i> -acetyl-L-cysteine |
| NCP | = | Non-capacitation |
| NPs | = | Nanoparticles |
| OAM | = | Outer acrosomal membrane |
| PMSG | = | Pregnant mare's serum gonadotropin |
| POU5F1 | = | POU class 5 homeobox1 |
| ROS | = | Reactive oxygen species |
| RT-qPCR | = | Real-time quantitative polymerase chain reaction |
| SEM | = | Scanning electron microscopy |
| SOD | = | Superoxide dismutase |
| SOX2 | = | Sex determining region Y-box 2 |
| TE | = | Trophectoderm cell |

LIST OF ABBREVIATIONS (Continued)

| | | |
|-----|---|----------------------------------|
| TEM | = | Transmission electron microscopy |
| UV | = | Ultraviolet |
| XRD | = | X-ray diffraction |
| ZP | = | Zona pellucida |



CHAPTER I

INTRODUCTION

1.1 Background

Nowadays, the pollutions of the industrial waste, severe environmental and contaminants are elements that have effected on health and reproductive abnormality in both humans and animals. Most of elements are nanoparticles, metal, heavy metals that cause toxicity in health. A large part of these elements exert their toxic effect by generating reactive oxygen species (ROS), that causing oxidative stress. People are exposed to these elements by contaminated ground and surface water, agricultural land, and aquatic life, even by many other products. By the way, a silver nanoparticle (AgNPs) is one of the most accepted nanomaterials that have been used in material science. For instance, most importantly used as, one of the constituent elements of dental alloys, catheters, and implant surfaces for treating of wounds and burns related infections, as well as in drug delivery in cancer and retinal therapies. As a result, not only the consumers but also the workers manufacturing these products are also exposed to AgNPs which may have destructive effects on them. Several studies have demonstrated that, the effects of sub-chronic oral or inhalation toxicity of AgNPs in experimental animals. They found that silver was accumulated in the blood as well as all tested organs, including the liver, spleen, kidneys, thymus, lungs, heart, brain, and testes (Kim et al., 2010; Park et al., 2010). NPs can induce cytotoxicity by the mechanism of intracellular oxidative stress and apoptosis (Nel et al., 2006; Oberdörster, 2004; Oberdörster et al., 2006; Smith et al., 2007; Usenko et al., 2007;

Xia et al., 2006; Zhu et al., 2006). Like other nanoparticles, AgNPs also show the risk of toxicity by generating ROS (AshaRani et al., 2009; Hussain et al., 2005). Several studies suggest that the toxicity of AgNPs is mainly mediated by the release of silver ions, Ag⁺ (Kvitek et al., 2009; Navarro et al., 2008). AgNPs can enter the cell by diffusion or endocytosis to cause mitochondrial dysfunction, leading to damage of proteins and nucleic acids and finally cause inhibition of cell proliferation (Ahamed et al., 2010; Foldbjerg et al., 2009; Lim et al., 2012; Roy et al., 2014). The influence of NPs on a single gamete may cause remarkable developmental differences as the gamete quality plays a crucial role in ontogenesis (Gandolfi and Brevini, 2010). Impairment of gametes due to NPs exposure may affect reproductive functions or have pathological influence on the later generation (Campagnolo et al., 2012). However, studies concerning the sensitivity of gametes towards NPs exposure are very limited. In spermatozoa, PVA and PVP-coated iron and europium hydroxide NPs do not show any toxicity (Makhluf et al., 2006, 2008). Titanium dioxide, gold, silver and zinc oxide NPs show moderate effects (Guo et al., 2009; Gopalan et al., 2009; Moretti et al., 2013; Wiwanitkit et al., 2009; Zakhidov et al., 2012). On the other hand, europium trioxide shows severe cytotoxicity in spermatozoa (Makhluf et al., 2008). There are only limited studies regarding the effects of AgNPs on fertility as well as sperm function. It has been shown that AgNPs exposure could affect testicular morphology, reduced sperm production, and increased the number of abnormal spermatozoa as well as germ cell DNA damage *in vivo* (Gromadzka-Ostrowska et al., 2012; Kyjovska et al., 2013; Lan and Yang, 2012; Sleiman et al., 2013). In another *in vivo* study in rats, Miresmaeili et al. (2013) showed that AgNPs exposure significantly decreased the number of spermatogenic cells including spermatogonia, spermatocytes, spermatids and spermatozoa as well as affected the acrosome reaction in sperm cells.

Several *in vitro* studies also showed that AgNPs caused cytotoxicity/apoptosis in testicular cells and embryos as well as affected the proliferation rate in spermatogonial stem cells (Asare et al., 2012; Braydich-Stolle et al., 2010; Li et al., 2010; Lucas et al., 2009). In another *in vitro* study, Moretti et al. (2013) showed that AgNPs exerted a significant dose-dependent effect on motility and viability of human spermatozoa.

Secondly, chromium (Cr) is a heavy metal that is mostly found in rocks, volcanic dust and gases, soils, as well as in animals and plants. It is extensively used in pigment and stainless steel production; leather tannery; wood processing; welding; cement manufacturing; chrome plating, textile, ceramic, glass, and photography industries; catalytic converters for automobiles; and cooling plant (Stohs et al., 2001). This kind of industrial waste releases an environmental pollution. Especially, Chromium can exist in a variety of oxidative states ranging from -2 to +6, among which the trivalent (III) and hexavalent (VI) forms have biological importance (Stoecker, 2004). Hexavalent chromium, Cr(VI), can readily cross cellular membranes via nonspecific anion transporters, whereas Cr(III) is poorly transported across membranes. Therefore, Cr (VI) is mainly toxicity. Cr(VI) has been reported to cause allergic dermatitis as well as cytotoxic, genotoxic, immunotoxic, and carcinogenic effects in both humans and laboratory animals (Stohs et al., 2001; Li et al., 2011). Moreover, Cr(VI) exposure has also been reported to induce reproductive toxicity in both humans and laboratory animals (Danadevi et al., 2003; Li et al., 2001; Subramanian et al., 2006). In welding industries and chromate factories, workers exposed to Cr (VI) suffer from increased risk of reduced semen quality and sperm abnormalities that ultimately lead to infertility (Danadevi et al., 2003; Kumar et al., 2005). Additionally, decreased sperm count and increased numbers of abnormal

spermatozoa have been reported in Cr-treated/exposed mice, rats, rabbits, and bonnet monkeys (Acharya et al., 2006; Li et al., 2001; Subramanian et al., 2006; Yousef et al., 2006). Women working in Cr industries or living around Cr-contaminated areas, who have high levels of Cr in blood and urine experience irregular menses and complications during pregnancy and childbirth (Shmitova, 1980; Zhang et al., 1992; Greene et al., 2010). In addition, toxic effects on embryos and fetuses in laboratory animals exposed to Cr(VI) have also been reported (Junaid et al., 1996; Marouani et al., 2011).

1.2 Research objectives

1. To examine the cytotoxic effect of AgNPs on spermatozoa, oocyte-fertilizing capacity of sperm via IVF or ICSI, and subsequent embryonic development.
2. To understand the role of AgNPs on cell proliferation in blastocysts, and explore the effect of AgNPs on inner cell mass (ICM)- and trophoctoderm cell (TE)-specific gene expression in blastocysts.
3. To study the cytotoxic effect of hexavalent chromium on spermatozoa, oocyte-fertilizing capacity of sperm, and subsequent embryonic development.

1.3 Research hypotheses

1. To examine the cytotoxic effect of AgNPs on spermatozoa, oocyte-fertilizing capacity of sperm via IVF or ICSI, and subsequent embryonic development.
2. Cr(VI) is a potential cytotoxic agent that involved in the induction of oxidative stress which may cause cytotoxic effect on sperm functions, embryo development and cell proliferation in blastocysts.

1.4 Scope of the study

1. The toxicity of AgNPs is mainly mediated by the release of silver ions (Ag^+), and their particles can enter easily into the cell may cause cytotoxic effect on sperm functions, embryo development and cell proliferation in blastocysts.

2. Cr(VI) is a potential cytotoxic agent that involved in the induction of oxidative stress which may cause cytotoxic effect on sperm functions, embryo development and cell proliferation in blastocysts.

1.5 References

- Ahamed, M., Posgai, R., Gorey, T. J., Nielsen, M., Hussain, S. M., and Rowe, J. J. (2010). Silver nanoparticles induced heat shock protein 70, oxidative stress and apoptosis in *Drosophila melanogaster*. **Toxicol. Appl. Pharmacol.** 242: 263-269.
- Asare, N., Instanes, C., Sandberg, W. J., Refsnes, M., Schwarze, P., Kruszewski, M., Schwarze, P., Kruszewski, M., and Brunborg, G. (2012). Cytotoxic and genotoxic effects of silver nanoparticles in testicular cells. **Toxicology** 291: 65-72.
- AshaRani, P. V., Mun, G. L. K., Hande, M. P., and Valiyaveetil, S. (2009). Cytotoxicity and Genotoxicity of Silver Nanoparticles in Human Cells. **ACS Nano.** 3: 279-290.
- Braydich-Stolle, L. K., Lucas, B., Schrand, A., Murdock, R. C., Lee, T., Schlager, J. J., Hussain, S. M., and Hofmann, M. C. (2010). Silver nanoparticles disrupt GDNF/Fyn kinase signaling in spermatogonial stem cells. **Toxicol. Sci.** 116: 577-589.

- Campagnolo, L., Massimiani, M., Magrini, A., Camaioni, A., and Pietroiusti, A. (2012). Physico-chemical properties mediating reproductive and developmental toxicity of engineered nanomaterials. **Curr. Med. Chem.** 19: 4488-4494.
- Danadevi, K., Rozati, R., Reddy, P. P., and Grover, P. (2003). Semen quality of Indian welders occupationally exposed to nickel and chromium. **Reprod. Toxicol.** 17: 451-456.
- Foldbjerg, R., Olesen, P., Hougaard, M., Dang, D. A., Hoffmann, H. J., and Autrup, H. (2009). PVP-coated silver nanoparticles and silver ions induce reactive oxygen species, apoptosis and necrosis in THP-1 monocytes. **Toxicol. Lett.** 190: 156-162.
- Gandolfi, F., and Brevini, T. A. (2010). In vitro maturation of farm animal oocytes: a useful tool for investigating the mechanisms leading to full-term development. **Reprod. Fertil. Dev.** 22: 495-507.
- Gopalan, R. C., Osman, I. F., Amani, A., de Matas, M., Anderson, D. (2009). The effect of zinc oxide and titanium dioxide nanoparticles in the comet assay with UVA photoactivation of human sperm and lymphocytes. **Nanotoxicology** 3: 33-39.
- Greene, L. E., Riederer, A. M., Marcus, M., and Lkhasuren, O. (2010). Associations of fertility and pregnancy outcomes with leather tannery work in Mongolia: a pilot study. **Int. J. Occup. Environ. Health.** 16: 60-68.
- Gromadzka-Ostrowska, J., Dziendzikowska, K., Lankoff, A., Dobrzyoska, M., Instanes, C., Brunborg, G., Gajowik, A., Radzikowska, J., Wojewódzka, M., and Kruszewski, M. (2012). Silver Nanoparticles effects on epididymal sperm in rats. **Toxicol. Lett.** 214: 251-258.

- Guo, L. L., Liu, X. H., Qin, D. X., Gao, L., Zhang, H. M., Liu, J. Y., and Cui, Y. G. (2009). Effects of nanosized titanium dioxide on the reproductive system of male mice. **Zhonghua. Nan. Ke. Xue.** 15: 517-522.
- Hussain, S. M., Hess, K. L., Gearhart, J. M., Geiss, K. T., and Schlager, J. J. (2005). In vitro toxicity of nanoparticles in BRL 3A rat liver cells. *Toxicol. in Vitro* 19: 975-983.
- Junaid, M., Murthy, R. C., and Saxena, D. K. (1996). Embryo-toxicity of orally administered chromium in mice: exposure during the period of organogenesis. **Toxicol. Lett.** 84: 143-148.
- Kim, Y. S., Song, M. Y., Park, J. D., Song, K. S., Ryu, H. R., Chung, Y. H., Chang, H. K., Lee, J. H., Oh, K. H., Kelman, B. J., Hwang, I. K., and Yu, I. J. (2010). Subchronic oral toxicity of silver nanoparticles. **Part. Fibre. Toxicol.** 7:20.
- Kvitek, L., Vanickova, M., Panacek, A., Soukupova, J., Dittrich M, Valentova E, Pucek, R., Bancirova, M., Milde, D., and Zboril, R. (2009). Initial Study on the Toxicity of Silver Nanoparticles (NPs) against *Paramecium caudatum*. **J. Phys. Chem. C.** 113: 4296-4300.
- Kyjovska, Z. O., Boisen, A. M., Jackson, P., Wallin, H., Vogel, U., and Hougaard, K. S. (2013). Daily sperm production: application in studies of prenatal exposure to nanoparticles in mice. **Reprod. Toxicol. (Elmsford, NY)** 36: 88-97.
- Lan, Z., and Yang, W. X. (2012). Nanoparticles and spermatogenesis: how do nanoparticles affect spermatogenesis and penetrate the blood–testis barrier. **Nanomedicine** 7:579-96.
- Lim, D., Roh, J. Y., Eom, H. J., Choi, J. Y., Hyun, J., and Choi, J. (2012). Oxidative stress-related PMK- 1 P38 MAPK activation as a mechanism for toxicity of

- silver nanoparticles to reproduction in the nematode *Caenorhabditiselegans*. **Environ. Toxicol. Chem.** 31:585-592.
- Li, H., Chen, Q., Li, S., Yao, W., Li, L., Shi, X., Wang, L., Castranova, V., Vallyathen, V., Ernst, E., and Chen, C. (2001). Effect of Cr(VI) exposure on sperm quality: human and animal studies. **Ann. Occup. Hyg.** 45: 505-511.
- Li, P. W., Kuo, T. H., Chang, J. H., Yeh, J. M., and Chan, W. H. (2010). Induction of cytotoxicity and apoptosis in mouse blastocysts by silver nanoparticles. **Toxicol. Lett.** 197: 82-87.
- Li, Z. H., Li, P., and Randak, T. (2011). Evaluating the toxicity of environmental concentrations of waterborne chromium (VI) to a model teleost, *oncorhynchus mykiss*: a comparative study of in vivo and in vitro. **Comp. Biochem. Physiol. C.** 153: 402-407.
- Lucas, B., Fields, C., and Hofmann, M. C. (2009). Signaling pathways in spermatogonial stem cells and their disruption by toxicants. **Birth. Defects. Res. C.** 87: 35-42.
- Makhluf, S. B. D., Qasem, R., Rubinstein, S., Gedanken, A., and Breitbart, H. (2006). Loading magnetic nanoparticles into sperm cells does not affect their functionality. **Langmuir.** 22:9480-9482.
- Makhluf, S. B. D., Arnon, R., Patra, C. R., Mukhopadhyay, D., Gedanken, A., Mukherjee, P., and Breitbart, H. (2008). Labeling of Sperm Cells via the Spontaneous Penetration of Eu^{3+} Ions as Nanoparticles Complexed with PVA or PVP. **Phys. Chem. C.** 112: 12801-12807.
- Marouani, N., Tebourbi, O., Mokni, M., Yacoubi, M. T., Sakly, M., Benkhalifa, M., and Ben Rhouma, K. (2011). Embryotoxicity and fetotoxicity following

intraperitoneal administrations of hexavalent chromium to pregnant rats. **Zygote** 19: 229-235.

- Miresmaeili, S. M., Halvaei, I., Fesahat, F., Fallah, A., Nikonahad, A., and Taherinejad, M. (2013). Evaluating the role of silver nanoparticles on acrosomal reaction and spermatogenic cells in rat. **Iran. J. Reprod.** 11(5): 423-430.
- Moretti, E., Terzuoli, G., Renieri, T., Iacoponi, F., Castellini, C., Giordano, C., Collodel, G. (2013). In vitro effect of gold and silver nanoparticles on human spermatozoa. **Andrologia** 45(6): 392-6.
- Navarro, E., Piccapietra, F., Wagner, B., Marconi, F., Kaegi, R., Odzak, N., Sigg, L., and Behra, R. (2008). Toxicity of Silver Nanoparticles to *Chlamydomonas reinhardtii*. **Environ. Sci. Technol.** 42: 8959-8964.
- Nel, A., Xia, T., Madler, L., and Li, N. (2006). Toxic potential of materials at the nanolevel. **Science** 311: 622-627.
- Oberdörster, E. (2004). Manufactured nanomaterials (Fullerenes, C60) induce oxidative stress in the brain of juvenile largemouth bass. **Environ. Health Perspect** 112: 1058-1062.
- Oberdörster, E., Zhu, S., Blickley, T. M., McClellan-Green, P., and Haasch, M. L. (2006). Ecotoxicology of carbon-based engineered nanoparticles: effects of fullerene (C60) on aquatic organisms. **Carbon** 44: 1112-1120.
- Park, E. J., Bae, E., Yi, J., Kim, Y., Choi, K., Lee, S. H., Yoon, J., Lee, B. C., and Park, K. (2010). Repeated-dose toxicity and inflammatory responses in mice by oral administration of silver nanoparticles. **Environ. Toxicol. Pharmacol.** 30: 162-8.

- Roy, R., Kumar, S., Tripathi, A., Das, M., and Dwivedi, P. D. (2014). Interactive threats of nanoparticles to the biological system. **Immunol. Lett.** 158: 79-87.
- Shmitova, L. (1980). Content of hexavalent chromium in the biological substrates of pregnant women and women in the immediate postnatal period engaged in the manufacture of chromium compounds. **Gig. Trud. Prof. Zabol.** 2: 32-35.
- Sleiman, H., Romano, R. M., Oliveira, C. A., and Romano, M. A. (2013). Effects of prepubertal exposure to silver nanoparticles on reproductive parameters in adult male Wistar rats. **J. Toxicol. Environ. Health. A.** 76: 1023-1032.
- Smith, C. J., Shaw, B. J., and Handy, R. D. (2007). Toxicity of single walled carbon nanotubes to rainbow trout, (*Oncorhynchus mykiss*): respiratory toxicity, organ pathologies, and other physiological effects. **Aquat. Toxicol.** 82: 94-109.
- Stoecker, J. B. (2004). Chromium in elements and their compounds in the environment 2nd edition, pp 709-729. Eds Merian E, Anke M, Ihnat M, Stoepler M. Copyright, Weinheim, Germany.
- Stohs, J. S., Bagchi, D., Hassoun, E., and Bagchi, M. (2001). Oxidative mechanism in the toxicity of chromium and cadmium ions. **J. Environ. Pathol. Toxicol. Oncol.** 20: 77-88.
- Subramanian, S., Rajendiran, G., and Sekhar, P. (2006). Reproductive toxicity of chromium in adult bonnet monkeys (*Macaca radiata* Geoffrey). **Toxicol. Appl. Pharmacol.** 215: 237-249.
- Usenko, C. Y., Harper, S. L., and Tanguay, R. L. (2007). In vivo evaluation of carbon fullerene toxicity using embryonic zebrafish. **Carbon** 45:1891-1898.
- Wiwanitkit, V., Sereemasun, A., and Rojanathanes, R. (2009). Effect of gold nanoparticles on spermatozoa: the first world report. **Fertil. Steril.** 91:e7-8.

- Xia, T., Kovochich, M., Brant, J., Hotze, M., Sempf, J., Oberley, T., Sioutas, C., Yeh, J. I., Wiesner, M. R., and Nel, A. E. (2006). Comparison of the abilities of ambient and manufactured nanoparticles to induce cellular toxicity according to an oxidative stress paradigm. **Nano. Lett.** 6:1794-1807.
- Yousef, M. I., El-Demerdash, F. M., Kamil, K. I., and Elaswad, F. A. M. (2006) Ameliorating effect of folic acid on chromium (VI)-induced changes in reproductive performance and seminal plasma biochemistry in male rabbits. **Reprod. Toxicol.** 21: 322-328.
- Zakhidov, S. T., Pavliuchenkova, S. M., Marshak, T. L., Rudoi, V. M., Dement'eva, O. V., Zelenina, I. A., Skuridin, S. G., Makarov, A. A., Khokhlov, A. N., Evdokimov Iu, M. (2012). Effect of gold nanoparticles on mouse spermatogenesis. **Izv. Akad. Nauk. Ser. Biol.** 3: 279-287.
- Zhu, S., Oberd'rster, E., and Haasch, M. L. (2006). Toxicity of an engineered nanoparticle (fullerene, C60) in two aquatic species, daphnia and fathead minnow. **Mar. Environ. Res.** 62: S5-S9.
- Zhang, J., Cai, W. W., and Lee, D. J. (1992). Occupational hazards and pregnancy outcomes. **Am. J. Ind. Med.** 21: 397-408.

CHAPTER II

LITERATURE REVIEWS

2.1 Nanoparticles

Nanoparticles (NPs) are materials with at least one dimension that is less than 100 nm (Klaine et al., 2008). In general, NPs are presented in the environment in forms as volcanic ash, as known free NPs. In field of manufacturing, NPs can be divided into different material classes, including metals, metal oxides, non-metals, polymer-based, carbon-based as well as those classified as semi-conductor materials (Klaine et al., 2008). Actually, NPs can be located on the surface of a material or contained within a material (Handy and Shaw, 2007), depending on composition of different materials and apart from their size.

In small size, NPs could be hazardous to biological systems by entering to body of organism more than slightly larger particles. Their size can also lead to act differently harmful on your body depend on materials. NPs have an extremely high surface area to volume ratio because of their small size (Buzea et al., 2007). Some researchers have indicated that decreasing size increases toxic responses such as lung inflammation (Brown et al., 2001); because of smaller NPs can easily pass through into plasma membrane.

In properties of NPs, agglomeration and aggregation may cause NPs to behave more like their bulk form (Buzea et al., 2007), depending on affinity of NPs which can lead to a state of loose association as agglomeration, or a stronger association of individual particles as aggregation. It is known that agglomeration does increase the

complexity of assessing the possible effects of NPs on biological systems. Some studies have shown that agglomerated NPs still have significant effects on exposed cells and organisms. For example, smaller diameter of TiO₂ NPs showed enhanced cytotoxicity in mouse keratinocytes compared to larger NPs when both size types agglomerated into clumps of similar diameters (Braydich-Stolle et al., 2009). However, it is not clear that agglomeration state always influences the toxicity of a particular NP, so it is reasonable that this may depend on the type of NP being examined.

In case of NP type, surface area and agglomeration state are important for toxicity test. Thus, there are some proposed general mechanisms to explain the toxicity seen after treatment of cells and organisms with NPs (Lacerda et al., 2006). Actually, NPs can enter to cell or organ system by passive diffusion (Buzea et al., 2007) or by directed uptake via endocytosis (Panyam and Labhasetwar, 2003; Kostarelos et al., 2007; Skebo et al., 2007; Jiang et al., 2008). After internalization, NPs can initiate an immune-type response with inflammation via the production of reactive oxygen species (ROS), which can react with various cellular macromolecules as well as can interfere with cellular signaling. NPs can also disturb mitochondrial functioning, affecting the ability of the cell to respire, which can contribute to cell death (Buzea et al., 2007). While ROS can oxidize DNA causing damage, some NPs have been shown to bind directly to the DNA (Yang et al., 2009).

2.2 Silver nanoparticles (AgNPs)

Silver nanoparticles are the names that used for particles of silver with size 1-100 nm in at least one of the dimensions as definition of other nanoparticles (Figure 2.1). Of note, AgNPs can form different inorganic and organic complexes, its

most stable oxidation states are +0 and +1 exist as well. Silver nitrate (AgNO_3) is often used as a precursor in the synthesis of the different forms of particle.

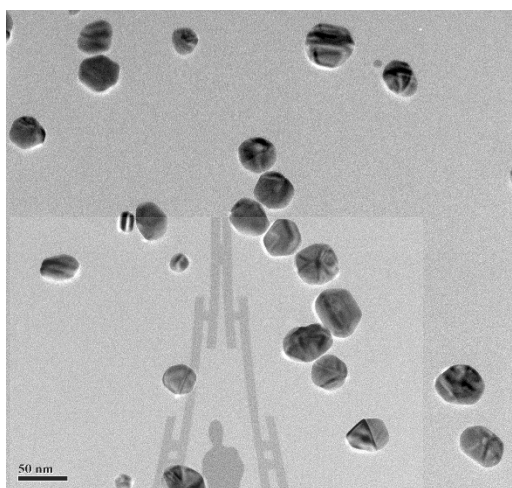


Figure 2.1 AgNPs derived from TEM picture.

2.2.1 History and applications

Silver is not a new discovery because of silver has been known for over 100 years. Previously, silver nanoparticles were referred to suspensions of silver as colloidal silver. Before the invention of penicillin in 1928, colloidal silver had been used to treat many infections and illnesses as well as antibacterial. In 1951, Turkevich et al. (1951) have first reported that AgNO_3 is reducing agent for a wet chemistry technique to synthesize AgNPs (Turkevich et al., 1951). However, the antibacterial derived from silver was not scientifically described until the late 19th century (Russell and Hugo 1994). Later, the use of AgNPs for treating medical conditions have found, particularly in the form of colloidal silver ingestion for treatment of cold symptoms, or as a topical cream for wounds. (Fung and Bowen, 1996). Medicinally used nanoparticles have some medicinal compounds containing silver in composition, such

as the silver sulfadiazine topical ointment and Ag-containing burn dressings (Fung and Bowen, 1996). With technology in present has growth as fast, AgNPs has resurgence with the development and production of AgNPs.

Nowaday, AgNPS were importantly used as products in industrial such as dental restoration material (Ohashi et al., 2004), water treatment facilities (Chou et al., 2005), medical devices and bandages (Asz et al., 2006), antibacterial properties (Le Pape et al., 2004; Panacek et al., 2006; Damm et al., 2008), probe for *in vitro* and *in vivo* imaging (Lee et al., 2007), clothing (Benn and Westerhoff, 2008), jewelry, silverware and the photographic industries (Wijnhoven et al., 2009), food packaging (Yang et al., 2009).

2.2.2 Behavior factors of AgNPs

The behavior of AgNPs undergoes a variety of transformations in environmental and biological media. The environmental fate, state of agglomeration or aggregation, and dissolution in environmental and biological media are dependent on size, types of surface coating are used, and surface oxidation as well as release of Ag^+ .

2.2.2.1 Size

Researchers have found the impact of AgNPs to be size-dependent (Johnston et al., 2010; Powers et al., 2011; Yen et al., 2009; Trickler et al., 2010). In case of small size, most toxic of AgNPs were found (Choi et al., 2008). Small nanoparticles is away explained that it easy uptake (Johnston et al., 2010), cells exposed with small size of AgNPs were showed higher levels of silver inside the cell than to larger AgNPs, indicating a size-dependent cellular uptake of the NPs

(Liu et al. 2010b). Moreover, some studies found smaller AgNPs have more cytotoxic than their larger counterparts after comparing AgNPs with different sizes (Braydich-Stolle et al., 2010; Carlson et al., 2008; Haase et al., 2011; Liu et al., 2010b). However, the toxicity of AgNPs may be involved the specific surface area of smaller particles leading to high reactivity or can enhance release of toxic silver ions from the particle surface. Of note, the studies mentioned above do not demonstrate a clear association between nanoscale phenomena such as quantum effects or surface plasmon resonances and toxicity. In contrast, a research was recently pointed out that observations on size-dependent toxicity of NPs often are scalable effects meaning that small particles show greater to behave in a certain way compared to large particles, but their behavior is predictable from that of larger particles (Maynard et al., 2011).

2.2.2.2 Surface coating

AgNPs are often coated for the purpose of promoting stability and dispensability (Tolaymat et al., 2010). A study reported that the polysaccharide-coated AgNPs caused the highest levels of toxicity (Ahamed et al., 2008). However, agglomeration for the uncoated AgNPs has found the differential toxicity and differences in bioavailability such as uptake and dissolution in the specific study. AgNPs with a hydrocarbon surface layer were more toxic than polysaccharide-coated AgNPs suggesting that other factors such as cell type and media may influence the toxicity. Recently, Suresh et al. (2012) had study on four types of AgNPs via uniform size and shape distribution but with different surface coatings (Suresh et al., 2012). The result of Poly (diallyldimethylammonium)-coated AgNPs were found to be the most toxic, whereas uncoated AgNPs were found to be the least toxic in both mouse macrophage and lung epithelial cells (Suresh et al., 2012). This result was consistent

to a study on gold NPs which concluded that positively (+) charged particles have greater efficiency in cell membrane penetration and cellular internalization (Cho et al., 2009). In contrast, Yang et al. (2012) had compared AgNPs with similar sizes but different coatings (citrate, PVP and gum Arabic) and found differential toxicity towards *C. elegans*. Gum Arabic-coated NPs were 9-fold more toxic than PVP-coated NPs, which in turn was 3-fold more toxic than citrate-coated NPs (Yang et al., 2012). These investigators concluded that toxicity was mainly due to NP dissolution which depended on the surface coating (Yang et al., 2012). In conclusion, the effect of AgNPs on the bioavailability or interaction of AgNPs with cellular systems depends on the surface charge and surface coatings. Moreover, the complexity of NP surface chemistry is further study in case of covered proteins when they come in contact with a biological medium (Monopoli et al., 2012). The formation of a protein at the surface of NPs usually referred to a new biological identity, which determines the subsequent cellular/tissue responses (Monopoli et al., 2012). A report has been found that AgNPs with different shapes the composition and thickness of the protein cluster can make significantly depending on the NP shape and the NP/protein ratio (Ashkarran et al., 2012). However, the dynamics of the AgNPs corona with response on protein concentrations, incubation time, NP size and NP surface coating are still unclear.

2.2.2.3 Silver ions (Ag^+) of AgNPs

In field of nanoparticles have believed that silver ions can strongly contribute to the biological activity of AgNPs depending influences of size, coating, concentration, temperature, pH, ionic strength, and time on the dissolution (Kittler et al., 2010; Liu and Hurt, 2010; Liu et al., 2010a; Liu et al., 2012). The ion release kinetics of AgNPs is major for toxicity by the release of silver ions (Ag^+) that

involved dissolved as well as toxicity may be highly informative for risk assessment. In the other hand, AgNPs have other toxicities from their nanoparticles form including composed of elemental silver (Ag^0), which is not soluble or reactive in pure water (Wiberg et al., 2001), but is soluble in acidic solutions (i.e., nitric acid). Of note, AgNPs can soluble in aqueous solutions under oxidizing conditions. Moreover the properties of AgNPs in aqueous solutions that involve two related processes: (i); oxidation with release of reactive oxygen species and (ii); photon-mediated release of dissolved silver (Liu et al., 2010a). Of course, ion release are involved the oxidation pathways, relating surface area (size), ligand binding, polymeric coatings, scavenging of peroxy-intermediates, and pre-oxidation treatments (Liu et al., 2010a). The oxidation of AgNPs can react with highly reactive ionic silver both adsorbed to the surface of NP and released to the surrounding element. Colloidal suspensions of AgNPs will contain at least three forms of silver including particles, dissolved silver (both ionic silver and soluble silver complexes), and ionic silver adsorbed to the surface of NPs (Liu and Hurt, 2010). In general, the dissolution rate is higher for lower concentrations of AgNPs. At higher concentrations, key factors that influence dissolution, like available oxygen and presence of protons (i.e., pH), may be depleted, and high concentrations of dissolved silver and ligands, which can inhibit surface reactions, might further inhibit dissolution (Liu and Hurt, 2010). Oxidative complex chemical reaction is influenced by pH, coatings, temperature and ligands in the surrounding fluid (Liu et al., 2012). The rates of dissolution were shown to be higher for PVP-stabilized AgNPs than for citrate-stabilized AgNPs and an increase in temperature led to increased dissolution (Kittler et al., 2010). The dissolution of AgNPs in soluble solution have dependent on significant amounts of sodium chloride, thus dissolution may have occurred followed by precipitation of silver-chloride

complexes. Rogers et al. (2012) examined that the synthetic stomach fluid (SSF, pH 1.5) mixed with citrate-stabilized AgNPs (1-10 nm and 40 nm) can agglomerate, release silver ions, and partially react to form silver-chloride complexes (Rogers et al., 2012). Thus, the chemical transformations of AgNPs and the toxicological role of AgNPs dissolution appear equivocal in biological environments have investigated by demonstrating that AgNPs cytotoxicity was not involved Ag^+ concentration and resulted primarily from oxidative stress (Eom and Choi, 2010; Kim et al., 2009a). Limbach et al. (2007) have observed that NPs could be carriers for heavy metal uptake into human lung epithelial cells, increasing the toxicity of the NP. However, several studies suggest that the toxicity of AgNPs is largely explained by Ag ions (Beer et al., 2012; Bouwmeester et al., 2011; Navarro et al., 2008; Yang et al., 2012). Furthermore, several studies also been suggested that AgNPs may combined mechanism of Trojan horse by passing typical barriers and then releasing silver ions that damage the cell machinery (Park et al., 2010). A recent study used AgNPs with various sizes and coatings to examine the mechanism of toxicity in *C. elegans*, and then they found a linear correlation between AgNP toxicity and NP dissolution (Yang et al., 2012). The cytotoxicity of AgNPs may largely be explained by silver ions (Beer et al., 2012), gene expression data indicating that AgNPs may affect cells in a more complex way than silver ions alone (Foldbjerg et al., 2012). In conclusion, it is still uncertain by which mechanisms and to what degree silver ions play a role in AgNP-mediated toxicity.

2.2.3 Mechanism of AgNPs cytotoxicity

The mechanism of AgNPs toxicity is involved surface oxidation, release of silver ions, and interaction with biological macromolecules by transformation in

biological and environmental media. Actually, when AgNPs enter to the cell through diffusion or endocytosis to cause mitochondrial dysfunction, generation of reactive oxygen species (ROS), leading to oxidative stress, cell death and genotoxicity as shown in Figure 2.2.

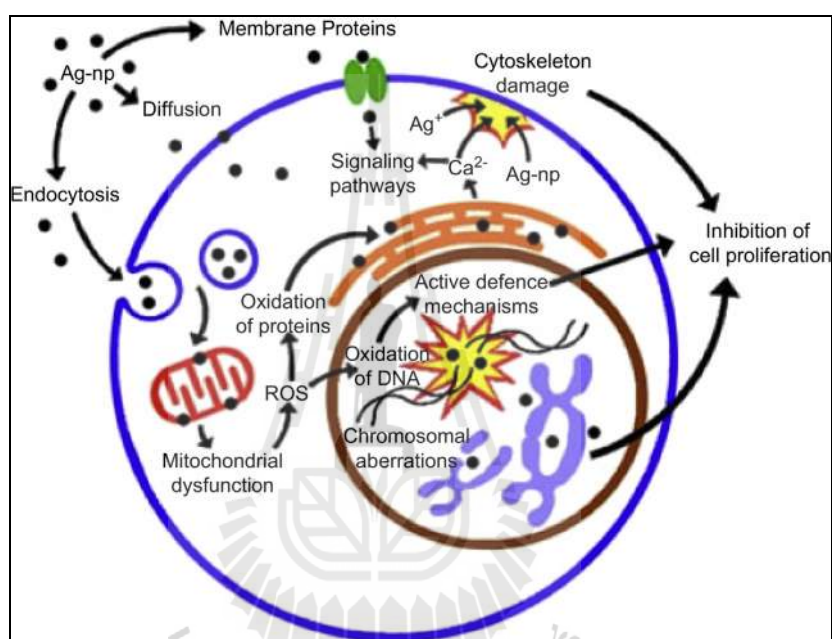


Figure 2.2 Mechanism of AgNPs cytotoxicity (AshaRani et al., 2009).

2.2.3.1 Oxidative stress

The generation of ROS in an organism is a mechanism that involves the main determinant for oxidative stress by unbalancing between the systemic manifestation of reactive oxygen species and a biological system's ability. Thus, the normal redox state of cells is disturbed through the generation of peroxides and free radicals which can damage all components of the cell, including proteins, lipids, mitochondria, and etc. ROS has important roles in cell signaling that involve redox signaling. Thus, to maintain the balance of ROS

production and consumption are most important. To achieve the balance of ROS in cell, antioxidants are molecule that inhibits oxidation by removing free radical intermediates (Figure 2.3). The important enzymes that involve antioxidant such as superoxide dismutase (SOD), catalase, glutathione peroxidase (GPx), glutathione S-transferase (GST) and the peroxiredoxins, as well as non-enzymatic factors such as glutathione (GSH) and vitamins (Franco et al., 2009). In case of AgNPs, the effect of AgNP exposure on cellular responses related to ROS by responding the oxidative related genes, decreasing antioxidant related genes are concerned. As shown in a study who reported that the oxidative dissolution of AgNPs is directly mediated a mechanism of AgNP by increasing reactive oxygen intermediates (Liu and Hurt, 2010). Moreover, ROS production in cell exposed AgNP was inhibited by cyanide, an inhibitor of the mitochondrial electron-transferring activity of cytochrome c oxidase leads to inhibition of ROS production (Hsin et al., 2008). Clearly, mitochondria are an organelle that related to AgNP-mediated ROS production. In another study, the antioxidant capacity of human serum was lowered by ex vivo AgNP treatment, indicating that the AgNPs induced depletion of antioxidants (Rogers et al., 2008). As previous describe, GSH is a major endogenous antioxidant that protects cells against oxidative stress through its ability to reduce ROS (Figure 2.3). Result of a report also suggested that AgNPs exposed could response levels of GSH which could be cellular responses by coping with AgNP-mediated oxidative damage (Kang et al., 2012). Silver ions strongly bind to GSH and other molecules with thiol groups that may play a role the depletion of GSH (Liu et al., 2012). Moreover, other examples have found that oxidative stress was increased in cellular response after AgNP exposure related to abnormal of oxidative stress-related gene expression (Bouwmeester et al., 2011;

Foldbjerg et al., 2012), lipid peroxidation (Arora et al., 2008; Piao et al., 2011). Furthermore, some report also suggested that oxidative stress may involve depletion of antioxidants, oxidative dissolution of AgNPs or following perturbation of mitochondria (Bouwmeester et al., 2011). Consistently, a recent study has suggested that the determining factor of AgNP toxicity was nanoparticle dissolution and also acted via oxidative stress (Yang et al., 2012).

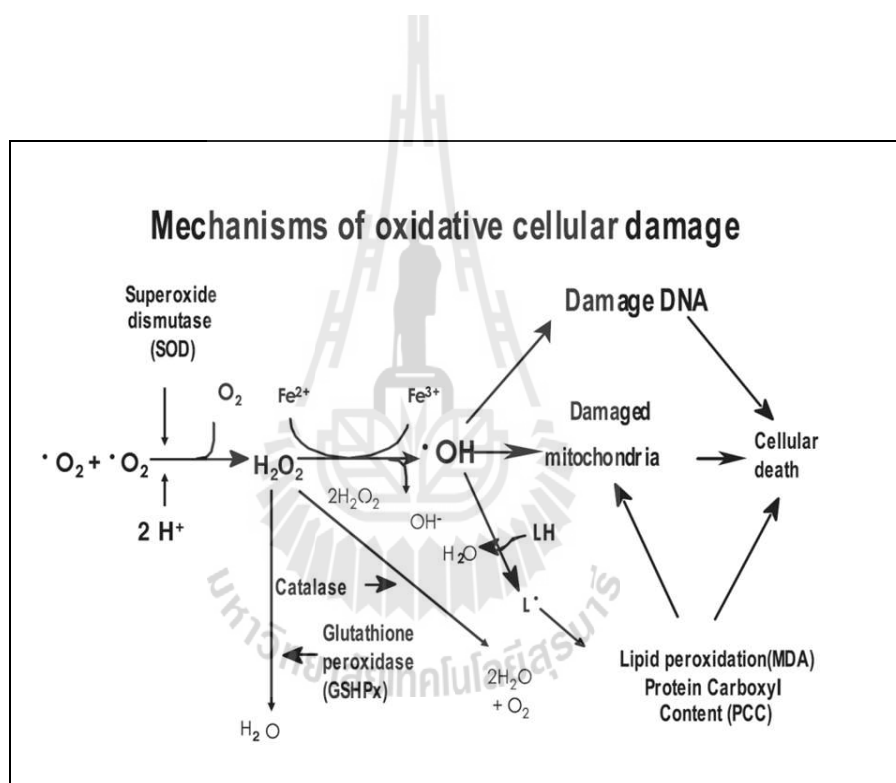


Figure 2.3 Mechanism of oxidative stress on cellular damage (Kang et al., 2012).

2.2.3.2 Cell death

Actually, cell death is often explained the necrosis or apoptosis by considering the programming and physiological mechanism. In term of program cell death is regulated by specific genes and involves the activation of specific molecular pathways which is related to receptor-mediated pathway or the intrinsic,

mitochondria-mediated pathway. Nodaway, a report has found that different nanomaterials may effect to activate several pathways of programmed cell death (Andon and Fadeel, 2012). Importantly, AgNPs had effect on the predominant mechanism of programmed cell death that involved being mitochondria-dependent apoptosis as well as intrinsic pathway (Andon and Fadeel, 2012). The apoptosis pathway is affected in numerous types of cellular stress including DNA damage, oxidative stress, cytosolic calcium overload, endoplasmic reticulum (ER) (Zhang et al., 2012). The mechanism of AgNPs expose on the intrinsic pathway as shown in Figure 2.4. It is characterized by insertion of Bax and/or Bak into the mitochondrial outer membrane. This is followed by the release of several proteins from the mitochondrial inter membrane space, including cytochrome c, which forms a cytosolic apoptosome complex with Apaf-1 (apoptosis activating factor-1) and procaspase-9 in the presence of dATP. This results in the activation of procaspase-9, which triggers the caspase cascade by activation of procaspase-3 leading to apoptotic cell death and phagocytosis by macrophages (Ott et al., 2007). In AgNP treatments, previously studies demonstrated that down-regulation of the pro-survival protein Bcl-2 and enhanced expression of pro-apoptotic gene products such as Bax and Bad (Bcl-2-associated death promoter) in human and animal cells were involved AgNPs expose (Gopinath et al., 2010; Piao et al., 2011). Moreover, Hsin et al. (2008) point out that AgNP exposure could trigger cytochrome c, releasing into the cytosol and translocation of Bax into the mitochondria in cells. Interestingly, AgNPs could activate the intrinsic apoptotic pathway by increasing protein levels of active caspase-9 in human liver cells; actually caspase-9 was activated by releasing cytochrome c from mitochondria (Arora et al., 2008; Arora et al., 2009; Gopinath et al., 2010; Piao et al., 2011). Clearly, AgNPs could activate procaspase-3 in case of AgNP treated

human and animal cell lines. In conclusion, AgNP can induce toxic effect on cellular by relating mechanism of apoptosis.

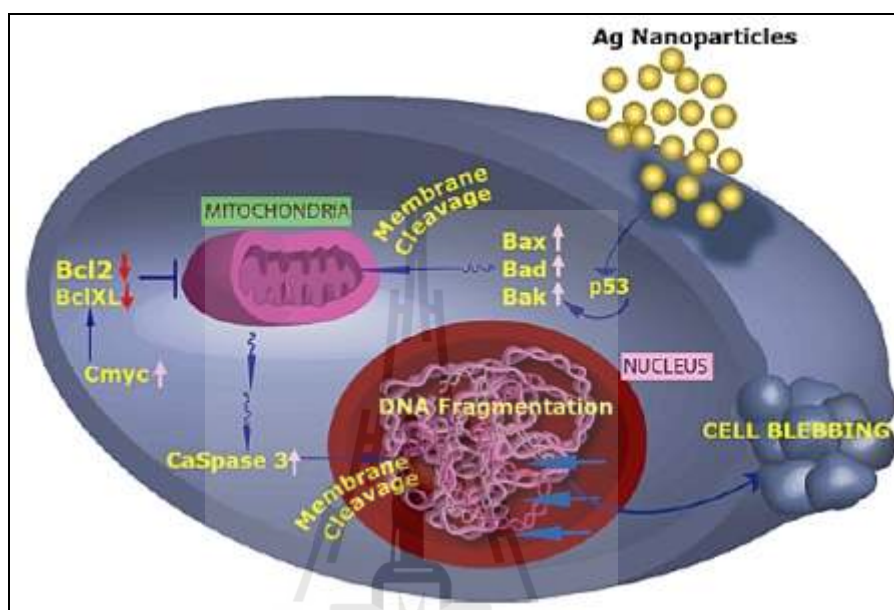


Figure 2.4 Representation of AgNPs induces apoptosis (Lim et al., 2015).

2.2.3.3 DNA damage

Actually, several studies have suggested that AgNPs has effected on genotoxicology in case of DNA damage in different types of human and mammalian cells, considering DNA strand breaks and micronuclei induction (Figure 2.5) (Ahamed et al., 2008; AshaRani et al., 2009; Kawata et al., 2009; Foldbjerg et al., 2011; Hackenberg et al., 2011; Kim et al., 2011a; Flower et al., 2012; Li et al., 2012; Nymark et al., 2012; Singh et al., 2009). DNA damage was detected after AgNPs exposures in cellular with dose-dependent (Kim et al. (2011a; Nymark et al., 2012). In another study showed DNA damage in human mesenchymal stem cells after 1, 3, and 24 h at AgNP concentrations from 0.1-10 $\mu\text{g/ml}$ by determining with both the comet

assay and chromosomal aberration test (Hackenberg et al., 2011). Furthermore, several studies have also shown that AgNPs in the size range 1–50 nm can induce DNA and chromosomal damage in different cell types (Ahamed et al., 2008; AshaRani, et al., 2009; Kawata et al., 2009; Li et al., 2012). The same study found AgNPs induced genotoxicity in the human lymphoblast TK6 cell depending on concentration (Li et al., 2012). Furthermore, protein expression was upregulated by determining the cell cycle checkpoint protein, p53, and the DNA damage repair proteins, Rad51, and phosphorylated-H2AX in mouse embryonic and fibroblast cells after AgNP exposure (Ahamed et al., 2008). However, some investigator showed that AgNPs has no significant genotoxic effects based on gene mutations in MEF-LacZ cells (Park et al., 2011b). Previous result was consistent with Asare et al. (2012) that AgNPs exposed has no statistically significant effect on DNA damage in a human testicular embryonic carcinoma cell line and in primary testicular cells from C57BL6 mice (Asare et al., 2012). In conclusion, AgNPs exposure in mammalian cell may effects on DNA damage depending on ROS level, it is also possible that AgNPs or liberated silver ions interact directly with proteins or DNA and thereby cause genotoxic effects

2.2.3.4 Protein and cell membrane damage

It is well known that silver have two forms including nanosilver and Ag^+ that can interact with cell membrane, proteins and amino acids to cause toxicity (Figure 2.6). It was well known that the most action of AgNPs is useful for antimicrobials because of mechanism particles can interaction with extracellular proteins, is dependent on pH (Khan et al., 2011). Other study also found that the binding of AgNPs could inhibit the activity of proteins on plasma membrane

(Grigor'Eva et al., 2013). By the way, AgNPs can make the formation of protein corona, protein unfolding, and altered protein function on surface of membrane led to toxicity as well (Figure 2.6) (Saptarshi et al., 2013). Especially, in term of in vitro study, to investigate the action of AgNPs on membrane proteins activity, it causes membrane damage involving permeability. Cheng et al. (2013) have found that AgNPs could disturb the cell membrane cause cell death through oxidative stress. Furthermore, the mitochondrial membrane potential variation was found after AgNPs expose with increasing ROS level (Cheng et al., 2013). Saptarshi et al. (2013) have also suggested that different size of AgNPs can cause different protein corona formation. They suggested that corona formation found on 20 nm nanosilver implies binding of more hydrophobic proteins compared to larger 110 nm particles (Saptarshi et al., 2013). In conclusion, AgNPs can disturb protein formation and cause membrane damage by imbalance of ROS level.

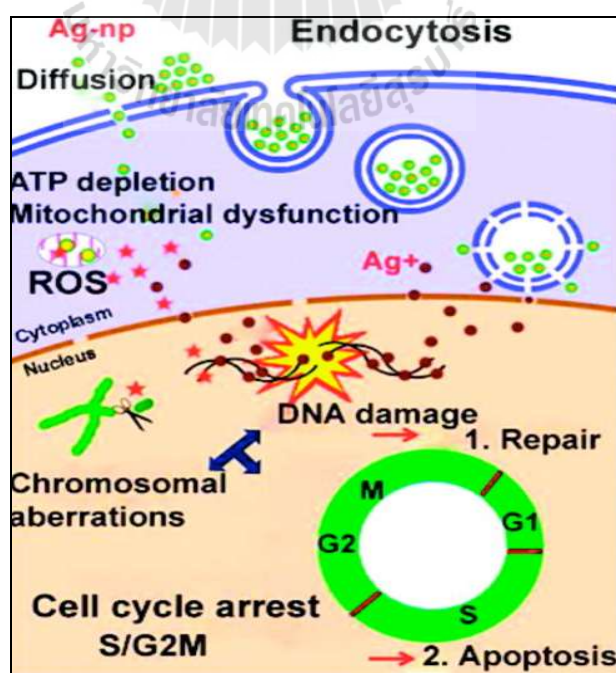


Figure 2.5 Mechanism of AgNPs cause DNA damage (Arcangeli et al., 2012).

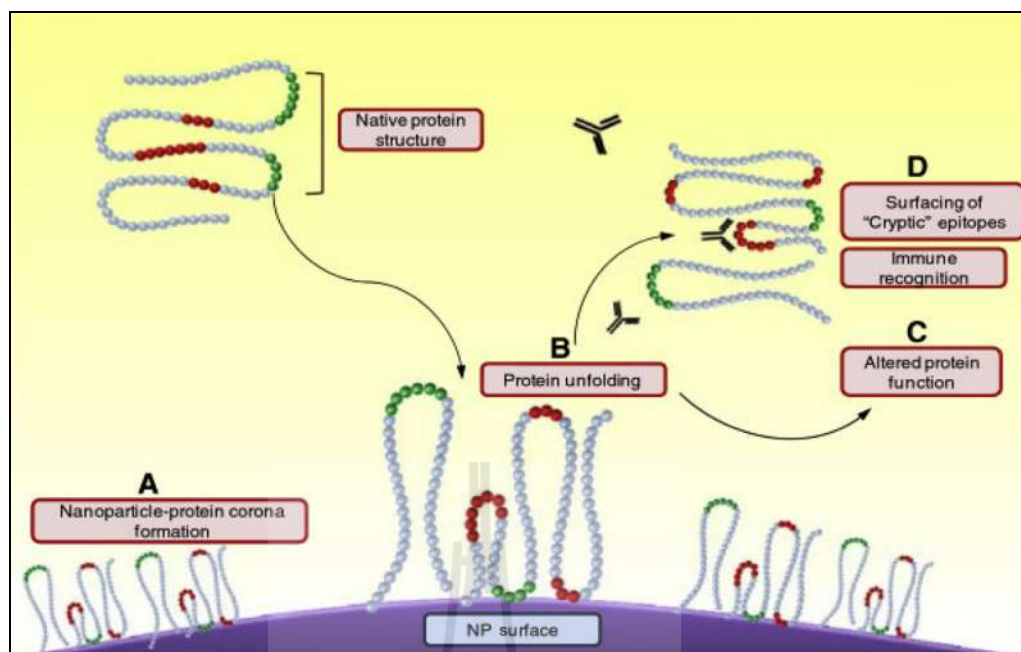


Figure 2.6 Interaction of nanoparticles with proteins: relation to bioreactivity of the nanoparticles (Saptarshi et al., 2013).

2.3 Mouse spermatozoa

The constituent of mammalian spermatozoa have specific structures that prepare it for travelling through the female reproductive tract and fertilizing with matured oocytes. Mammalian sperm must undergo multiple changes after leaving the testis to gain the capacity to fertilize an oocyte in the term capacitation (Yanagimachi et al., 1994). Sperm progressive motility and the ability to fertilize as they pass through the epididymis, attaining full fertilizing capability by the time they reach the proximal cauda epididymis (Quill et al., 2002). Mammalian sperm also experience modifications of both integral and surface plasma membrane glycoproteins during epididymal maturation. Modifications to protein distribution and protein expression, as well as lipid and protein substitutions also occur during this maturation period (Parks et al., 1985). Membrane alterations occur not only in the plasma membrane

overlying the head and the principal piece, but in the outer acrosomal membrane and are presumed to prevent premature capacitation and stimulation of the acrosome reaction (Yanagimachi et al., 1994).

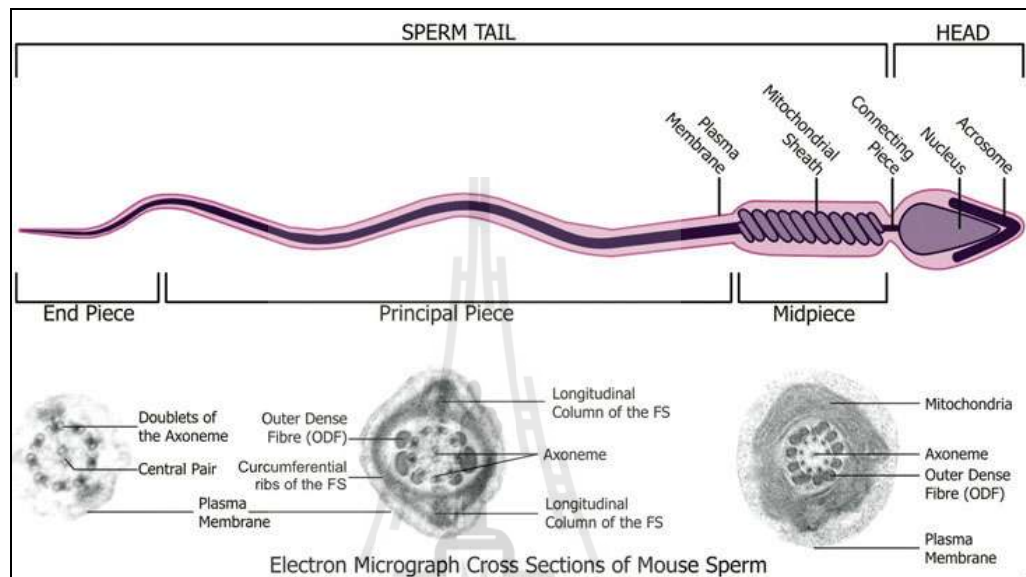


Figure 2.7 Spermatozoa (mouse) cross-sections of tail (EM) and diagram (Borg et al., 2009).

2.3.1 Mouse sperm morphology

As shown in Figure 2.7. The Spermatozoa is containing two main regions containing the head and the tail. The forward portion of the head is covered by the cap as well as acrosome. Moreover, the head of sperm is connected with the tail by the connecting piece. For tail, it is divided into three regions which are the midpiece, principal piece, and the end-piece. In figure 2.7, the electron micrographs cross sections showed the tail structure containing the axoneme, outer dense fibers (ODF), the mitochondrial sheath (midpiece) and fibrous sheath (FS) (principal piece).

2.3.2 Sperm capacitation

Actually, capacitation is the near final step of the maturation of mammalian spermatozoa and is required for the ability to fertilize (Yanagimachi, 1994). The process of capacitation is biochemical events that involve the sperm movement. In vivo capacitation typically occurs after ejaculation, occurring in the female reproductive tract (Cheng et al., 1998). In vitro, capacitation can occur by incubating sperms in a defined medium for several hours. The steps of capacitation by secreting sterol binding albumin, lipoproteins, proteolytic and glycosidic enzymes such as heparin (Tateno et al., 2013). Non-mammalian spermatozoa do not require this capacitation step because of it ready to fertilize an oocyte immediately after release from male ejaculation. After this capacitation the sperm must undergo activation involving the acrosome reaction.

Such mechanism of capacitation in spermatozoa (Figure 2.8) are involved an increase in intracellular pH (pH_i), an increase in intracellular Ca^{2+} concentration (Ca^{2+}), activation of a cAMP/PKA pathway, hyperpolarization of the sperm plasma membrane potential, loss of membrane cholesterol (cholesterol efflux) and lipid modifications, and an increase in protein tyrosine phosphorylation then lead to hyperactive motility.

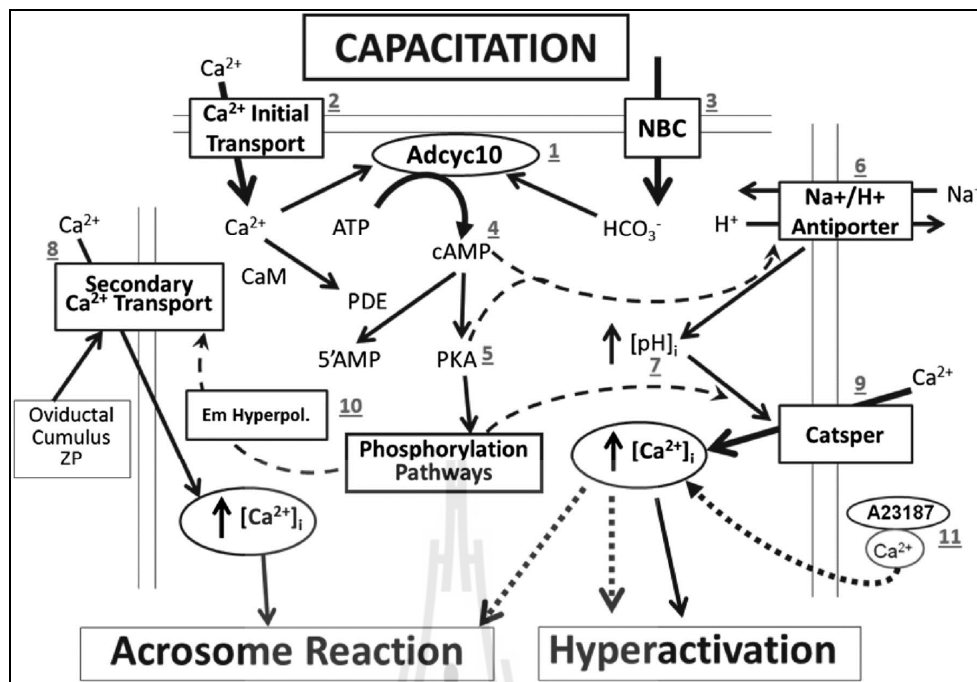


Figure 2.8 Working model of the sequence of events involved in preparation of spermatozoa for the capacitation (Tateno et al., 2013).

2.3.3 Acrosome reaction

It was known that a sperm must release a cap of head sperm namely acrosome before the plasma membrane of them will fuse and penetrate the female egg in order to fertilize it. Therefore sperm cells go through a process known as the acrosome reaction which is the reaction that occurs in the acrosome of the sperm as it approaches the egg (Flesch et al., 2000). Only capacitated spermatozoa are able to acrosome reaction. Because of the most superficial membrane that covers the apical surface of the sperm head is the plasma membrane. As shown in Figure 2.9, beneath the plasma membrane localized at the apical region of the head that is the outer acrosomal membrane (OAM). Intermittent of these two membranes has resultant vesiculation and fenestration of the combined membranes after reaction. The acrosomal matrix underlies the outer acrosomal membrane that contains nonstructural

(non-enzymatic and enzymatic) components will release of non-adherent components of the acrosomal matrix to expose the inner acrosomal membrane (IAM) that covers the nuclear envelope. Thus, the acrosome reaction leads to the release of a variety of hydrolytic and proteolytic enzymes, mainly acrosin and hyaluronidase, which are essential for sperm penetration through the oocyte envelopes (Yanagimachi, 1994). The acrosome reaction also results in the modification of some plasma membrane proteins at the acrosomal equatorial segment and post acrosomal level necessary for the fusion with the oocyte membrane.

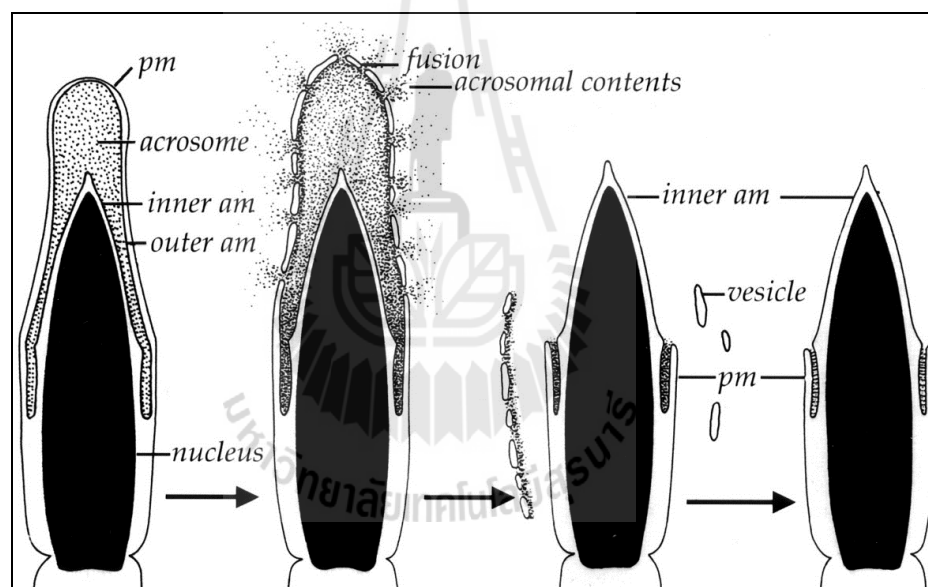


Figure 2.9 Schematic diagram of acrosome reaction in mammals (<http://pixgood.com/sperm-slide-acrosome.html>).

2.3.3.1 Acrosome reaction measurement

Of course, methods for detection of acrosome using dye staining and observed under phase contrast of microscopy have been used several years. Of note, the final step of the acrosome reaction is determined when the inner acrosomal membrane is exposed. By the way, there are many methods have been used to detect

the acrosome reaction such as coomassie blue staining (Miller et al., 1993), quinacrine (Amin et al., 1996), fluorochrome-coupled lectins such as *Pisum sativum* agglutinin (PSA) or *Arachis hypogaea* agglutinin (Cross et al., 1986; Mortimer et al., 1987). Moreover, the glycoproteins of the inner acrosomal membrane are labeled with lectins such as concanavalin ensiformis agglutinin (Holden et al., 1990). In addition, an assay based on the chlortetracycline (CTC) staining has been proposed (Saling and Storey, 1979). Nodaway, based on fluorescence light microscopy, methods labeling the acrosomal content or the outer acrosomal membrane are used. The glycoproteins of the inner acrosomal membrane are labeled specific monoclonal antibody (anti- CD46) (Figure 2.10) which is a fluorochrome (Fénichel et al., 1989; Tao et al., 1993). These methods are positive staining that only acrosome-reacted spermatozoa are labeled.

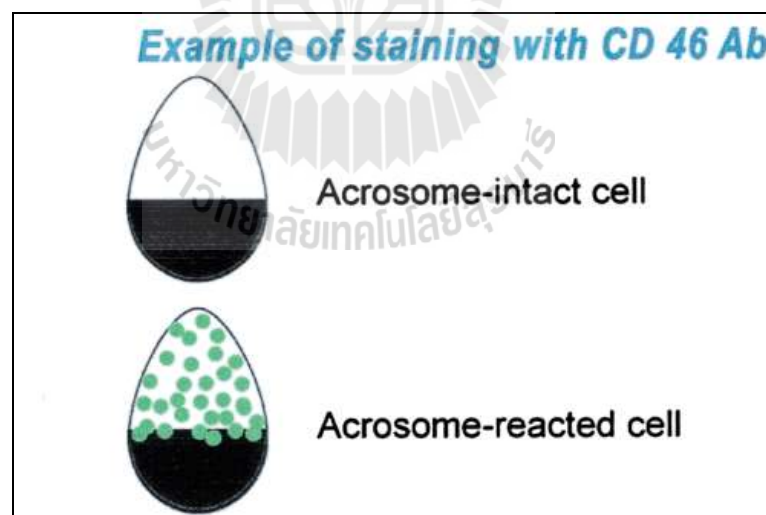


Figure 2.10 The glycoproteins of the inner acrosomal membrane are labeled specific monoclonal antibody (anti- CD46) (Patrat et al., 2000).

2.4 Fertilization

In case of sperm, receptor proteins in the sperm plasma membrane to dissolve, releasing acrosomal enzymes. In the oocyte, mammalian oocyte is contained the two layers, which are the cumulus cells and the zona pellucida. Before, the sperm penetrate to both layers, the sperm capacitation and acrosome reaction is importantly required. Then, sperm bind to the zona pellucida. In mouse, the three glycoproteins (ZP1, ZP2 and ZP3) are preventers for cross-species fertilization (Yanagimachi, 1994). After sperm binding, (Na^+) channel is opened and change their gradient into the oocyte and the plasma membrane is depolarized. These process causes block to polyspermy. The depolarization activates calcium ions (Ca^{2+}) channels in endoplasmic reticulum (ER) of the oocyte. Calcium signal transduction pathway is then initiated as well as “calcium oscillations”. The sperm head fuses to the cytoplasm and forms a male pronucleus. The pronucleus fuses with the egg nucleus and generate diploid (2N) chromosomes. The cleavage of oocytes was then occurred. Finally, fertilization is complete.

2.5 Mouse embryo development

After fertilization, meiosis is completed and first cleavage is begin. After that mouse zygote produces more two cells and then divides again to four cells, 8 cells, 16 cells. The 2 cell stages take around 18-22 h depending on the strain of mice. In mice, the embryo develops to 16-32 cells at the third day called a morula stage. The morula cells atomically then form blastocyst stage. The outer layer of the blastocyst is the Trophoectoderm (TE) and the cells inside is inner cell mass (ICM). The cells of the ICM are the three embryonic germ layers such as ectoderm, mesoderm, and endoderm as well as “pluripotent cells”.

2.6 TE and ICM formation

In mice, blastocyst formation occurs at Day 4. The TE cells arising from the trophoblast at the blastocyst stage develops a sphere of epithelial cells surrounding the ICM and blastocoel. These TE cells are required for the development of embryonic portion of the placenta and mammalian conceptus (Kunath et al., 2004; Cross, 2005). Moreover, the ICM is a group of pluripotent cells that gives rise to the embryonic tissue that comprises the ectoderm, endoderm, and mesoderm (Marikawa and Alarcon, 2009). Our results showed that Cr(VI)-exposed sperm not only significantly inhibited the ICM/TE cell proliferation in blastocysts but also downregulated the ICM/TE-associated genes, which play crucial roles in ICM and TE cell formation, reflecting a negative effect on embryo development.

2.7 Cytotoxic of AgNPs on biology fields

With AgNPs have small within nanometer, enormous specific surface area, releasing the silver ion due to to generate reactive oxygen species, and potentially disturb the functioning of biomolecules such as proteins, enzymes and DNA, thus result of AgNPs have effect toxic on biology (Table 2.1).

Table 2.1 Cytotoxic of AgNPs on biology fields.

| Targets | Size (nm) | Coating | Sample | Results | Reference |
|---------|-------------|---------|--------------------|--|--|
| Organs | 11.6±3.5 | Citrate | Zebra fish embryos | - Silver nanoparticles passively diffuse into developing embryos via chorion pore canals, abnormalities in zebrafish are highly dependent dose of AgNPs. | Lee et al., 2007 |
| | 25 | Not | Mice | - AgNPs have effect on apoptotic related genes expression in brain, caused by free radical-induced oxidative stress. | Rahman et al., 2009 |
| | 20, 80, 110 | Not | Wistar rats | - AgNPs distributed and injuries to all organs (liver, lungs, spleen, brain, heart, kidneys and testes). | Lankveld et al., 2010; Dhawan & Sharma, 2010; Dziendzikowska, et al., 2012 |

Table 2.1 (Continued).

| Targets | Size (nm) | Coating | Sample | Results | Reference |
|----------------|--------------------------------|-----------------------------|---|--|------------------------------|
| Cellular | 7-20 | Not | Fibroblasts and liver cells from Swiss albino mice | - AgNPs internalized in mitochondria and cytoplasm due to oxidative stress. | Arora et al., 2009 |
| | 10, 15, 25-30, 80 | Hydrocarbon, polysaccharide | Mouse spermatogonial | - Small-sized nanoparticles (10–25 nm) are more likely to promote apoptosis or the production of ROS. | Braydich-Stolle et al., 2010 |
| | 28.3±9.6, 47.5±5.6, 102.2±32.8 | PVP | Primary rat brain microvessel endothelial cells (rBMEC) | - Blood-brain barrier permeability - size-dependent increase, probably correlated with increased immunotoxicity. | Trickler et al., 2010 |

Table 2.1 (Continued).

| Targets | Size (nm) | Coating | Sample | Results | Reference |
|----------------|----------------------------|----------------|-------------------------------|--|--------------------------|
| Cellular | 20±2, 34±3, 61±5, 113±8 | Not | Caco-2 and M-cells co-culture | - AgNPs caused changes in gene expression in a range of stress responses including oxidative stress, endoplasmatic stress response, and apoptosis. | Bouwmeester et al., 2011 |
| | 60-70 | PVP | A549 | - DNA damage induced by ROS. | Foldbjerg et al., 2011 |
| | 20, 40 | Small peptide | THP-1 cells | - Significant oxidative stress insides macrophages after exposure to 20 nm silver NPs. | Haase et al., 2011 |
| | 46±21 | Not | Human mesenchymal stem cells | - DNA damage was induced by AgNPs, caused oxidative stress. | Hackenberg et al., 2011 |
| | 21, 75 | Citrate, PVP | PC12 cell line | - AgNPs impaired neurodevelopment differentiation | Power et al., 2011 |

Table 2.1 (Continued).

| Targets | Size (nm) | Coating | Sample | Results | Reference |
|-------------------------|------------------|-------------------------------------|---|--|-----------------------|
| Cellular | 20, 40 | Peptide | Neurons and astrocytes cell from Wistar rats | - Strong size-dependent cytotoxicity of silver nanoparticles on astrocytes, oxidative stress response. | Haase et al., 2012 |
| | <10 | chloride-Ag, biogenic-Ag, oleate-Ag | Mice macrophage RAW-264.7 and mice lung epithelial C-10 | - Membrane damage depends on surface charge and coating, materials used in the synthesis, particle aggregation, and the cell-type. | Suresh et al., 2012 |
| Reproductive -Female | 13 | Not | Mouse embryos | - AgNPs induced apoptosis in mouse embryos at the blastocyst stage, reduction of implantation frequency and delay in post-implantation development of embryos. | Li et al., 2010 |
| | 20 | Not | Pregnancy CD-1 mice | - Administration of AgNPs to the pregnant CD-1 mice resulted in the reduced fetus viability. | Phibrook et al., 2011 |

Table 2.1 (Continued).

| Targets | Size (nm) | Coating | Sample | Results | Reference |
|-----------------------|------------------|----------------|-------------------|--|----------------------------------|
| Reproductive -Male | 20, 200 | Not | Male rat | - Size-dependent (20 nm and 200 nm), dose-dependent (5 and 10 mg/kg body mass) and time-dependent (24 h, 7 and 28 days) decrease the epididymal sperm count. | Gromadzka-Ostrowska et al., 2012 |
| | 70 | Not | Male Wistar rats | - AgNPs can decrease human sperm motility and sperm viability with increasing dose (25, 50, 100 and 200 mg/kg concentration) after received oral feeding AgNPs every 12 h (48 days). | Moretti et al., 2012 |
| | 60, 120 | PVP | Human spermatozoa | - Motility and viability of human spermatozoa were decreased with increasing dose of AgNPs (30, 60, 125, 250 and 500 μ M). | Moretti et al., 2013 |
| | N/A | Not | Male mice | - The different concentrations (100, 500 and 1000 mg/kg) of silver nanoparticles (AgNPs) were injected into i.p. of male mice, it was shown that sperm motility, viability was deceased after AgNPs injection for totally 3 months | Attia, 2014 |

Table 2.1 (Continued).

| Targets | Size (nm) | Coating | Sample | Results | Reference |
|-----------------------|------------------|----------------|------------------|--|----------------------|
| Reproductive -Male | 70 | Not | Male Wistar rats | - After 45 days of feeding AgNPs with different concentration (25, 50, 100, and 200 mg/kg/day), resulting of sperm motility and normal sperm morphology were decreased after feeding with AgNPs dose dependent. | Baki et al., 2014 |
| | N/A | Not | Male Wistar rats | - Male Wistar rats were orally treated with 15 or 30 mg/kg/day AgNPs, it was shown that AgNPs reduced the acrosome and plasma membrane integrities, reduced the mitochondrial activity and increased the abnormalities of sperm with dose dependent. | Mathias et al., 2014 |

N/A = Not analysis

2.8 Chromium

Elemental chromium was first discovered and characterized by a French chemist Nicolas in 1797 (Costa and Klein 2008). It is naturally elements in crustal abundance and is found virtually in all pahses including air, water, soil and biota (Losi et al., 1994). The major industries using chromium are the metallurgical, chemical and refracotyr brick industries (Losi at al., 1994). Major uses of hexavalent chromium (Cr (VI)) compounds are mostly found in rocks, volcanic dust and gases, soils, as well as in animals and plants. It is extensively used in pigment and stainless steel production; leather tannery; wood processing; welding; cement manufacturing; chrome plating, textile, ceramic, glass, and photography industries; catalytic converters for automobiles; and cooling plant (Stohs et al., 2001); disposal of these kinds of industrial waste creates severe environmental pollution.

- Hexavalent chromium

Hexavalent chromium, or Cr(VI), compounds are those that contain the metallic element chromium (Cr) in its +6 valence (hexavalent) state. In this document these compounds are denoted as chromium (hexavalent compounds), or Cr(VI) compounds. Chromium has six oxidation states. The hexavalent state is one of the three most stable forms in which chromium is found in the environment. The other two of these forms are the 0 (metal and alloys), and the +3 (trivalent chromium, Cr(III)) valence states. In addition to occupational exposure of workers (via inhalation and skin contact), people are also exposed to Cr when it contaminates ground and surface water, agricultural land, and aquatic life. Cr can exist in a variety of oxidative states ranging from -2 to +6, among which the trivalent (III) and hexavalent (VI)

forms have biological importance (Stoecker, 2004). Cr(VI), can readily cross cellular membranes via nonspecific anion transporters, whereas the trivalent form, Cr(III), is poorly transported across membranes. Therefore, Cr toxicity is mainly attributed to Cr(VI).

Mechanism of hexavalent chromium – As shown in Fig. 2.11, Cr(VI) can enter the cell by anionic transporters and is rapidly reduced to Cr(V), Cr(IV), and Cr(III). Both Cr(III) and Cr(VI) display an appreciable affinity for both DNA bases and the phosphate backbone leading to the formation of Cr–DNA monoadducts, ICLs and ternary adducts. Cr(VI) can directly oxidize DNA bases (guanine, 8-oxo-dG) and sugars (hydrogen abstraction) and make DNA strand breaks. Cr(III) is the ultimate DNA reactive species and is critical for the formation of monoadducts, DNA-Cr-DNA interstrand crosslinks and protein-Cr-DNA crosslinks. Moreover, Cr(VI) may generate the hydroxyl radical in the presence of elevated levels of H₂O₂ and lead to “oxidative” DNA damage. During the reduction process, reactive oxygen species (ROS) are generated (Valko et al., 2005). It is believed that the reduction of Cr(VI) is the most important factor in the induction of chromium cytotoxicity (Bagchi et al., 2001). In certain cell types, such as lung epithelial cells and rat hepatoma cells, it was found that, via the effects of ROS, Cr(VI) could activate cell signaling, including the Akt, NF- κ B, and MAPK pathways (Beaver et al., 2009, Chuang et al., 2000 and Kim and Yurkow, 1996). Cr(VI) could also stimulate the release of cytokines, such as TNF- α and IL-1 α (Gueniche et al., 1994 and Curtis et al., 2007). Recent studies have demonstrated that the production of TNF- α and IL-1 α , are related to cell signaling activation, particularly in the Akt, NF- κ B, and MAPK pathways (Dumitru et al., 2000, Feldmeyer et al., 2007, Gaestel et al., 2009 and Rommel et al., 2007).

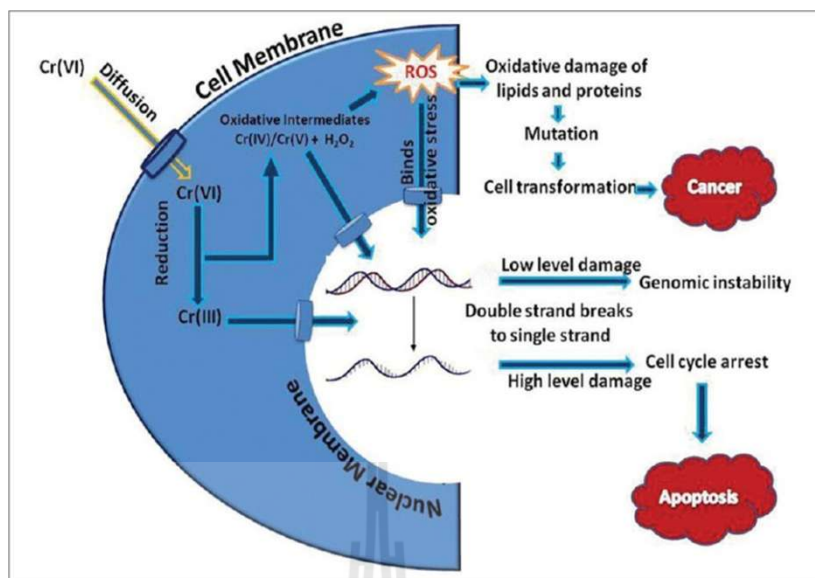


Figure 2.11 Role of cellular response, repair and recovery mechanisms (O'Brien et al., 2003).

Hexavalent chromium cytotoxicity – In humans and animals, Cr(VI) is an essential nutrient that plays a role in glucose, fat, and protein metabolism by potentiating the action of insulin. The biologically active form of chromium, called chromodulin, is an oligopeptide complex containing with four chromic ions (Jacquemet et al. 2003). Both humans and animals are capable of converting inactive inorganic Cr(VI) compounds to physiologically active forms. For Cr(VI), it can readily be transported into cells make DNA strand breaks as describe in 2.5.2.1. Thus, many reports have been determined the cytotoxicity of Cr (VI) on biological fields as shown in Table 2.2.

Table 2.2 Hexavalent chromium cytotoxicity.

| Route of exposure | Lowest-observed-adverse-effect level (mg/m ³) | Expose duration | Targets | Species | Results | Reference |
|-------------------|---|--------------------|--------------------|---------|--|----------------------|
| Inhalation | 1.15 | 10 days | Respiratory | Rat | - Decrease of activity, alopecia and nasal hemorrhage. The lung showed inflammation reactions caused by Cr exposure. | Kim et al., 2004 |
| | 0.025 | 90 days | Respiratory, other | Human | - Ulcerated nasal septum, irritated skin, and perforated eardrum. | Glaser et al., 2000a |
| | 0.05 | 90 days | Respiratory | Rat | - Increased lung weight, hyperplasia, and macrophage infiltration. | Glaser et al., 1990 |
| | 0.36 | 2-4 weeks (5d/wk) | Immune | Rat | - Increased neutrophils, monocytes, and decreased macrophage in BAL fluid. | Cohen et al., 1998 |
| | 0.0042 | Worker | Renal | Human | - Increased prevalence of high N-acetyl-B-glucosaminidase. | Liu et al., 1998 |
| | 0.001 | Worker (5.8 years) | Immune | Human | - Increased response of peripheral blood mononucleocytes to concavalin A. | Mignini et al., 2004 |

Table 2.2 (Continued).

| Route of exposure | Lowest-observed-adverse-effect level (mg/m³) | Expose duration | Targets | Species | Results | Reference |
|--------------------------|--|--------------------------|------------------|----------------|--|------------------------|
| Oral | 357 | Ingestion | - | Human | - Death (35 year old women ingested chromic acid solution containing Cr(VI). | Loubieres et al., 1999 |
| | 89 | 2 weeks (drinking water) | Reproductive | Rat | - Reduction in number of implantations and number of fetuses, increase in number of resorptions and pre-implantation and post-implantation losses. | Kanojia et al., 1998 |
| | 10 | 8 days (drinking water) | Gastrointestinal | Rat | - Villous atrophy and crypt cell hyperplasia in duodenum and jejunum. | Thompson et al., 2012 |
| | 152.4 | 9 days | Body weight | Mouse | - 23% decrease in gestational weight gain, increased resorptions. | Junaid et al., 1996b |
| | 30 | 8 days (drinking water) | Gastrointestinal | Mouse | - Cr(VI) in drinking water can induce oxidative stress, villous cytotoxicity, and crypt hyperplasia in the mouse intestine. | Thompson et al., 2011 |

Table 2.2 (Continued).

| Route of exposure | Lowest-observed-adverse-effect level (mg/m³) | Expose duration | Targets | Species | Results | Reference |
|--------------------------|--|---------------------------------|-------------------|----------------|---|-----------------------|
| Oral | 35.5 | 3 days (intragastic intubation) | Reproductive | Rat | - Cr(VI) induced failure of pregnancy and produce fetotoxic or fetal resorptive potentials. | Bataineh et al., 2007 |
| | 5.2 | 6 days (intragastic intubation) | Reproductive | Rat | - Cr(VI) to rats significantly reduced the epididymal sperm counts, also significantly increased the sperm abnormality. | Li et al., 2001 |
| | 6.25 | 10 days (gavage) | Body | Rat | - Cr(VI) have effect on body and mandibular growth and tooth eruption in suckling Wistar rats. | de Lucca et al., 2009 |
| | 8 | Gestation period (adlibitum) | Reproductive | Rat | - Increased pre and post implantation loss, dead fetus, resorptions. | Elsaieed & Nada, 2002 |
| | 1.3 | 22 weeks (drinking water) | Hepatic and renal | Rat | - Increased serum ALT and AST, histopathological changes, degeneration of Bowman's capsule. | Acharya et al., 2001 |

Table 2.2 (Continued).

| Route of exposure | Lowest-observed-adverse-effect level (mg/m³) | Expose duration | Targets | Species | Results | Reference |
|--------------------------|--|------------------------------|----------------|----------------|--|----------------------------|
| Oral | 42 | 12 weeks (drinking water) | Body | Rat | - Loss body weight (57%). | Bataineh et al., 1997 |
| | 40 | 90 days (gavage) | Body | Rat | - Loss body weight. | Chowghury & Mitra, 1995 |
| | 73 | 30 days (drinking water) | Endocrine | Rat | - Decreased in serum prolactin. | Quinteros et al., 2007 |
| | 3.7 | 10 days (drinking water) | Hepatic | Rat | - Increased serum ALT and AST, histopathological changes in vascularization. | Rafael et al., 2007 |
| | 3.4 | 21 days (drinking water) | Renal | Rat | - Induced proximal tube necrosis. | Soudani et al., 2010a |
| | 9.4 | 21 days (drinking water) | Ranal | Rat | - Kidney hemorrhage and necrosis. | Soudani et al., 2010b |

Table 2.2 (Continued).

| Route of exposure | Lowest-observed-adverse-effect level (mg/m³) | Expose duration | Targets | Species | Results | Reference |
|--------------------------|--|------------------------------|----------------|----------------|---|-----------------------------|
| Oral | 9.4 | 21 days (drinking water) | Hepatic | Rat | - Liver necrosis; antioxidant enzyme activities were reduced in liver. | Soudani et al., 2011a |
| | 26 | 3 weeks (drinking water) | Cardio | Rat | - Chromium caused oxidative stress in heart tissue. | Soudani et al., 2011c |
| | 14 | 210 days (drinking water) | Body | Mouse | - Loss body weight. | de Flora et al., 2006 |
| | 16 | 10 weeks | Immune | Mouse | - Increased proliferation of T and B lymphocytes. | Snyder & Valle et al., 2007 |
| | 2.1 | 180 days (drinking water) | - | Monkey macaca | - Histopathological changes to epididymis including ductal obstruction. | Aruldas et al., 2004 |
| | 2.1 | 180 days (drinking water) | - | Monkey macaca | - Decreased testis weight, disrupted spermatogenesis. | Aruldas et al., 2005 |

Table 2.2 (Continued).

| Route of exposure | Lowest-observed-adverse-effect level (mg/m³) | Expose duration | Targets | Species | Results | Reference |
|--------------------------|--|--------------------------------------|----------------|----------------|---|--------------------------|
| Oral | 2.1 | 180 days (drinking water) | Reproductive | Monkey macaca | - Histopathological changes to basal cells and principal cells of epididymis. | Aruldas et al., 2006 |
| | 1.1 | 180 days (drinking water) | Reproductive | Monkey macaca | - Sperm count and motility were decreased by Cr(VI) expose. | Subramanian et al., 2006 |
| | 15.2 | 7 weeks (feed) | Reproductive | Mouse | - Decreased spermatogenesis. | Zahid et al., 1990 |
| | 2.6 | 10 weeks (gavage) | - | Rabbit | - Sperm count, viability, mortality were decreased by Cr(VI). | Yousef et al., 2006 |
| | 11.4 | Lactational day (drinking water) | Reproductive | Rat | - Delay follicle development. | Banu et al., 2008 |
| | 11.4 | Lactational day (drinking water)) | Reproductive | Rat | - Reduced pup's body weight, increased free radicals in uterus. | Samuel et al., 2011 |
| | 66 | Gastation period (ad libitum) | - | Mouse | - Delayed time of vaginal opening and impaired fertility in female offspring. | Al-Hamood et al., 1998 |

2.9 Why use mouse as a model?

There are many researches using the mouse as a model. Because of their anatomy, physiology, and genetics are similarity to humans. Actually, the mouse genome is also similar to humans. Thus, we usually found mouse as model for the genetic research apply to human disease and the development of drug therapies. Importantly, mouse are a cost-effective, small size, have a short generation time and an accelerated lifespan. Moreover, the inbred strain provides an essential system to study complex diseases involving the interaction of multiple genes. Because of many genes shared between mice and humans. Thus, research in mice is important for the risk factors in the human population. BDF1 strain is a mouse model for our research. Because these strain is cross between female C57BL/6 and male DBA/2. They are also small size, short life cycle and easy to take care. Importantly, this strain is reposed on hormone synchronization during superovulation and produced large numbers of oocytes.

2.10 References

- Acharya, S., Mehta, K., Krishnan, S., and Rao, C. V. (2001). A subtoxic interactive toxicity study of ethanol and chromium in male Wistar rats. **Alcohol** 23(2): 99-108.
- Amin, A. H., Bailey, J. L., Storey, B. T., Blasco, L., Heyner, S., (1996). A comparison of the three methods for detecting the acrosome reaction in human spermatozoa. **Hum. Reprod.** 11: 741-745.
- Al-Hamood, M. H., Elbetieha, A., and Bataineh, H. (1998). Sexual maturation and fertility of male and female mice exposed prenatally and postnatally to

- trivalent and hexavalent chromium compounds. **Reprod. Fertil. Dev.** 10: 179-183.
- Andon, F. T., and Fadeel, B. (2012). Programmed Cell Death: Molecular Mechanisms and Implications for Safety Assessment of Nanomaterials. **Acc. Chem. Res.** 46(3): 733-42.
- Arora, S., Jain, J., Rajwade, J., and Paknikar, K. (2008). Cellular responses induced by silver nanoparticles: In vitro studies. **Toxicol. Lett.** 179(2): 93-100.
- Arora, S., Jain, J., Rajwade, J., and Paknikar, K. (2009). Interactions of silver nanoparticles with primary mouse fibroblasts and liver cells. **Toxicol. Appl. Pharmacol** 236(3): 310-318.
- Asharani, P. V., Low Kah Mun, G., Hande, M. P., and Valiyaveetil, S. (2009). Cytotoxicity and genotoxicity of silver nanoparticles in human cells. **ACS Nano.** 3: 279-290.
- Ashkarran, A. A., Ghavami, M., Aghaverdi, H., Stroeve, P., and Mahmoudi, M. (2012). Bacterial effects and protein corona evaluations: crucial ignored factors in the prediction of bioefficacy of various forms of silver nanoparticles. **Chem. Res. Toxicol.** 25(6): 1231-1242.
- Attia, A. A. (2014). Evaluation of the Testicular Alterations Induced By Silver Nanoparticles in Male Mice: Biochemical, Histological and Ultrastructural Studies. **Res. J. Pharm. Biol. Chem.** 5(4): 1558-1589.
- Ahamed, M., Karns, M., Goodson, M., Rowe, J., Hussain, S. M., Schlager, J. J., and Hong, Y. (2008). DNA damage response to different surface chemistry of silver nanoparticles in mammalian cells. **Toxicol. Appl. Pharmacol.** 233(3): 404-410.

- Arcangeli, C., Brunori, C., Celino, M., Pacchierrotti, F., and della Sala. (2012). Approaching the responsible use of nanotechnologies. **Energia. Ambiente Innovazione**. 1: 66-76.
- Aruldhas, M. M., Subramanian, S., Sekhar, P., Hasan, G. C., Govindarajulu, P., Akbarsha, M. A. (2004). Microcanalization in the epididymis to overcome ductal obstruction caused by chronic exposure to chromium a study in the mature bonnet monkey (*Macaca radiata Geoffroy*). **Reproduction** 128: 127-137.
- Aruldhas, M. M., Subramanian, S., Sekhar, P., Vengatesh, G., Chandrahasan, G., Govindarajulu, P., and Akbarsha, M. A. (2005). Chronic chromium exposure-induced changes in testicular histoarchitecture are associated with oxidative stress: Study in a non-human primate (*Macaca radiata Geoffroy*). **Hum. Reprod.** 20(10): 2801-2813.
- Aruldhas, M. M., Subramanian, S., Sekhar, P., Vengatesh, G., Govindarajulu, P., and Akbarsha, M. A. (2006). *In vivo* spermatotoxic effect of chromium as reflected in the epididymal epithelial principal cells, basal cells, and intraepithelial macrophages of a nonhuman primate (*Macaca radiata Geoffroy*). **Fertil. Steril.** 86(Suppl 3): 1097-1105.
- Asare, N., Instanes, C., Sandberg, W. J., Refsnes, M., Schwarze, P., Kruszewski, M., and Brunborg, G. (2012). Cytotoxic and genotoxic effects of silver nanoparticles in testicular cells. **Toxicology** 291(1-3): 65-72.
- Asz, J., Asz, D., Moushey, R., Seigel, J., Mallory, S. B., and Foglia, R. P. (2006). Treatment of toxic epidermal necrolysis in a pediatric patient with a nanocrystalline silver dressing. **J. Pediatr. Surg.** 41: e9-e12.

- Baki, M. E., Miresmaili, S. M., Pouretezari, M., Amraii, E., Yousefi, V., Spenani, H. R., Talebi, A. R., Anvari, M., Fazilati, M., Fallah, A. A., and Mango, E. (2014). Effects of silver nanoparticles on sperm parameters, number of Leydig cells and sex hormones in rats. **Iran J. Reprod. Med.** 12(2): 139-44.
- Bagchi, D., Bagchi, M., and Stohs, S. J., (2001). Chromium (VI)-induced oxidative stress, apoptotic cell death and modulation of p53 tumor suppressor gene. **Mol. Cell. Biochem.** 222: 149-158.
- Banu, S. K., Samuel, J. B., Arosh, J. A., Burghardt, R. C., and Aruldhas, M. M. (2008). Lactational exposure to hexavalent chromium delays puberty by impairing ovarian development, steroidogenesis and pituitary hormone synthesis in developing Wistar rats. **Toxicol. Appl. Pharmacol.** 232(2): 180-189.
- Bataineh, H., Al-Hamood, M. H., Elbetieha, A., and Bani Hani, I. (1997). Effect of long-term ingestion of chromium compounds on aggression, sex behavior and fertility in adult male rat. **Drug Chem. Toxicol.** 20(3): 133-149.
- Bataineh, H., Bataineh, Z., and Daradka, H. (2007). Short-term exposure of female rats to industrial metal salts: Effect on implantation and pregnancy. **Reprod. Med. Biol.** 6(3): 179-183.
- Beaver, L. M., Stemmy, E. J., Constant, S. L., Schwartz, A., Little, L. G., Gigley, J. P., Chun, G., Sugden, K. D., Ceryak, S. M., and Patierno, S. R., (2009). Lung injury, inflammation and Akt signaling following inhalation of particulate hexavalent chromium. **Toxicol. Appl. Pharmacol.** 235: 47-56.
- Benn, T. M., and Westerhoff, P. (2008). Nanoparticle silver released into water from commercially available sock fabrics. **Environ. Sci. Technol.** 42: 4133-4139.

- Beer, C., Foldbjerg, R., Hayashi, Y., Sutherland, D. S., and Autrup, H. (2012). Toxicity of silver nanoparticles - nanoparticle or silver ion? **Toxicol. Lett.** 208(3): 286-292.
- Bouwmeester, H., Poortman, J., Peters, R. J., Wijma, E., Kramer, E., Makama, S., Puspitaninganindita, K., Marvin, H. J., Peijnenburg, A. A., and Hendriksen, P. J. (2011). Characterization of translocation of silver nanoparticles and effects on wholegenome gene expression using an in vitro intestinal epithelium coculture model. **ACS Nano.** 5(5): 4091-4103.
- Borg, C. L., Wolski, K. M., Gibbs, G. M., and O'Bryan, M. K. (2009). Phenotyping male infertility in the mouse: how to get the most out of a 'non-performer'. **Hum. Reprod. Update** 16(2): 205-24.
- Braydich-Stolle, L. K., Schaeublin, N. M., Murdock, R. C., Jiang, J., Biswas, P., Schlager, J. J., and Hussain, S. M. (2009). Crystal structure mediates mode of cell death in TiO₂ nanotoxicity. **J. Nanopart. Res.** 11: 1361-1374.
- Braydich-Stolle, L. K., Lucas, B., Schrand, A., Murdock, R. C., Lee, T., Schlager, J. J., Hussain, S. M., and Hofmann, M. C. (2010). Silver nanoparticles disrupt GDNF/Fyn kinase signaling in spermatogonial stem cells. **Toxicol. Sci.** 116(2): 577-589.
- Brown, D. M., Wilson, M. R., MacNee, W., Stone, V., and Donaldson, K. (2001). Size-dependent proinflammatory effects of ultrafine polystyrene particles: a role for surface area and oxidative stress in the enhanced activity of ultrafines. **Toxicol. Appl. Pharmacol.** 175: 191-199.
- Burd, A., Kwok, C. H., Hung, S. C., Chan, H. S., Gu, H., Lam, W. K., and Huang, L. (2007). A comparative study of the cytotoxicity of silver-based dressings in

- monolayer cell, tissue explant, and animal models. **Wound Repair Regen.** 15: 94-104.
- Buzea, C., Pacheco, I. I., and Robbie, K. (2007). Nanomaterials and nanoparticles: sources and toxicity. **Biointerphases** 4: MR17-MR71.
- Carlson, C., Hussain, S. M., Schrand, A. M., Braydich-Stolle, L. K., Hess, K. L., Jones, R. L., and Schlager, J. J. (2008). Unique cellular interaction of silver nanoparticles: size-dependent generation of reactive oxygen species. **J. Phys. Chem. B.** 112(43): 13608-13619.
- Cheng, F. P., Fazeli, A. R., Voorhout, W. F., Tremoleda, J. L., Bevers, M. M., Colenbrander, B. (1998). Progesterone in mare follicular fluid induces the acrosome reaction in stallion spermatozoa and enhances in vitro binding to the zona pellucida. **Int. J. Androl.** 21: 57-66.
- Cheng, X., Zhang, W., Ji, Y., Meng, J., Guo, H., Liu, J., Wu, X., and Xu, H. (2013). Revealing silver cytotoxicity using Au nanorods/Ag shell nanostructures: disrupting cell membrane and causing apoptosis through oxidative damage. **RSC Adv.** 3: 2296-305.
- Cho, E. C., Xie, J., Wurm, P. A., and Xia, Y. (2009). Understanding the role of surface charges in cellular adsorption versus internalization by selectively removing gold nanoparticles on the cell surface with a I₂/KI etchant. **Nano. Lett.** 9(3): 1080-1084.
- Choi, O., and Hu, Z. (2005). Size dependent and reactive oxygen species related nanosilver toxicity to nitrifying bacteria. **Environ. Sci. Technol.** 42: 4583-4588.

- Chou, W. L., Yu, D. G., and Yang, M. C. (2005). The preparation and characterization of silver-loading cellulose acetate hollow fiber membrane for water treatment. **Polym. Adv. Technol.** 16: 600-607.
- Chowdhury, A. R., and Mitra, C. (1995). Spermatogenic and steroidogenic impairment after chromium treatment in rats. **Indian J. Exp. Biol.** 33: 480-484.
- Chuang, S. M., Liou, G. Y., Yang, J. L., (2000). Activation of JNK, p38 and ERK mitogenactivated protein kinases by chromium(VI) is mediated through oxidative stress but does not affect cytotoxicity. **Carcinogenesis** 21: 1491-1500.
- Cohen, M. D., Zelikoff, J. T., Chen, L. C., and Schlesinger, R. B. (1998). Immunotoxicologic effects of inhaled chromium: Role of particle solubility and co-exposure to ozone. **Toxicol. Appl. Pharmacol.** 152: 30-40.
- Costa, M., and Klein, C. B. (2008). Toxicity and carcinogenicity of chromium compounds in humans. **Crit. Rev. Toxicol.** 36(2): 155-163.
- Cross, N. L., Morales, P., Overstreet, J. W., and Hanson, F. W., (1986). Two simple methods for detecting acrosome-reacted human sperm. **Gam. Res.** 15: 213-226.
- Curtis, A., Morton, J., Balafa, C., MacNeil, S., Gawkrödger, D. J., Warren, N. D., and Evans, G. S., 2007. The effects of nickel and chromium on human keratinocytes: differences in viability, cell associated metal and IL-1alpha release. **Toxicol. In Vitro** 21: 809-819.
- Damm, C., Münstedt, H., and Rösch, A. (2008). The antimicrobial efficacy of polyamide 6/silver-nano-and microcomposites. **Mater. Chem. Phys.** 108: 61-66.

- Dhawan, A., and Sharma, V. (2010). Toxicity assessment of nanomaterials: methods and challenges. **Anal. Bioanal. Chem.** 398: 589-605.
- de Flora, S., Ilcheva, M., and Balansky, R. M. (2006). Oral chromium(VI) does not affect the frequency of micronuclei in hematopoietic cells of adult mice and of transplacentally exposed fetuses. **Mutat. Res.** 610: 38-47.
- de Lucca, R. C., Dutrey, P. L., Villarino, M. E., and Ubios, A. M. (2009). Effect of different doses of hexavalent chromium on mandibular growth and tooth eruption in juvenile Wistar rats. **Exp. Toxicol. Pathol.** 61(4): 347-352.
- Dumitru, C. D., Ceci, J. D., Tsatsanis, C., Kontoyiannis, D., Stamatakis, K., Lin, J. H., Patriotis, C., Jenkins, N. A., Copeland, N. G., Kollias, G., Tsihchlis, P. N., (2000). TNF-alpha induction by LPS is regulated posttranscriptionally via a Tpl2/ERK-dependent pathway. **Cell** 103: 1071-1083.
- Dziendzikowska, K., Gromadzka-Ostrowska, J., Lankoff, A., Oczkowski, M., Krawczynska, A., Chwastowska, J., Sadowska-Bratek, M., Chajduk, E., Wojewodzka, M., Dusinska, M., and Kruszewski, M. (2012). Time-dependent biodistribution and excretion of silver nanoparticles in male Wistar rats. **J. Appl. Toxicol.** 32(11): 920-928.
- Elsaieed, E. M., and Nada, S. A. (2002). Teratogenicity of hexavalent chromium in rats and the beneficial role of ginseng. **Bull Environ. Contam. Toxicol.** 68: 361-368.
- Eom, H. J., and Choi, J. (2010). p38 MAPK activation, DNA damage, cell cycle arrest and apoptosis as mechanisms of toxicity of silver nanoparticles in Jurkat T cells. **Environ. Sci. Technol.** 44(21): 8337-8342.

- Feldmeyer, L., Keller, M., Niklaus, G., Hohl, D., Werner, S., and Beer, H. D. (2007). The inflammasome mediates UVB-induced activation and secretion of interleukin-1 β by keratinocytes. **Curr. Biol.** 17: 1140-1145.
- Fénichel, P., Hsi, B. L., Farahifar, D., Donzeau, M., Barrier-Delpech, N., Yeh, C. J. G. (1989). Evaluation of the sperm acrosome reaction using a monoclonal antibody, GB24, and the fluorescence-activated cell sorter. **J. Reprod. Fert.** 87: 699-706.
- Flesch, F. M., and Gadella, B. M. (2000). Dynamics of the mammalian sperm plasma membrane in the process of fertilization. **Biochimica et Biophysica Acta.** 1469: 197-235.
- Flower, N. A., Brabu, B., Revathy, M., Gopalakrishnan, C., Raja, S.V., Murugan, S. S., and Kumaravel, T. S. (2012). Characterization of synthesized silver nanoparticles and assessment of its genotoxicity potentials using the alkaline comet assay. **Mutat. Res.** 742(1-2): 61-65.
- Foldbjerg, R., Dang, D. A., and Autrup, H. (2011). Cytotoxicity and genotoxicity of silver nanoparticles in the human lung cancer cell line, A549. **Arch. Toxicol.** 85(7): 743-750.
- Foldbjerg, R., Irving, E. S., Hayashi, Y., Sutherland, D. S., Thorsen, K., Autrup, H., and Beer, C. (2012). Global gene expression profiling of human lung epithelial cells after exposure to nanosilver. **Toxicol. Sci.** 130(1): 145-157.
- Franco, R., Sanchez-Olea, R., Reyes-Reyes, E. M., and Panayiotidis, M. I. (2009). Environmental toxicity, oxidative stress and apoptosis: menage a trois. **Mutat. Res.** 674(1-2): 3-22.
- Fung, M. C., and Bowen, D. L. (1996). Silver products for medical indication: Risk benefit assessment. **Clin. Toxicol.** 34: 119-126.

- Gaestel, M., Kotlyarov, A., and Kracht, M., 2009. Targeting innate immunity protein kinase signalling in inflammation. **Nat. Rev. Drug Discov.** 8: 480-499.
- Gibb, H. J., Lees, P. S. J., Pinsky, P. F., Rooney, B. C. (2000a). Clinical findings of irritation among chromium chemical production workers. **Am. J. Ind. Med.** 38: 127-131.
- Glaser, U., Hochrainer, D., and Steinhoff, D. (1990). Investigation of irritating properties of inhaled CrVI with possible influence on its carcinogenic action. **Environ. Hyg.** 2: 235-245.
- Gopinath, P., Gogoi, S. K., Sanpui, P., Paul, A., Chattopadhyay, A., and Ghosh, S. S. (2010). Signaling gene cascade in silver nanoparticle induced apoptosis. **Colloid. Surf. B. Biointerfac.** 77(2): 240-245.
- Grigor'Eva, A., Saranina, I., Tikunova, N., Timoshenko, N., Rebrov, A., and Ryabchikova, E. (2013). Fine mechanisms of the interaction of silver nanoparticles with the cells of *Salmonella typhimurium* and *Staphylococcus aureus*. **BioMetals** 26: 479-88.
- Gromadzka-Ostrowska, J., Dziendzikowska, K., Lankoff, A., Dobrzyoska, M., Instanes, C., and Brunborg, G. (2012). Silver Nanoparticles effects on epididymal sperm in rats. **Toxicol. Lett.** 214: 251 - 258.
- Gueniche, A., Viac, J., Lizard, G., Charveron, M., and Schmitt, D. (1994). Effect of various metals on intercellular adhesion molecule-1 expression and tumour necrosis factor alpha production by normal human keratinocytes. **Arch. Dermatol. Res.** 286: 466-470.
- Haase, A., Arlinghaus, H. F., Tentschert, J., Jungnickel, H., Graf, P., Manton, A., Draude, F., Galla, S., Plendl, J., Goetz, M. E., Masic, A., Meier, W.,

- Thunemann, A. F., Taubert, A., and Luch, A. (2011). Application of laser postionization secondary neutral mass spectrometry/time-of-flight secondary ion mass spectrometry in nanotoxicology: visualization of nanosilver in human macrophages and cellular responses. **ACS Nano**. 5(4): 3059-3068.
- Haase, A., Rott, S., Mantion, A., raf, P., Plendl, J., Thünemann, A. F., Meier, W. P., Taubert, A., Luch, A., and Reiser, G. (2012). Effects of silver nanoparticles on primary mixed neural cell cultures: uptake, oxidative stress and acute calcium responses. **Toxicol. Sci.** 126: 457-68.
- Hackenberg, S., Scherzed, A., Kessler, M., Hummel, S., Technau, A., Froelich, K., Ginzkey, C., Koehler, C., Hagen, R., and Kleinsasser, N. (2011). Silver nanoparticles: evaluation of DNA damage, toxicity and functional impairment in human mesenchymal stem cells. **Toxicol. Lett.** 201(1): 27-33.
- Handy, R. D., and Shaw, B. J. (2007). Toxic effects of nanoparticles and nanomaterials: implications for public health, risk assessment and the public perception of nanotechnology. **Health, Risk & Society** 9: 125-144.
- Holden, C. A., Hyne, R. V., Sathananthan, A. H., and Trounson, A. O. (1990). Assessment of the human sperm acrosome reaction using concanavalin A lectin. **Mol. Reprod. Dev.** 25: 247–257.
- Hsin, Y. H., Chen, C. F., Huang, S., Shih, T. S., Lai, P. S., and Chueh, P. J. (2008). The apoptotic effect of nanosilver is mediated by a ROS-and JNK-dependent mechanism involving the mitochondrial pathway in NIH3T3 cells. **Toxicol. Lett.** 179: 130-139.
- Jacquamet, L., Sun, Y., Hatfield, J., Gu, W., Cramer, S. P., Crowder, M. W., Lorigan, G. A., Vincent, J. B., and Latour, J. M. (2003). Characterization of

- chromodulin by x-ray absorption and electron paramagnetic resonance spectroscopies and magnetic susceptibility measurements. **J. Am. Chem. Soc.** 125: 774-780.
- Jiang, W., Kim, B. Y. S., Rutka, J. T., and Chan, W. C. W. (2008). Nanoparticle mediated cellular response is size-dependent. **Nat. Nanotechnol.** 3: 145-150.
- Johnston, H. J., Hutchison, G., Christensen, F. M., Peters, S., Hankin, S., Stone, V. A. (2010). Review of the *in vivo* and *in vitro* toxicity of silver and gold particulates: Particle attributes and biological mechanisms responsible for the observed toxicity. **Crit. Rev. Toxicol.** 4: 328-346.
- Junaid, M., Murthy, R. C., Saxena, D. K. (1996b). Embryotoxicity of orally administered chromium in mice: Exposure during the period of organogenesis. **Toxicol. Lett.** 84: 143-148.
- Kang, S. J., Lee, Y. J., Lee, E. K., and Kwak, M. K. (2012). Silver nanoparticles mediated G2/M cycle arrest of renal epithelial cells is associated with NRF2 GSH signaling. **Toxicol. Lett.** 211(3): 334-341.
- Kanojia, R. K., Junaid, M., and Murthy, R. C. (1998). Embryo and fetotoxicity of hexavalent chromium: A long-term study. **Toxicol. Lett.** 95: 165-172.
- Kawata, K., Osawa, M., and Okabe, S. (2009). In vitro toxicity of silver nanoparticles at noncytotoxic doses to HepG2 human hepatoma cells. **Environ. Sci. Technol.** 43(15): 6046-6051.
- Khan, S. S., Mukherjee, A., and Chandrasekaran, N. (2011). Studies on interaction of colloidal silver nanoparticles (SNPs) with five different bacterial species. **Colloids Surf B Biointerfaces.** 87:129-38.

- Kittler, S., Greulich, C., Diendorf, J., Koller, M., and Epple, M. (2010). Toxicity of Silver Nanoparticles Increases during Storage Because of Slow Dissolution under Release of Silver Ions. **Chem. Materl.** 22(16): 4548-4554.
- Kim, G., and Yurkow, E. J. (1996). Chromium induces a persistent activation of mitogenactivated protein kinases by a redox-sensitive mechanism in H4 rat hepatoma cells. **Cancer Res.** 56: 2045-2051.
- Kim, H. Y., Lee, S. B., and Jang, B. S. (2004). Subchronic inhalation toxicity of soluble hexavalent chromium trioxide in rats. **Arch. Toxicol.** 78: 363-368.
- Kim, S., Choi, J. E., Choi, J., Chung, K. H., Park, K., Yi, J., and Ryu, D. Y. (2009a). Oxidative stress-dependent toxicity of silver nanoparticles in human hepatoma cells. **Toxicol. In Vitro.** 23(6): 1076-1084.
- Kim, H. R., Kim, M. J., Lee, S. Y., Oh, S. M., and Chung, K. H. (2011a). Genotoxic effects of silver nanoparticles stimulated by oxidative stress in human normal bronchial epithelial (BEAS-2B) cells. **Mutat. Res.** 726(2): 129-135.
- Klaine, S. J., Alvarez, P. J., Batley, G. E., Fernandes, T. F., Handy, R. D., Lyon, D. Y., Mahendra, S., McLaughlin, M. J., and Lead, J. R. (2008). Nanomaterials in the environment: behavior, fate, bioavailability, and effects. **Environ. Toxicol. Chem.** 27: 1825-1851.
- Kostarelos, K., Lacerda, L., Pastorin, G., Wu, W., Wieckowski, S., Luangsivilay, J., Godefroy, S., Pantarotto, D., Briand, J. P., and Muller, S. (2007). Cellular uptake of functionalized carbon nanotubes is independent of functional group and cell type. **Nat. Nanotechnol.** 2: 108-113.
- Lacerda, L., Bianco, A., Prato, M., and Kostarelos, K. (2006). Carbon nanotubes as nanomedicines: from toxicology to pharmacology. **Adv. Drug. Deliv. Rev.** 58: 1460-1470.

- Lankveld, D. P., Oomen, A. G., Krystek, P., Neigh, A., Troost-de, J. A., Noorlander, C. W., Van Eijkeren, J. C., Geertsma, R. E., and De Jong, W. H. (2010). The kinetics of the tissue distribution of silver nanoparticles of different sizes. **Biomaterials** 31(32): 8350-8361.
- Le Pape, H., Solano-Serena, F., Contini, P., Devillers, C., Maftah, A., and Leprat, P. (2004). Involvement of reactive oxygen species in the bactericidal activity of activated carbon fibre supporting silver: Bactericidal activity of ACF (Ag) mediated by ROS. **J. Inorg. Biochem.** 98: 1054-1060.
- Lee, K. J., Nallathamby, P. D., Browning, L. M., Osgood, C. J., and Xu, X. H. N. (2007). *In vivo* imaging of transport and biocompatibility of single silver nanoparticles in early development of zebrafish embryos. **ACS Nano.** 1: 133-143.
- Li, H., Chen, Q., Li, S., Yao, W., Li, L., Shi, X., Wang, L., Castranova, V., Vallyathan, V., Ernst, E., and Chen, C. (2001). Effect of Cr(VI) exposure on sperm quality: Human and animal studies. **Ann. Occup. Hyg.** 45(7): 505-511.
- Li, Y., Chen, D. H., Yan, J., Chen, Y., Mittelstaedt, R. A., Zhang, Y., Biris, A. S., Heflich, R. H., and Chen, T. (2012). Genotoxicity of silver nanoparticles evaluated using the Ames test and in vitro micronucleus assay. **Mutat. Res.** 745(1-2): 4-10.
- Limbach, L. K., Wick, P., Manser, P., Grass, R. N., Bruinink, A., and Stark, W. J. (2007). Exposure of engineered nanoparticles to human lung epithelial cells: influence of chemical composition and catalytic activity on oxidative stress. **Environ. Sci. Technol.** 41(11): 4158-4163.

- Lim, H. J., Kim, J. K., and Park, J. S. (2015). Complexation of Apoptotic Genes with Polyethyleneimine (PEI)-Coated Poly-(DL)-Lactic-Co-Glycolic Acid Nanoparticles for Cancer Cell Apoptosis. **J. Biomed. Nanotechnol.** 15: 211-225.
- Liu, C. S., Kuo, H. W., Lai, J. S., and Lin, T. I. (1998). Urinary N-acetyl-beta glucosaminidase as an indicator of renal dysfunction in electroplating workers. **Int. Arch. Occup. Environ. Health.** 71(5): 348-352.
- Liu, J., and Hurt, R. H. (2010). Ion release kinetics and particle persistence in aqueous nano-silver colloids. **Environ. Sci. Technol.** 44(6): 2169-2175.
- Liu, J., Sonshine, D. A., Shervani, S., and Hurt, R. H. (2010a). Controlled release of biologically active silver from nanosilver surfaces. **ACS Nano.** 4(11): 6903-6913.
- Liu, W., Wu, Y., Wang, C., Li, H. C., Wang, T., Liao, C. Y., Cui, L., Zhou, Q. F., Yan, B., and Jiang, G. B. (2010b). Impact of silver nanoparticles on human cells: effect of particle size. **Nanotoxicol.** 4(3): 319-330.
- Liu, J., Wang, Z., Liu, F. D., Kane, A. B., and Hurt, R. H. (2012). Chemical transformations of nanosilver in biological environments. **ACS Nano.** 6(11): 9887-9899.
- Loubieres, Y., de Lassence, A., Bernier, M., Vieillard-Baron, A., Schmitt, J. M., Page, B., Jardin, F. (1999). Acute, fatal, oral chromic acid poisoning. **J. Toxicol. Clin. Toxicol.** 37(3): 333-336.
- Losi, M. E., Amrhein, C., Frankenberger, and Jr, W. T. (1994) Environmental biochemistry of chromium. **Rev. Environ. Contam. Toxicol.** 136: 91-121.
- Mathias, F. T., Romano, R. M., Kizys, M. M. L., Kasamatsu, T., Giannocco, G., Chiamolera, M. I., Dias-da-Silva, M. R., and Romano, M. A. (2014). Daily

- exposure to silver nanoparticles during Prepubertal development decreases adult sperm and reproductive parameters. **Nanotoxicology**. DOI:10.3109/17435390.2014.889237.
- Maynard, A. D., Warheit, D. B., and Philbert, M. A. (2011). The new toxicology of sophisticated materials: nanotoxicology and beyond. **Toxicol. Sci.** 120 (1): S109-S129.
- Mignini, F., Streccioni, V., Baldo, M., Vitali, M., Indraccolo, U., Bernacchia, G., and Cocchioni, M. (2004). Individual susceptibility to hexavalent chromium of workers of shoe, hide, and leather industries. Immunological pattern of HLA B8,DR3-positive subjects. **Prev. Med.** 39(4): 767-775.
- Miller, D. J., Gong, X., and Shur, B. D. (1993). Sperm requires beta N-acetylglucosaminidase to penetrate through the zona pellucida. **Development** 118: 1279-1289.
- Monopoli, M. P., Aberg, C., Salvati, A., and Dawson, K. A. (2012). Biomolecular coronas provide the biological identity of nanosized materials. **Nat. Nanotechnol.** 7(12): 779-786.
- Moretti, E., Terzuoli, G., Renieri, T., Iacoponi, F., Castellini, C., Giordano, C., Collodel, G. (2012). In vitro effect of gold and silver nanoparticles on human spermatozoa. **Andrologia** 45(6): 392-6.
- Moretti, E., Terzuoli, G., Renieri, T., Iacoponi, F., Castellini, C., Giordano, C., and Collodel, G. (2013). In vitro effect of gold and silver nanoparticles on human spermatozoa. **Andrologia** 45(6): 392-396.
- Mortimer, D., Curtis, E. F., and Miller, R. G., (1987). Specific labeling by peanut agglutinin of the outer acrosomal membrane of the human spermatozoon. **J. Reprod. Fertil.** 81: 127-135.

- Navarro, E., Piccapietra, F., Wagner, B., Marconi, F., Kaegi, R., Odzak, N., Sigg, L., and Behra, R. (2008). Toxicity of Silver Nanoparticles to *Chlamydomonas reinhardtii*. **Environ. Sci. Tech.** 42(23): 8959-8964.
- Nymark, P., Catalan, J., Suhonen, S., Jarventaus, H., Birkedal, R., Clausen, P. A., Jensen, K. A., Vippola, M., Savolainen, K., and Norppa, H. (2012). Genotoxicity of polyvinylpyrrolidone-coated silver nanoparticles in BEAS 2B cells. **Toxicology** 313(1): 38-48.
- O'Brien, T. J., Ceryak, S., Patierno, S. R. (2003) Complexities of chromium carcinogenesis: role of cellular response, repair and recovery mechanisms. **Mutation Research** 533: 3-36.
- Ohashi, S., Saku, S., and Yamamoto, K. (2004). Antibacterial activity of silver inorganic agent YDA filler. **J. Oral. Rehabil.** 31: 364-367.
- Ott, M., Gogvadze, V., Orrenius, S., and Zhivotovsky, B. (2007). Mitochondria, oxidative stress and cell death. **Apoptosis** 12(5): 913-922.
- Panyam, J., and Labhasetwar, V. (2003). Biodegradable nanoparticles for drug and gene delivery to cells and tissue. **Adv. Drug. Deliv. Rev.** 55: 329-347.
- Panacek, A., Kvitek, L., Pucek, R., Kolar, M., Vecerova, R., Pizurova, N., Sharma, V. K., Nevecna, T., and Zboril, R. (2006). Silver colloid nanoparticles: synthesis, characterization, and their antibacterial activity. **J. Phys. Chem. B.** 110: 16248 (1-5).
- Parks, J. E., and Hammerstedt, R. H. (1985). Developmental changes occurring in the lipid of ram epididymal sperm plasma membranes. **Biol. Reprod.** 32: 653-668.

- Park, E. J., Yi, J., Kim, Y., Choi, K., and Park, K. (2010). Silver nanoparticles induce cytotoxicity by a Trojan-horse type mechanism. **Toxicol. In Vitro** 24(3): 872-878.
- Park, K., Park, E. J., Chun, I. K., Choi, K., Lee, S. H., Yoon, J., and Lee, B. C. (2011a). Bioavailability and toxicokinetics of citratecoated silver nanoparticles in rats. **Arch. Pharm. Res.** 34(1): 153-158.
- Patrat, C., Serres, C. and Jouannet, P. (2000). The acrosome reaction in human spermatozoa. **Biol. Cell.** 92: 255-266.
- Philbrook, N. A., Winn, L. M., Afrooz, A. R., Saleh, N. B., and Walker, V. K. (2011). The effect of TiO₂ and Ag nanoparticles on reproduction and development of *Drosophila melanogaster* and CD-1 mice. **Toxicol. Appl. Pharmacol.** 257(3): 429-36.
- Piao, M. J., Kang, K. A., Lee, I. K., Kim, H. S., Kim, S., Choi, J. Y., Choi, J., and Hyun, J. W. (2011). Silver nanoparticles induce oxidative cell damage in human liver cells through inhibition of reduced glutathione and induction of mitochondria-involved apoptosis. **Toxicol. Lett.** 201(1): 92-100.
- Powers, C. M., Badireddy, A. R., Ryde, I. T., Seidler, F. J., Slotkin, T. A. (2011). Silver nanoparticles compromise neurodevelopment in pc12 cells: Critical contributions of silver ion, particle size, coating, and composition. **Environ. Health Persp.** 119: 37-44.
- Quill, T. A., and Garbers, D. L. (2002). Capacitation. In: Hardy DM, editor. Fertilization. New York: Academic Press, 2002. p. 57-99.
- Quinteros, F. A., Poliandri, A. H. B., Machiavelli, L. I., Cabilla, J. P., and Duvilanski, B. H. (2007). *In vivo* and *in vitro* effects of chromium VI on anterior pituitary hormone release and cell viability. **Toxicol. Appl. Pharmacol.** 218: 79-87.

- Rahman, M. F., Wang, J., Patterson, T. A., Saini, U. T., Robinson, B. L., Newport, G. D., Murdock, R. C., Schlager, J. J., Hussain, S. M., and Ali, S. F. (2009). Expression of genes related to oxidative stress in the mouse brain after exposure to silver 25 nanoparticles. **Toxicol. Lett.** 187(1): 15-21.
- Rafael, A. I., Almeida, A., Santos, P., Parreira, I., Madeira, V. M., Alves, R., Cabrita, A. M., and Alpoim, M. C. (2007). A role for transforming growth factor-beta apoptotic signaling pathway in liver injury induced by ingestion of water contaminated with high levels of Cr(VI). **Toxicol. Appl. Pharmacol.** 224: 163-173.
- Rathi, R., Colenbrander, B., Bevers, M. M., Gadella, B. M. (2001). Evaluation of *in vitro* capacitation of stallion spermatozoa. **Biol. Reprod.** 65: 462-470.
- Rogers, E. J., Hsieh, S. F., Organti, N., Schmidt, D., and Bello, D. (2008). A high throughput *in vitro* analytical approach to screen for oxidative stress potential exerted by nanomaterials using a biologically relevant matrix: human blood serum. **Toxicol. In Vitro** 22(6): 1639-1647.
- Rogers, K. R., Bradham, K., Tolaymat, T., Thomas, D. J., Hartmann, T., Ma, L., and Williams, A. (2012). Alterations in physical state of silver nanoparticles exposed to synthetic human stomach fluid. **Sci. Total Environ.** 420: 334-339.
- Rommel, C., Camps, M., Ji, H. (2007). PI3K delta and PI3K gamma: partners in crime in inflammation in rheumatoid arthritis and beyond? **Nat. Rev. Immunol.** 7: 191-201.
- Russell, A. D., and Hugo, W. B. (1994). Antimicrobial activity and action of silver. **Prog. Med. Chem.** 31: 351-370.

- Saling, P. M., and Storey, B. T. (1979). Mouse gamete interactions during fertilization in vitro: chlortetracycline as a fluorescent probe for the mouse sperm acrosome reaction. **J. Cell Biol.** 83: 544–555.
- Samuel, J. B., Stanley, J. A., Roopha, D. P., Vengatesh, G., Anbalagan, J., Banu, S. K., and Aruldas, M. M. (2011). Lactational hexavalent chromium exposure-induced oxidative stress in rat uterus is associated with delayed puberty and impaired gonadotropin levels. **Hum. Exp. Toxicol.** 30(2): 91-101.
- Saptarshi, S. R., Duschl, A., and Lopata, A. L. (2013). Interaction of nanoparticles with proteins: relation to bio-reactivity of the nanoparticle. **J. Nanobiotech.** 11: 26.
- Singh, N., Manshian, B., Jenkins, G. J., Griffiths, S. M., Williams, P. M., Maffei, T. G., Wright, C. J., and Doak, S. H. (2009). NanoGenotoxicology: The DNA damaging potential of engineered nanomaterials. **Biomaterials** 30(23-24): 3891-3914.
- Skebo, J. E., Grabinski, C. M., Schrand, A. M., Schlager, J. J., and Hussain, S. M. (2007). Assessment of metal nanoparticle agglomeration, uptake, and interaction using high-illuminating system. **Int. J. Toxicol.** 26: 135-141.
- Snyder, C. A., and Valle, C. D. (1991). Immune function assays as indicators of chromate exposure. **Environ. Health Perspect.** 92: 83-86.
- Soudani, N., Bouaziz, H., Sefi, M., Chtourou, Y., Boudawara, T., and Zeghal, N. (2011a). Toxic effects of chromium (VI) by maternal ingestion on liver function of female rats and their suckling pups. **Environ. Toxicol.** 28(1): 11-20.

- Soudani, N., Ibtissem Ben, A., Troudi, A., Bouaziz, H., Boudawara, T., Zeghal, N. (2011b). Oxidative stress induced by chromium (VI) in bone of suckling rats. **Toxicol. Ind. Health.** 27(8): 724-734.
- Soudani, N., Sefi, M., Bouaziz, H., Chtourou, Y., Boudawara, T., and Zeghal, N. (2010b). Nephrotoxicity induced by chromium (VI) in adult rats and their progeny. *Hum. Exp. Toxicol.* 30(9): 1233-1245.
- Soudani, N., Sefi, M., Ben Amara, I., Boudawara, T., and Zeghal, N. (2010a). Protective effects of Selenium (Se) on Chromium (VI) induced nephrotoxicity in adult rats. **Ecotoxicol. Environ. Saf.** 73(4): 671-678.
- Soudani, N., Troudi, A., Bouaziz, H., Ben Amara, I., Boudawara, T., and Zeghal, N. (2011c). Cardioprotective effects of selenium on chromium (VI) induced toxicity in female rats. **Ecotoxicol. Environ. Saf.** 74(3): 513-520.
- Stoecker, J. B. (2004). Chromium In Elements and their compounds in the environment 2nd edition, pp 709-729. Eds Merian E, Anke M, Ihnat M, Stoepler M. Copyright, Weinheim, Germany.
- Stohs, J. S., Bagchi, D., Hassoun, E., and Bagchi, M. (2001). Oxidative mechanism in the toxicity of chromium and cadmium ions. **J. Environ. Pathol. Toxicol. Oncol.** 20: 77-88.
- Subramanian, S., Rajendiran, G., Sekhar, P., Gowri, C., Govindarajulu, P., Aruldas, M.M. (2006). Reproductive toxicity of chromium in adult bonnet monkeys (*Macaca radiata Geoffrey*). Reversible oxidative stress in the semen. **Toxicol. Appl. Pharmacol.** 215: 237-249.
- Suresh, A. K., Pelletier, D. A., Wang, W., Morrell-Falvey, J. L., Gu, B., and Doktycz, M. J. (2012). Cytotoxicity induced by engineered silver nanocrystallites is dependent on surface coatings and cell types. **Langmuir.** 28(5): 2727-2735.

- Tateno, H., Krapf, D., Hino, T., Sánchez-Cárdenas, C., Darszon, A., Yanagimachi, R., Visconti, P. E. (2013). Ca^{2+} ionophore A23187 can make mouse spermatozoa capable of fertilizing in vitro without activation of cAMP-dependent phosphorylation pathways. **Proc. Natl. Acad. Sci. USA.** 110(46): 18543-18548.
- Tao, J., Du, J., Crister, E. S., and Crister, J. K. (1993). Assessment of the acrosomal status and viability of human spermatozoa simultaneously using flow cytometry. **Hum. Reprod.** 8: 1879-1885.
- Tolaymat, T. M., El Badawy, A. M., Genaidy, A., Scheckel, K. G., Luxton, T. P., and Suidan, M. (2010). An evidence-based environmental perspective of manufactured silver nanoparticle in syntheses and applications: a systematic review and critical appraisal of peer-reviewed scientific papers. **Sci. Total Environ.** 408(5): 999-1006.
- Trickler, W. J., Lantz, S. M., Murdock, R. C., Schrand, A. M., Robinson, B. L., Newport, G. D., Schlager, J. J., Oldenburg, S. J., Paule, M. G., Slikker, W., Jr., Hussain, S. M., and Ali, S. F. (2010). Silver nanoparticle induced blood-brain barrier inflammation and increased permeability in primary rat brain microvessel endothelial cells. **Toxicol. Sci.** 118: 160-170.
- Thompson, C. M., Proctor, D. M., Haws, L. C., Hébert, C. D., Grimes, S. D., Shertzer, H. G., Kopec, A. K., Hixon, J. G., Zacharewski, T. R., and Harris, M. A. (2011). Investigation of the mode of action underlying the tumorigenic response induced in B6C3F1 mice exposed orally to hexavalent chromium. **Toxicol. Sci.** 123(1): 58-70.
- Thompson, C. M., Proctor, D. M., Suh, M., Haws, L. C., Hébert, C. D., Mann, J. F., Shertzer, H. G., Hixon, J. G., and Harris, M. A. (2012). Comparison of the

- effects of hexavalent chromium in the alimentary canal of F344 rats and B6C3F1 mice following exposure in drinking water: Implications for carcinogenic modes of action. **Toxicol. Sci.** 125(1): 79-90.
- Turkevich, J., Stevenson, P., and Hillier, J. (1951). A study of the nucleation and growth processes in the synthesis of colloidal gold. **Discuss. Faraday Soc.** 55-75.
- Valko, M., Morris, H., and Cronin, M. T. (2005). Metals, toxicity and oxidative stress. **Curr. Med. Chem.** 12: 1161-1208.
- Wijnhoven, S. W. P., Peijnenburg, W. J. G. M., Herberts, C. A., Hagens, W. I., Oomen, A. G., Heugens, E. H. W., Roszek, B., Bisschops, J., Gosens, I., van de Meent, D., Dekkers, S., de Jong, W. H., van Zijverden, M., Sips, A. J. A. M., and Geertsma, R. E. (2009). Nanosilver – a review of available data and knowledge gaps in human and environmental risk assessment. **Nanotoxicology** 3(2): 109-138.
- Yang, W., Shen, C., Ji, Q., An, H., Wang, J., Liu, Q., and Zhang, Z. (2009). Food storage material silver nanoparticles interfere with DNA replication fidelity and bind with DNA. **Nanotechnology.** **20**: 085102 (1-7).
- Yang, X., Gondikas, A. P., Marinakos, S. M., Auffan, M., Liu, J., Hsu-Kim, H., and Meyer, J. N. (2012). Mechanism of silver nanoparticle toxicity is dependent on dissolved silver and surface coating in *Caenorhabditis elegans*. **Environ. Sci. Technol.** 46(2): 1119-1127.
- Yanagimachi, R. (1994). Mammalian fertilization. In:Knobil E, Neill JD, editors. The physiology of reproduction. New York: Raven Press. p. 189-317.
- Yen, H. J., Hsu, S., Tsai, C. L. (2009). Cytotoxicity and immunological response of gold and silver nanoparticles of different sizes. **Small** 5: 1553–1561.

- Yousef, M. I., El-Demerdash, F. M., Kamil, K. I., and Elaswad, F. A. (2006). Ameliorating effect of folic acid on chromium(VI)-induced changes in reproductive performance and seminal plasma biochemistry in male rabbits. **Reprod. Toxicol.** 21(3): 322-328.
- Zahid, Z. R., Al-Hakkak, Z. S., Kadhim, A. H. H., Elias, E. A., and Al-Jumaily, I. S. (1990). Comparative effects of trivalent and hexavalent chromium on spermatogenesis of the mouse. **Toxicol. Environ. Chem.** 25: 131-136.
- Zhang, R., Piao, M. J., Kim, K. C., Kim, A. D., Choi, J. Y., Choi, J., and Hyun, J. W. (2012). Endoplasmic reticulum stress signaling is involved in silver nanoparticles-induced apoptosis. **Int. J. Biochem. Cell Biol.** 44(1): 224-232.

<http://pixgood.com/sperm-slide-acrosome.html>.



CHAPTER III

**INTERNALIZATION OF SILVER NANOPARTICLES
INTO MOUSE SPERMATOZOA RESULT IN POOR
OOCYTE FERTILIZATION AND COMPROMISED
EMBRYO DEVELOPMENT**

3.1 Abstract

Silver nanoparticles (AgNPs) have many features that make them attractive as medical devices, especially in therapeutic agents and drug delivery systems. Here we have introduced AgNPs into mouse spermatozoa and then determined the cytotoxic effects of AgNPs on sperm function and subsequent embryo development. Scanning electron microscopy and transmission electron microscopy analyses showed that AgNPs could be internalized into sperm cells. Furthermore, exposure to AgNPs inhibited sperm viability and the acrosome reaction in a dose-dependent manner, whereas sperm mitochondrial copy numbers, morphological abnormalities, and mortality due to reactive oxygen species were significantly increased. Likewise, sperm abnormalities due to AgNPs internalization significantly decreased the rate of oocyte fertilization and blastocyst formation. Blastocysts obtained from AgNPs-treated spermatozoa showed lower expression of trophectoderm-associated and pluripotent marker genes. Overall, we propose that AgNPs internalization into spermatozoa may alter sperm physiology, leading to poor fertilization and embryonic

development. Such AgNPs-induced reprotoxicity may be a valuable tool as models for testing the safety and applicability of medical devices using AgNPs.

3.2 Introduction

Nanoparticles (NPs) are defined as materials having diameter between 1 nm to 100 nm that behaves as a full unit with respect to its transport and properties. These properties are derived from specific characteristics including size, distribution and morphology of the NPs. Nowadays, the application of NPs is widespread and it has been extensively used in therapeutic and diagnostic agents, drug delivery systems, medical devices, food products and cosmetics. Silver nanoparticles (AgNPs) are one of the most popular nanomaterials that have been used in material science, most importantly as one of the constituent elements of dental alloys, catheters, implant surfaces and for treating of wounds and burns related infections, as well as in drug delivery in cancer and retinal therapies. Therefore, not only the consumers but also the workers manufacturing these products are exposed to AgNPs which may have harmful effects on them.

Several studies have demonstrated the effects of subchronic oral or inhalation toxicity of AgNPs in experimental animals. They also found that silver was accumulated in the blood as well as all tested organs, including the liver, spleen, kidneys, thymus, lungs, heart, brain, and testes (Kim et al., 2010; Park et al., 2010). NPs can induce cytotoxicity by the mechanism of intracellular oxidative stress and apoptosis (Nel et al., 2006; Oberdörster, 2004; Oberdörster et al., 2006; Smith et al., 2007; Usenko et al., 2007; Xia et al., 2006; Zhu et al., 2006). Like other nanoparticles, AgNPs also show the risk of toxicity by generating ROS (AshaRani et al., 2009; Hussain et al., 2005). Several studies suggest that the toxicity of AgNPs is mainly

mediated by the release of silver ions, Ag⁺ (Kvitek et al., 2009; Navarro et al., 2008). AgNPs can enter the cell by diffusion or endocytosis to cause mitochondrial dysfunction, leading to damage of proteins and nucleic acids and finally cause inhibition of cell proliferation (Ahamed et al., 2010; Foldbjerg et al., 2009; Lim et al., 2012; Roy et al., 2014).

The influence of NPs on a single gamete may cause remarkable developmental differences as the gamete quality plays a crucial role in ontogenesis (Gandolfi and Brevini, 2010). Impairment of gametes due to NPs exposure may affect reproductive functions or have pathological influence on the later generation (Campagnolo et al., 2012). However, studies concerning the sensitivity of gametes towards NPs exposure are very limited. In spermatozoa, PVA and PVP-coated iron and europium hydroxide NPs do not show any toxicity (Makhluf et al., 2006, 2008). Titanium dioxide, gold, silver and zinc oxide NPs show moderate effects (Guo et al., 2009; Gopalan et al., 2009; Moretti et al., 2013; Wiwanitkit et al., 2009; Zakhidov et al., 2012). On the other hand, europium trioxide shows severe cytotoxicity in spermatozoa (Makhluf et al., 2008).

There are only limited studies regarding the effects of AgNPs on fertility as well as sperm function. It has been shown that AgNPs exposure could affect testicular morphology, reduced sperm production, and increased the number of abnormal spermatozoa as well as germ cell DNA damage *in vivo* (Gromadzka-Ostrowska et al., 2012; Kyjovska et al., 2013; Lan and Yang, 2012; Sleiman et al., 2013). In another *in vivo* study in rats, Miresmaeili et al. (2013) showed that AgNPs exposure significantly decreased the number of spermatogenic cells including spermatogonia, spermatocytes, spermatids and spermatozoa as well as affected the acrosome reaction in sperm cells.

Several *in vitro* studies also showed that AgNPs caused cytotoxicity/apoptosis in testicular cells and embryos as well as affected the proliferation rate in spermatogonial stem cells (Asare et al., 2012; Braydich-Stolle et al., 2010; Li et al., 2010; Lucas et al., 2009). In another *in vitro* study, Moretti et al. (2013) showed that AgNPs exerted a significant dose-dependent effect on motility and viability of human spermatozoa. However, extensive *in vitro* studies related to the effects of AgNPs on sperm parameters, sperm fertilizing ability during *in vitro* fertilization (IVF) of oocytes, as well as subsequent development of embryos are limited and not yet been studied. Discrepancies between the results obtained from *in vivo* and *in vitro* research might be explained by the mismatch between the ‘defined’ environments of an *in vitro* set up versus the ‘uncontrollable’ *in vivo* environment. More specifically, mechanisms of AgNP trafficking and uptake, compensating mechanisms of the surrounding tissues, or other potential confounders might be responsible factors explaining differences between *in vivo* and *in vitro* data.

So far, the researchers focused on the AgNPs binding or internalization into sperm cells and its dose dependent cytotoxic effects in spermatozoa before IVF, but the present study is the first to investigate the effects of AgNPs-exposed sperm on subsequent IVF- or ICSI-derived embryo development. Therefore, the objectives of this study were to: (i) determine the cytotoxic effect of AgNPs on spermatozoa; (ii) evaluate the effect of AgNPs on sperm acrosome reaction; (iii) assess the effect of AgNPs on sperm fertilizing ability during *in vitro* fertilization (IVF) of oocytes and embryo development; (iv) understand the role of AgNPs on cell proliferation in blastocysts; and (v) explore the effect of AgNPs on inner cell mass (ICM) and trophoctoderm cell (TE) specific gene expression in blastocysts.

3.3 Materials and methods

3.3.1 Animal

Male and female BDF1 mice (8-12 weeks old) were housed in wire cages at $22^{\circ}\text{C} \pm 1^{\circ}\text{C}$ with 70% humidity under a 12/12 h light–dark cycle. Mice had access to food and water *ad libitum*. These BDF1 mice are cross between female C57BL/6 and male DBA/2 mice. They are small in size, have short life cycle and easy to take care. Importantly, they are reposed on hormone injection during super ovulation and produce large number of oocytes. That is why we used BDF1 mice in our present study. This study was carried out in strict accordance with the recommendations in the Guide for the Care and Use of the Konkuk University Animal Care and Experimentation Community. The protocol was approved by the Committee on the Ethics of Animal Experiments of the Konkuk University (IACUC approval number: KU11035). All surgeries were performed under sodium pentobarbital anesthesia, and all efforts were made to minimize suffering.

3.3.2 Materials

AgNPs were obtained from Nano High Tech (South Korea) as a clear colloidal aqueous suspension with a concentration of 1000 PPM (or mg/l). AgNPs were dissolved in a modified Whitten's medium (or capacitation medium, CP media) (118.5mM NaCl, 4.7mM KCl, 1.18mM KH_2PO_4 , 2.54mM CaCl_2 , 1.18mM MgSO_4 , 24.9mM NaHCO_3 , 5.56mM Glucose, and 3mg/mL BSA) or non-capacitation (NCP, without BSA) and prepared in a final concentration of 0.1, 1, 10, and 50 $\mu\text{g}/\text{mL}$ just before treatment. NaCl, KCl, KH_2PO_4 , CaCl_2 , MgSO_4 , NaHCO_3 , Glucose and BSA were purchased from Sigma-Aldrich (St. Louis, MO, USA).

3.3.3 AgNPs characterizations

AgNPs were primarily characterized by UV-visible spectroscopy. Ultraviolet-visible (UV-vis) spectra were obtained using WPA (Mechasys, south korea). The particle size distribution analysis was carried out by using dynamic light scattering (DLS) measured by Zetasizer Nano ZS90 (Malvern Instruments, Ltd., UK). X-ray diffraction (XRD) analyses were carried out on an X-ray diffractometer (Bruker D8 DISCOVER, Bruker AXS GmbH, Karlsruhe, Germany). A Transmission electron microscopy (TEM, JEM-1200EX) was used to determine the size and shape of AgNPs.

3.3.4 Spermatozoa preparation and AgNPs treatment

Spermatozoa derived from the ampulla of the vas deferens of male BDF1 mice (8-12 weeks old) mice. The ampulla was dissected with scissors, and then squeezed by compression of forceps. The fluid was rapidly collected and gently suspended in 200 μ l of a modified Whitten's medium (or capacitation medium, CP media) containing 3 mg/mL BSA. After that, the suspension was incubated at 37°C under humidified atmosphere of 5% CO₂ in air for 30 min. Spermatozoa solution was placed in the bottom of a 5 ml snap tube containing 1 ml of modified Whitten's medium and incubated at 37°C under humidified atmosphere of 5% CO₂ in air for 30 min to allow live spermatozoa to swim up. The spermatozoa suspension (800 μ l) was collected from the top of the tube and centrifuged at 3000 rpm for 5 min. The pellets were re-suspended in modified Whitten's medium for adjusting the concentration of spermatozoa before incubation with different concentration of AgNPs. Ten microliter of spermatozoa suspension (2×10^4 cells/ μ l) were dropped into pre-warmed modified Whitten's medium or non-capacitation medium (NCP)

containing 0.1, 1, 10, and 50 $\mu\text{g/mL}$ AgNPs and incubated at 37°C under humidified atmosphere of 5% CO_2 in air for 3h. In the *N*-acetyl-L-cysteine (NAC) pre-treated group, the sperm were first treated with 5 mM NAC for 30 min and followed by AgNPs- treatment with different doses for additional 3 h.

3.3.5 Sperm morphology analysis

The samples were diluted by a factor of 10 in a buffered formal saline solution (34.72mM Na_2HPO_4 , 18.68mM KH_2PO_4 , 92.4mM NaCl , 4% (v/v) formaldehyde) and examined by wet preparations and observed by phase contrast microscopy (Mathias et al., 2014). A minimum of 100 spermatozoa were used for each experiments. Three independent experiments were done for evaluating morphology and classified into 5 categories: normal morphology, detached head, coiled tail, roll tail, and bent tails.

3.3.6 ROS assay

After treatment sperm cells were incubated with 10 μM 2',7'-dichlorodihydrofluorescein diacetate (DCFH-DA; Sigma-Aldrich, D6883) at 37°C for 30 min in modified Whitten's medium and washed with PBS. DCFH-DA-positive cell populations were identified using a FACSCalibur cell analyzer (Becton Dickinson, Franklin Lakes, NJ, USA).

3.3.7 Dead and living analysis of spermatozoa

The number of the dead and living of spermatozoa were assessed by using a LIVE/DEAD Sperm Viability Kit (Molecular Probes). Briefly, the samples were incubated with 100 nM of SYBR 14 dye at 37°C under humidified atmosphere of

5% CO₂ in air for 10 min in a dark, and then incubated with 12μM of Propidium Iodide (PI) for 5 min. After that, the samples were analyzed by fluorescence microscopy and flow cytometer. For fluorescence microscopy, the stained spermatozoa were placed on a microscope slide coated with 0.1% poly-D-lysine (Sigma) and covered with a cover glass. The spermatozoa showing a bright green fluorescence were considered to be alive while spermatozoa with red fluorescence were rated as dead. Dead or living of spermatozoa was calculated by the following formula: (number of dead or live spermatozoa×100) / number of total sperm count. Moreover, Dead or living of spermatozoa was confirmed by using flow cytometer. Briefly, quantitative data on the fluorescently stained sperm populations were collected through EPICS PROFILE II (Coulter Corporation). The Profile II uses an air-cooled argon ion laser emitter which was equipped with the PowerPak option that provided for detection of the side and forward light scatter parameters. Gates were set for the side and forward light scatter parameters so that only those cells possessing the light scatter characteristics of spermatozoa were analyzed for fluorescence intensity. The green fluorescence that passed through a 525-nm band pass filter was collected as the log of green fluorescence 1 (FL1). The red fluorescence parameter was operated as fluorescence 2 (FL2), through 575-nm band-pass filters. Compensation (30%) was used to minimize spillover of green fluorescence into the 575-nm red channel. The adjustment does not change the number of spermatozoa that reside within any given population. For each sample, a total of 10,000 spermatozoa per sample were analyzed for the log of their fluorescence for each sample. The generated data were then analyzed for the relative fluorescence of the LFL1 and LFL2 using the Coulter Histogram Analysis program.

3.3.8 Sperm acrosome reaction analysis

Sperm cells were washed two times by centrifuging at 3000 rpm for 5 min. The samples were fixed with 2% paraformaldehyde for 10 min at room temperature and washed two times. After that, the samples were incubated in PBS containing 1% BSA to block nonspecific sites for overnight, followed by washing the blocker off with PBS. The pellet was suspended in PBS and divided into two aliquots. To 1 aliquot 1:50 diluted mouse anti-CD46 was added and incubated at 4°C for 30 min, followed by washing with PBS two times. Then, the pellet was resuspended with secondary antibody (1:200) and incubated in dark for 30 min. After washing, spermatozoa were placed on a microscope slide coated with 0.1% poly-D-lysine and covered with a cover glass, observed by fluorescence microscope. The other aliquoted samples were then analyzed by flowcytometric analysis (FACS) as described previously. The generated data were then analyzed for the relative fluorescence of the LFL1 and cell number using the Coulter Histogram Analysis program.

3.3.9 Scanning electron microscope (SEM) and transmission electron microscope (TEM) analyses

For SEM analysis, AgNP-treated sperms were fixed in 2.5% paraformaldehyde-glutaraldehyde (4°C, phosphate buffer, pH 7.4) for 2 h and then post-fixed in 1% OsO₄ (4°C, phosphate buffer) for 2 h. Samples were rinsed with PBS to remove the fixative. Fixed sperm cells were dehydrated in EtOH (70%>80%>90%>95%>100%). Sperm cells were then dried in critical point dryer (Hitachi SCP-II) and coated with gold using IB-5 ion coater (Eiko) and observed under SEM (S-4700, Hitachi, Japan, 15kV). Backscattered electron images in the

SEM display compositional contrast that results from different atomic number elements and their distribution. Energy Dispersive Spectroscopy (EDS) allows one to identify what those particular elements are and their relative proportions (Atomic % for example).

For TEM analysis, sperm cells were fixed, washed and then dehydrated in EtOH like before. After that, sperm cells were embedded in Epon-Araldite mix solution and made block in 60°C in vacuum drying oven (Yamato, DPF-31) for 36 h. Firstly semi-thin slides were made by ultra-microtome (LKB-2088) and stained with 1% toluidine blue (1% borax) at 60°C hot plate for 2 min. After that to observe micro-structure in sperm cell, we made ultra-thin slide and stained with uranyl acetate and lead citrate. Examination of sections was performed with a transmission electron microscope operation at 100 kV.

3.3.10 *In vitro* fertilization (IVF)

Female BDF1 mice (6-8 weeks) were superovulated by intraperitoneal injection of pregnant mare's serum gonadotropin, PMSG (10 units). After 48 h, they were injected by human chorionic gonadotropin, hCG (10 units). Metaphase II (MII) oocytes with cumulus cells were collected from the oviductal ampulla 12-14 h after hCG injection, and then placed in a 50 µL drop of a modified Whitten's medium covered with mineral oil. MII oocytes were incubated in modified Whitten's medium at 37°C under humidified atmosphere of 5% CO₂ in air at least 1 h before co-incubation with sperm treated. Spermatozoa derived from each AgNPs treatment were washed by centrifugation with 3000 rpm for 5 min two times. Then, spermatozoa pellets were resuspended with 50 µL of modified Whitten's medium and mixed with the above 50µL drop of modified Whitten's medium. The oocytes were

counted and divided into groups equally. After that, the spermatozoa and oocytes were co-incubated with modified Whitten's medium at 37°C under humidified atmosphere of 5% CO₂ in air for 6 h. Finally, zygotes were washed and cultured in KSOM medium at 37°C under humidified atmosphere of 5% CO₂ in air for 96 h.

3.3.11 Intracytoplasmic sperm injection (ICSI)

To make spermatozoa was completely dead; spermatozoa were treated with 50 µg/mL AgNPs for 6 h in high dose for 6h. Spermatozoa were then suspended in 50 µL of 7 %PVP medium, in a 90 mm culture dish covered with oil. A piezo micromanipulator (PMAS-CT150; Prime Tech, Ibaraki, Japan) was connected with inverted microscope (IX71; Olympus, Tokyo, Japan). The blunt tip of the ICSI-piezo pipette with 7 to 8 µm inner diameter was used to draw spermatozoa. The oocytes were transferred to ICSI dish with CZB-H medium drop. The holding pipette was connected with the micromanipulator (Narishige, Tokyo, Japan) used to hold oocyte. the oocyte was rotated with 1st polar body at the 6 or 12 O'clock position using the blunt tip of the ICSI-piezo pipette. The spermatozoa heads were sucked into the ICSI-piezo pipette, and then the blunt-end of the ICSI-piezo pipette was used to cut the zona pellucida by using intensity and frequency of piezopulse about 2-3. The blunt-end of the ICSI-piezo pipette was pushed through the zona pellucida. The plasma membrane was penetrated by switching on the piezo set up and applying one piezo pulse with intensity and frequency equal to 1. Only one spermatozoa was injected into the cytoplasm and then the ICSI-piezo pipette was gently pulled out from the oocyte. This procedure was repeated until all spermatozoa heads in the pipette were injected. The injected oocytes were remained in the ICSI dish for 10 min at

room temperature and then transferred to KSOM culture medium for culturing at 37°C under humidified atmosphere of 5% CO₂ in air for 96 h.

3.3.12 Inner cell mass (ICM) and trophectoderm cell (TE) analysis

At 96 h after IVC, the blastocysts were collected and washed in PBS containing 1% BSA. The blastocysts were then fixed in 4% paraformaldehyde for 40 min at room temperature. After that, the blastocysts were washed twice in 1% BSA in PBS. The embryos were incubated in 1% BSA and 0.1% Triton-X 100 in PBS for overnight at 4°C. The blastocysts were washed twice in 1% BSA in PBS (15 min each time) and incubated with rabbit anti-OCT4 and mouse anti-CDX2 (1:50) (1:100) for 1h at room temperature. After incubation in primary antibody, samples were washed with 1% BSA in PBS for 3 times (15 min each time). Then, samples were incubated with secondary antibody (1:200) in dark for 1h at room temperature. After incubation, samples were washed three times and mounted on slide, observed with fluorescence microscope. The expressions of OCT4 and CDX2 in blastocyst were used to determine ICM and TE cell respectively.

3.3.13 Gene expression analysis

Fifteen blastocysts derived from each treatment were collected at 96 h after fertilization. The blastocysts were washed with diethylpyrocarbonate (DEPC) water. After that, blastocysts were collected into 5 µl of DEPC water, and kept at -80°C. For total mRNA extraction, the mRNA from collected blastocysts was extracted by freezing in LN₂ and thawing in water (37°C) for 5 times. cDNA was synthesized by Reverse Transcription Kit (Roche) in a final volume of 20 µL following manufacturer's instructions. The quantification of all gene transcripts (sex determining region Y-box 2; *SOX2*, POU class 5 homeobox1; *POU5F1*, Kruppel-like

factor 4; *KLF4*, Eomesodermin; *EOMES*, caudal type homeobox 2; *CDX2*, and keratin 8; *KRT8*) was approved out in three replicates by quantitative real-time RT-PCR on Lightcycler apparatus using Lightcycler®FastStart DNA Master SYBR Green I via AB applied biosystems machine. The primer sequences for each gene were shown in Table 3.1. The reaction mixture of total 10 µL volume consisted of 5 µL of Lightcycler®FastStart DNA Master SYBR Green I, 0.5 µl of each primer (10 µM), 1 µL of cDNA template and 3 µL of nuclease free water. The PCR program was as follows: denaturation (95°C for 10 min), amplification and quantification repeated 45 times (95°C for 10 sec, 55-60°C for 30 sec, and 72°C for 30 sec with a single fluorescent measurement), melting curve analysis (65-95°C, with a heating rate 0.2°C/sec and continuous fluorescence measurement) and final cooling to 12°C. The relative quantification of gene expression was analyzed by the 2-ddCt method. In all experiment, GAPDH mRNA was used as an internal standard.

3.3.14 Mitochondrial DNA copy number analysis

For quantification of mitochondrial DNA (mtDNA), essentially the same protocol was used as for qPCR, with 20 ng total DNA used as template, and normalization of cytochrome b (*CYTB*) (forward primer, ATTGACCTACCTGCC CCATC; reverse primer, CTCGTCCGACATGAAGGAAT) amplification level against the nuclear β-actin (forward primer, TCGCCATGGATGACGATA; reverse primer, CACGATGGAGGGGAATACAG) gene.

Table 3.1 Primers sets used for real-time qRT-PCR.

| Primer name | Primer sequence | Annealing (°C) | Size (bp) |
|--------------------|---|-----------------------|------------------|
| <i>GAPDH</i> | F: AGGTCGGTGTGAACGGATTTG R: TGTAGACCATGTAGTTGAGGTCA | 57 | 123 |
| <i>Pou5fl</i> | F: CTCCCTACAGCAGATCACTCACA R: AACCATACTCGAACCACATCCT | 63 | 220 |
| <i>Sox2</i> | F: CACAACCTCGGAGATCAGCAA R: CTCCGGGAAGCGTGTACTTA | 60 | 190 |
| <i>Klf4</i> | F: CTGAACAGCAGGGACTGTCA R: GTGTGGGTGGCTGTTCTTTT | 58 | 218 |
| <i>Cdx2</i> | F: AGACAAATACCGGGTGGTGTA R: CCAGCTCACTTTTCCTCCTGA | 60 | 153 |
| <i>Eomes</i> | F: GAGCTTCAACATAAACGGACTCAA R: CGGCCAGAACCACTTCCA | 60 | 210 |
| <i>Krt8</i> | F: ATCGAGATCACACCTACCG R: TGAAGCCAGGGCTAGTGAGT | 63 | 151 |

3.3.15 Statistical analysis

All the experiments were performed at least in triplicate, and statistical analyses were performed. Figures show representative experiments. For statistical analysis, one-way analysis of variance (ANOVA) was performed to determine whether there were differences within the groups ($P < 0.01$), and Dunnett's *t*-test was performed to determine the significance of difference between the treatment and

control group. Statistical tests were performed using Stat View version 5.0 (SAS institute, Cary, NC, USA).

3.4 Results

3.4.1 Characterization of AgNPs

The diameter and morphology of AgNPs, shown in Figure 3.1A and 3.1B, were analyzed by transmission electron microscopy (TEM). The representative TEM image indicated well-dispersed particles that were more or less spherical. We measured the size of more than 300 particles and the size-distribution is represented in Figure 3.1B. Although the average size was 40 nm, the AgNPs colloidal suspension contained different sized particles having diameter range mostly between 34 nm to 46 nm. Therefore, we actually used the AgNPs having particles diameter ranging from 34 nm to 46 nm (with average diameter of 40 nm) in our present study. We also measured the size of AgNPs by dynamic light scattering (DLS) and the size distribution is depicted in Figure 3.1C. It was found that the average diameter of AgNPs analyzed by DLS was approximately 61.51 nm (Figure 1C). Further, AgNPs were characterized by ultraviolet (UV)-visible spectroscopy and X-ray diffraction (XRD). The UV-visible absorption spectra were measured in the range of 350-600 nm. The UV-visible spectra showed a strong and broad surface peak located at 420 nm (Figure3. 1D). The XRD pattern of AgNPs is shown in Figure3.1E. We obtained five peaks at 2θ values of 38.2, 44.4, 64.5, 77.3 and 81.5° corresponded to Bragg's reflections from the (111), (200) (220), (311) and (222) planes respectively. The XRD results clearly showed that the AgNPs are crystalline in nature.

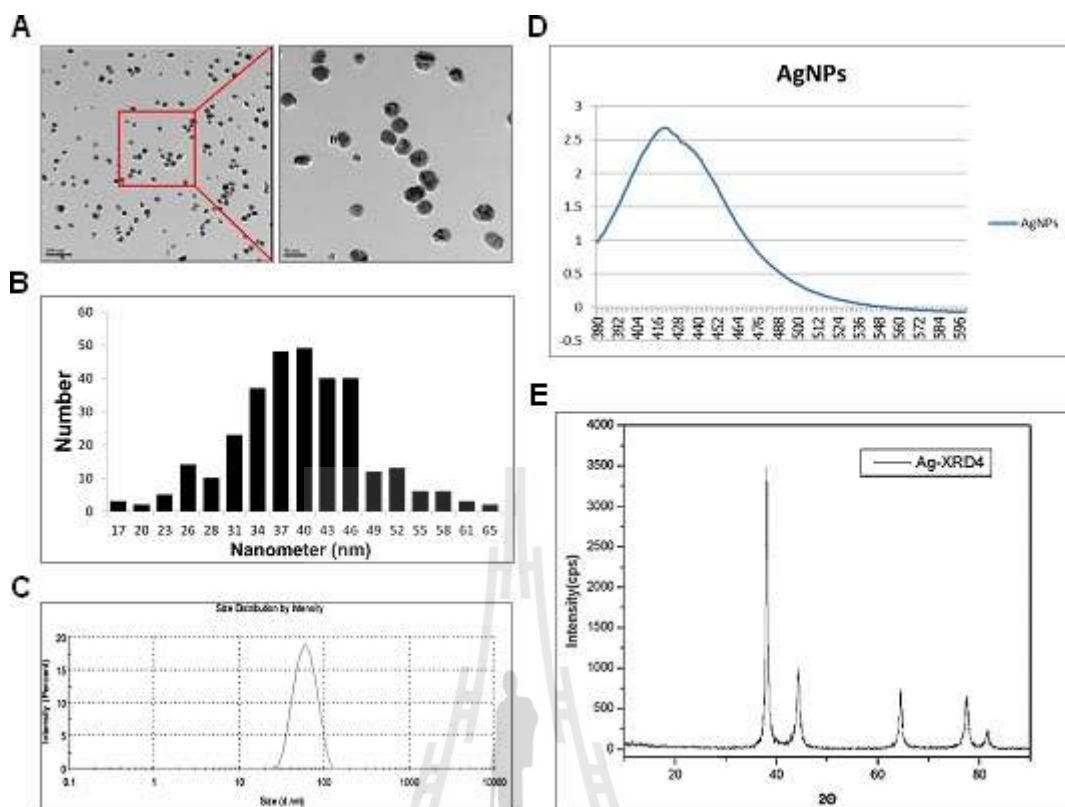


Figure 3.1 The characterizations of AgNPs. A) diameter and morphology of AgNPs analysis by TEM. B) Several fields were photographed and were used to determine the diameter of nanoparticles. The average range of observed diameter was 40 nm. C) Size distribution analysis by DLS. D) The absorption spectrum of AgNPs. The absorption spectrum of AgNPs exhibited a strong broad peak at 420 nm, and observation of such a band is assigned to surface plasmon resonance of the particles. The samples were visualized in UV-vis spectra. E) XRD pattern of AgNPs.

3.4.2 Internalization of AgNPs in spermatozoa

Energy dispersive spectroscopy (EDS) profiling of sperm cells showed a weak signal for Ag along with weak signals of Cl, whereas we did not observe Ag in

any of the control-treated spermatozoa (Figure 3.2A). On the basis of these findings, we examined AgNP binding on spermatozoa using scanning electron microscopy (SEM). As shown in Figure 3.2C–G, we found that AgNPs cluster on the midpiece or head of spermatozoa. SEM images of AgNPs indicated that they were more or less spherical in shape. Of note, EDS profiling of a sperm head showed a mild Ag signal (Figure 3.2G), indicating that AgNPs were localized on the sperm head (Figure 3.2F).

Next, we examined whether the 40 nm AgNPs had the ability to internalize into spermatozoa using TEM. Since AgNPs have high atomic numbers, it is possible to distinguish them from cellular structures using TEM. As the AgNP dosage increased, internalization of AgNPs became more obvious inside the spermatozoa head from sperm plasma membrane and evenly dispersed in the sperm head and midpiece including the mitochondrial area (Figure 3.2I, J, and L). The degree of AgNP internalization was clearly dose-dependent in the studied concentration range of 0.1 $\mu\text{g}/\text{mL}$ to 50 $\mu\text{g}/\text{mL}$: at low dosages, AgNPs mainly localized on the sperm plasma membrane (Figure 3.2I and K; Figure 3.3 and 3.4), whereas with increasing dosage, AgNPs were internalized into the head and mitochondrial area of the spermatozoa (Figure 3.2J, L, and M).

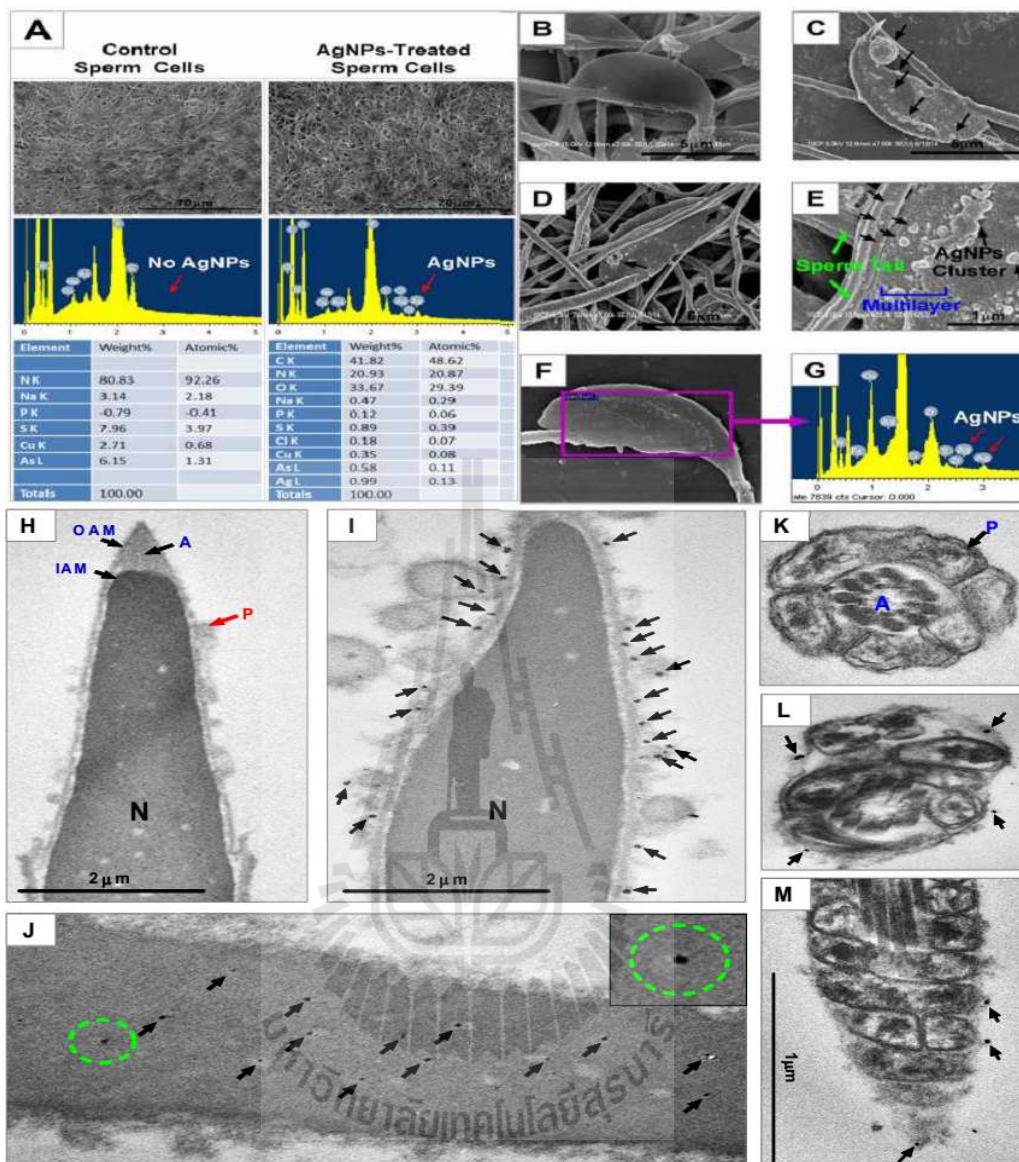


Figure 3.2 SEM and TEM analysis of AgNP-treated sperms. SEM-EDS analysis: A) Sperm cells were co-cultured with or without AgNPs for 3 h. AgNPs were detected in the AgNP-treated group but not in the control. Energy dispersive spectroscopy (EDS) analysis showed an Ag peak only in AgNP-treated group (red arrow) and contained 0.03% Ag among all atomic masses. B) A representative SEM figure of a control sperm cell. B, D, E) AgNP detection in AgNP-treated sperm cells: AgNP cluster covered the head and tails of sperm cells. F and G) Identification of

AgNPs in sperm cells using EDS. Arrows indicate the AgNP peak. TEM analysis: H) Control sperm cell. I and J) AgNPs were bound to the plasma membrane (I) or internalized into the head (J) of sperm cells. Open circle of (J) was magnified in the lower panel of (J). Of note, AgNP internalization caved in the sperm head. K) Control mitochondria. L and M) Detection of AgNP in mitochondria. Arrows indicate AgNPs. Note, due to internalization or binding of AgNPs, the sperm cell mitochondria and axoneme were severely disorganized and/or distorted. P, A, OAM, and IAM indicate the plasma membrane, acrosome, outer acrosome membrane, and inner acrosome membrane, respectively.

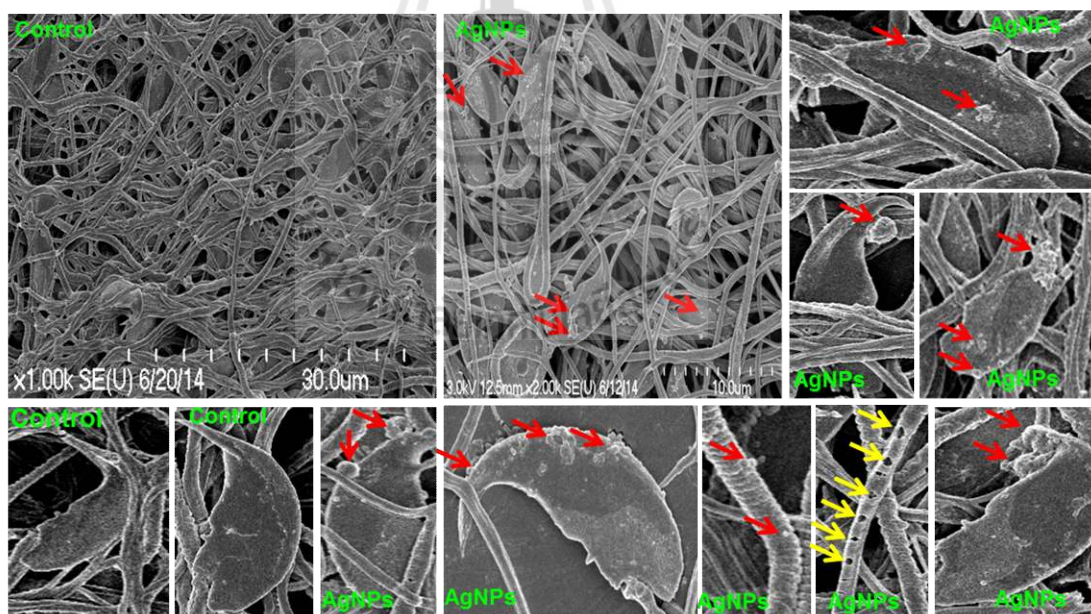


Figure 3.3 Localization of AgNPs in sperm cells by SEM. Sperm cells were co-cultured with or without AgNPs (1, 10 and 50g/mL) for 3 h. AgNPs were detected in the AgNP-treated group (indicated by arrows) but not in the control. AgNPs-1, 10, and 50 indicate sperm cells treated with 1, 10 and 50g/mL dosage of AgNPs, respectively.

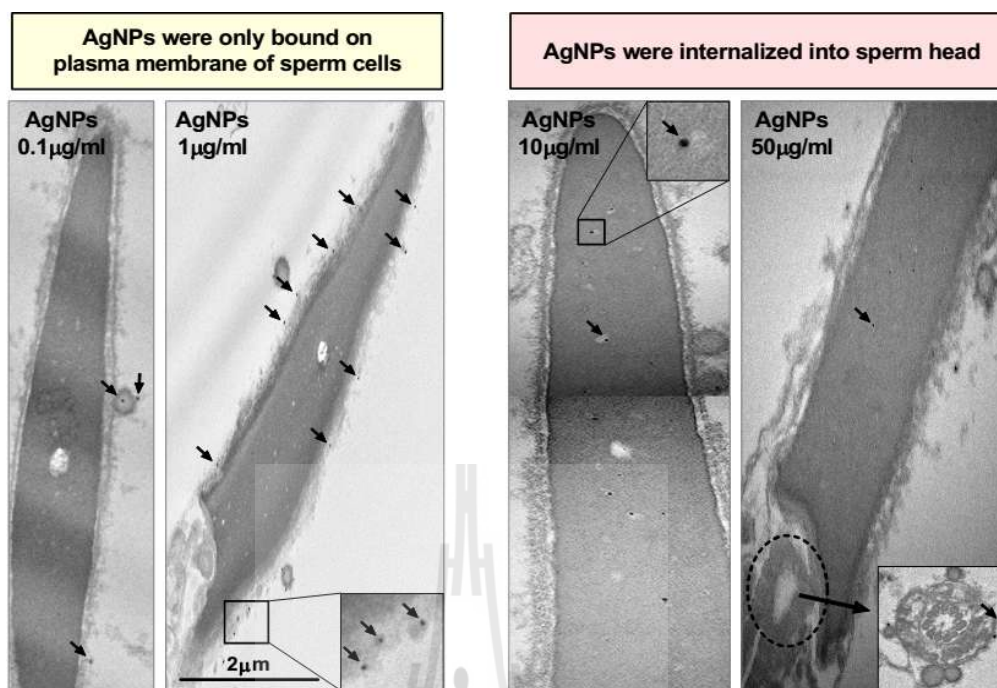


Figure 3.4 Localization of AgNPs in sperm cells by TEM. Sperm cells were co-cultured with AgNPs (0.1, 1, 10 and 50g/mL) for 3 h. Arrows indicate AgNPs inside sperms. At low dosages, AgNPs mainly localized on the sperm plasma membrane, whereas with increasing dosage, AgNPs were internalized into the head of the spermatozoa.

3.4.3 Mitochondrial DNA copy number and reactive oxygen species analysis in AgNPs-treated spermatozoa

After co-incubation with AgNPs for 3 h, the AgNP-treated spermatozoa and control sperm cells were subjected to TEM for mitochondrial abnormality analysis and real-time quantitative polymerase chain reaction (qPCR) for determination of mitochondrial DNA (mtDNA) copy number. As shown in Figure 3.5A (AgNP-treated group, lower panel), most of the mitochondria derived from the AgNP-treated spermatozoa were swollen, whereas control-derived spermatozoa were regular in shape. Axoneme and longitudinal fiber microtubules

in different tail regions of many sperm cells were degenerated and had lost their architectural appearance. Completely distorted mitochondrial cristae were also observed in the midpieces of many sperm. Next, we examined mtDNA copy number. To estimate relative mtDNA copy number, we used real-time qPCR to amplify cytochrome b (Cytb) in mtDNA and actin beta (ACTB) in nuclear DNA. The mtDNA/ACTB ratio, which represents the average copy number per sperm cell, was determined in the 3 different samples. We found that AgNPs-treated sperm cells showed increased mtDNA copy number with increasing dose (correlation coefficient, $r = 0.991$) (Figure 3.5B). In order to investigate the relationship between AgNPs-induced reactive oxygen species (ROS) formation and subsequent mitochondrial abnormalities in spermatozoa, the spermatozoa were pre-treated with *N*-acetyl-L-cysteine (NAC) followed by AgNPs intoxication, because NAC is a well-known ROS scavenger. NAC pre-treatment for 30 min reduced the AgNPs-induced increased mtDNA copy number in spermatozoa. This observation suggested that mtDNA copy number appeared to be closely associated with AgNPs-induced oxidative stress.

To examine the relationship between the increased mitochondrial damage induced by AgNPs and oxidative stress, reactive oxygen species (ROS) formation was quantified in spermatozoa exposed to AgNPs with or without NAC. As shown in Figure 3.5C, 3.5D, flow cytometry analysis showed that AgNP exposure significantly enhanced dichlorofluorescein (DCF)-positive signals in spermatozoa in a dose-dependent manner (correlation coefficient, $r = 0.989$). However, NAC pre-exposure reduced the percentage of DCF-positive sperm cells, indicating that ROS generation was reduced. These results were confirmed by fluorescence microscopy. Consistently, ROS generation induced by AgNPs results in high FITC fluorescence intensity (Figure 3.6), whereas pre-exposure to NAC inhibited AgNPs-induced ROS production.

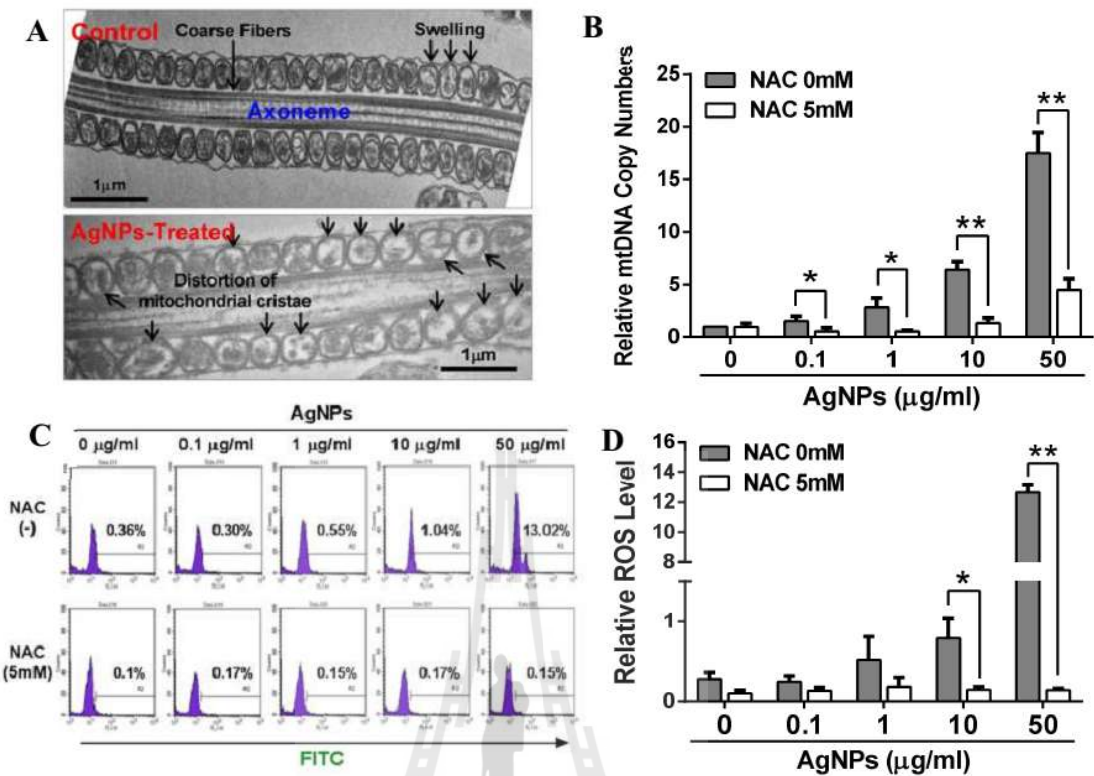


Figure 3.5 Mitochondrial damage and ROS analysis in AgNP-treated sperm cells. A) The mitochondrial sheath in control and AgNP-treated sperm cells was analyzed using TEM. Arrows indicate swelling of mitochondria in the mitochondrial sheath. B) Determination of mitochondrial copy number in AgNP-exposed sperms in presence or absence of NAC pretreatment. The mtDNA/ACTB ratio, which represents the average copy number per sperm cell, was determined by qPCR. C) and D) ROS in NAC-pretreated or untreated sperm cells after exposure to AgNPs was analyzed using flow cytometry by staining with DCFH-DA-FITC. Experiments were performed in triplicate; data represent the percentage of the mean of three independent experiments. Error bars represent the standard error of the mean (SEM). * $p < 0.05$ and ** $p < 0.01$ versus the control group (Dunnett's t -tests).

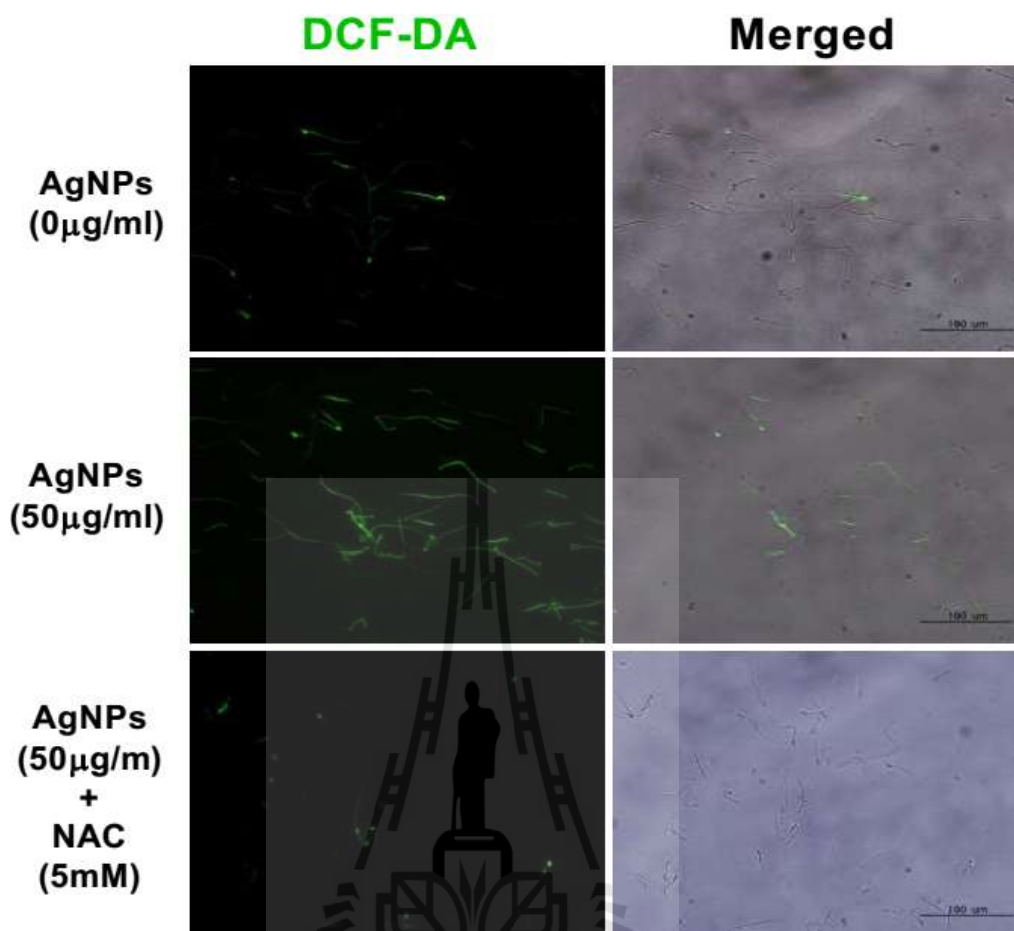


Figure 3.6 Localization of AgNPs in sperm cells by TEM. Sperm cells were co-cultured with AgNPs (0.1, 1, 10 and 50g/mL) for 3 h. Arrows indicate AgNPs inside sperms. At low dosages, AgNPs mainly localized on the sperm plasma membrane, whereas with increasing dosage, AgNPs were internalized into the head of the spermatozoa.

3.4.4 Effect of AgNPs on sperm morphology and sperm viability

As shown in Figure 3.7, sperm morphology was examined after incubation with different concentrations of AgNPs. In this study, there were 5 characteristics of spermatozoa: normal, detached head, coiled tails, roll tails, and bent tails (Figure 3.7A). We found significant abnormal morphological changes in spermatozoa, such as

coiled tails, roll tails, and bent tails at high concentrations of AgNPs (10 $\mu\text{g}/\text{mL}$ and 50 $\mu\text{g}/\text{mL}$) (Figure 3.7B). These results show that the morphology of spermatozoa was significantly changed after treating with high concentration of AgNPs when compared to control spermatozoa.

The major populations of live spermatozoa that stained with SYBR-14 (green color), dead spermatozoa that stained with propidium iodide (PI; red color), and merged spermatozoa that stained with both green and red (yellow color) are shown in Figure 3.8A. Exposure of spermatozoa to AgNPs had a negative effect on sperm motility as measured by flow cytometry analysis. As shown in Figure 3.8B, incubation of spermatozoa with AgNPs slightly increased the population of dead spermatozoa (correlation coefficient, $r = 0.988$). To confirm these results, sperm viability was checked by counting the number of dead and live spermatozoa, which were stained red and green, respectively. These results showed that only at the highest dose, AgNP exposure increased the percentage of dead spermatozoa, whereas the number of live spermatozoa was decreased (Figure 3.8C). Since silver ion (Ag^+) exposure formed precipitation in the Modified Whitten's medium, we could not examine whether Ag^+ exposure significantly reduced sperm viability. Of note, pre-treatment with NAC for 30 min decreased the AgNP-induced alterations in sperm viability (Figure 3.8C). However, the motility of spermatozoa cultured in non-capacitation (NCP) medium containing different AgNP dosages (0.1, 1, 10, and 50 $\mu\text{g}/\text{mL}$ AgNPs for 3 h) was more significantly decreased than those cultured in capacitation (CP) medium (Figure 3.9).

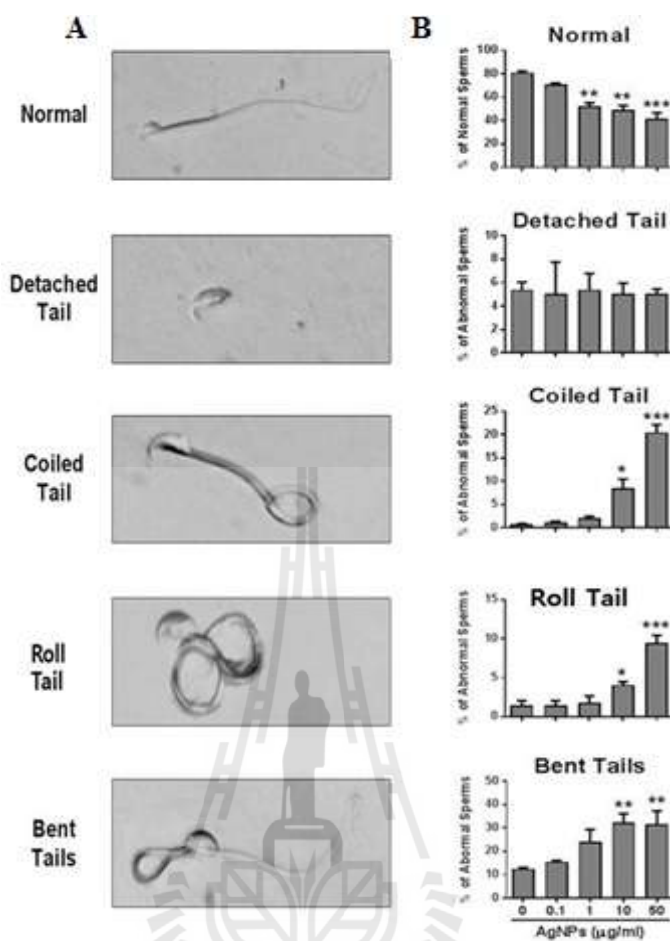


Figure 3.7 Abnormal sperm morphology analysis after treatment with different concentrations of AgNPs. A) A representative sperm morphological pattern, which was observed by phase contrast microscopy. B) A minimum of 100 sperm cells per replicate with three replicates were investigated for morphology analysis and classified into five categories: normal morphology, detached head, coiled tail, roll tails, and bent tails. * $P < 0.05$, ** $P < 0.01$, and *** $P < 0.001$ versus the control group (Dunnett's t -tests).

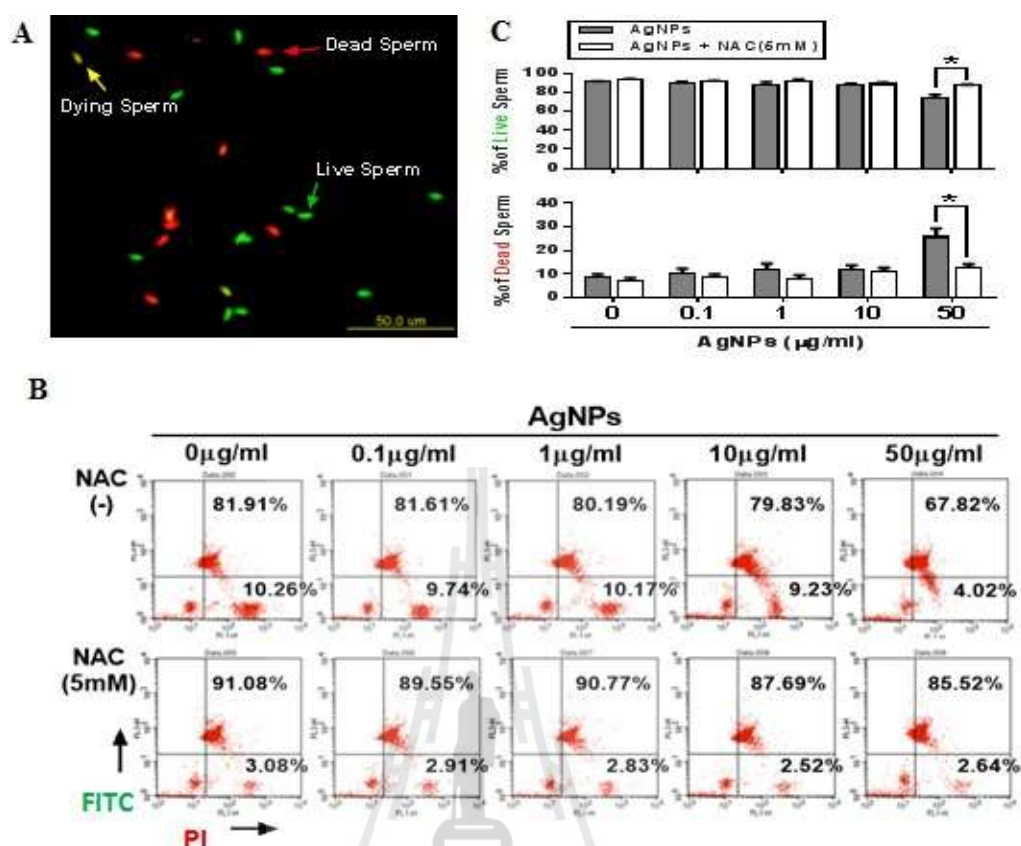


Figure 3.8 Sperm mortality and acrosome reaction analysis. Sperm cells were treated with 0, 0.1, 1, 10, or 50 µg/mL AgNPs. For the ROS inhibitor group, sperm were pretreated with 5 mM NAC for 30 min, and then, 0-50 µg/mL of AgNPs was added. Dead and live sperm cells were counted using the Dead/Live kit. A) Fluorescence microscopy image. Live sperm cells were stained with SYBR 14 dye (green fluorescence), whereas dead sperm cells were stained with propidium iodide (PI; red fluorescence). Yellow color in the merged image indicates dying sperm cells. B and C) Dead and live sperm cells were calculated by flow cytometry: FL1 represents green (living sperm), FL2 represents red (dead). * $P < 0.05$ and *** $P < 0.001$ versus the control group (Dunnett's t -tests). For the acrosome reaction analysis, sperm cells were cultured in capacitation medium with different concentrations of AgNPs for 3 h. D)

A representative immunofluorescence staining pattern obtained using mouse anti-CD46 (green) antibody. Nuclei are counterstained with DAPI (blue). Blue box depicts the magnified image (40×magnification). E and F) Flow cytometry analysis of CD46-positive sperm populations. Data for F) was obtained from the flow cytometry experiment in E). The experiments were performed in triplicate; data represent the mean of three independent experiments. *** $P < 0.001$ versus the control group (Dunnett's t -tests).

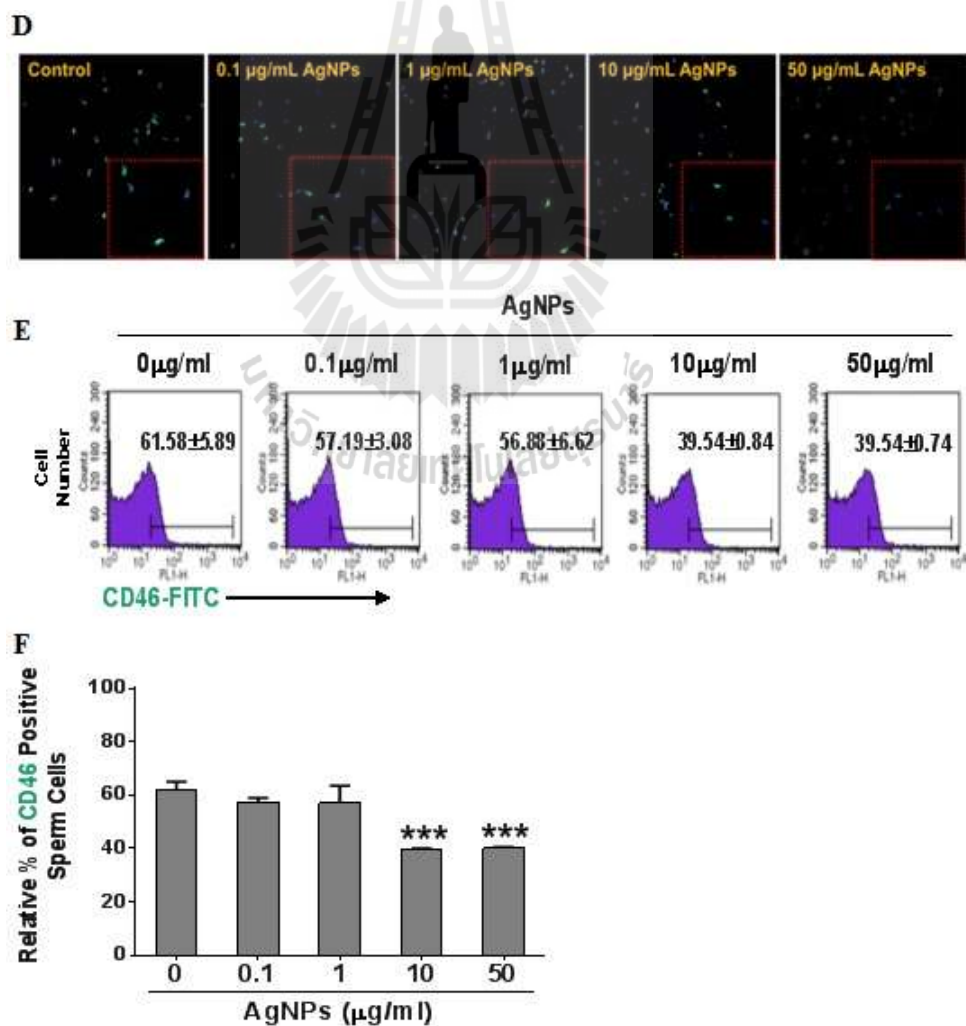


Figure 3.8 (Continued).

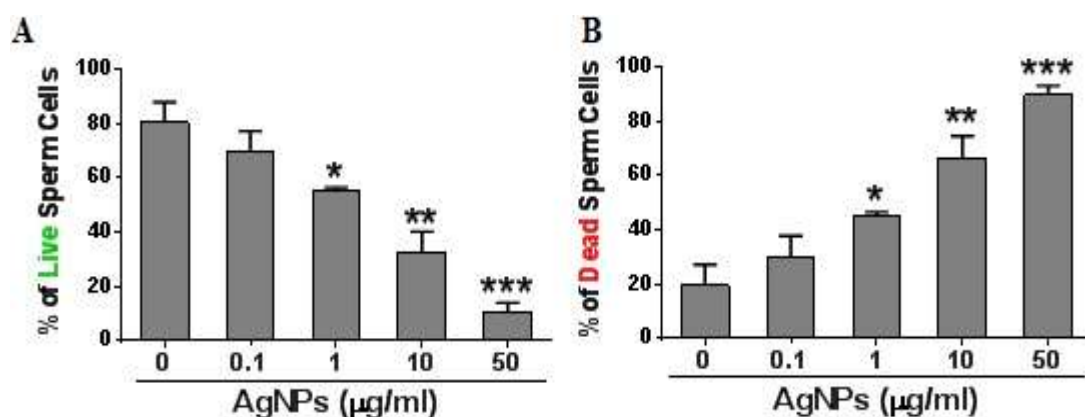


Figure 3.9 Analysis of dead and live sperm cells in non-capacitation medium after AgNP exposure. Sperm cells were cultured in non-capacitation medium with different concentration of AgNPs for 3 h. Dead and live sperm cells were stained using the Dead/Live kit and counted by flow cytometry. * $P < 0.05$, ** $P < 0.01$, *** $P < 0.001$ versus the control group (Dunnett's t -tests).

3.4.5 Impact of AgNPs exposure on acrosome reaction

In this study, spermatozoa undergoing the acrosome reaction were evaluated with the help of CD46-positive signals using immunofluorescence staining (Figure 3.8D). The population of CD46-positive spermatozoa was measured by flow cytometry analysis (Figure 3.8E and 3.8F). AgNP exposure affected the acrosome reaction of spermatozoa, causing significant ($P < 0.001$) reduction of CD46 expression in capacitation medium containing 10 ($39.53\% \pm 0.84\%$) and 50 ($40.08\% \pm 0.74\%$) µg/mL of AgNPs when compared to the control group ($61.58\% \pm 5.89\%$) (Figure 3.8D-F). To further confirm our results, spermatozoa were exposed to different concentrations of AgNPs in NCP medium. Our results suggested that AgNPs did not trigger the acrosome reaction (Figure 3.10 and 3.11), and we found that AgNP

exposure to spermatozoa reduced the acrosome reaction, as evident by decreased proportions of CD46-positive sperm.

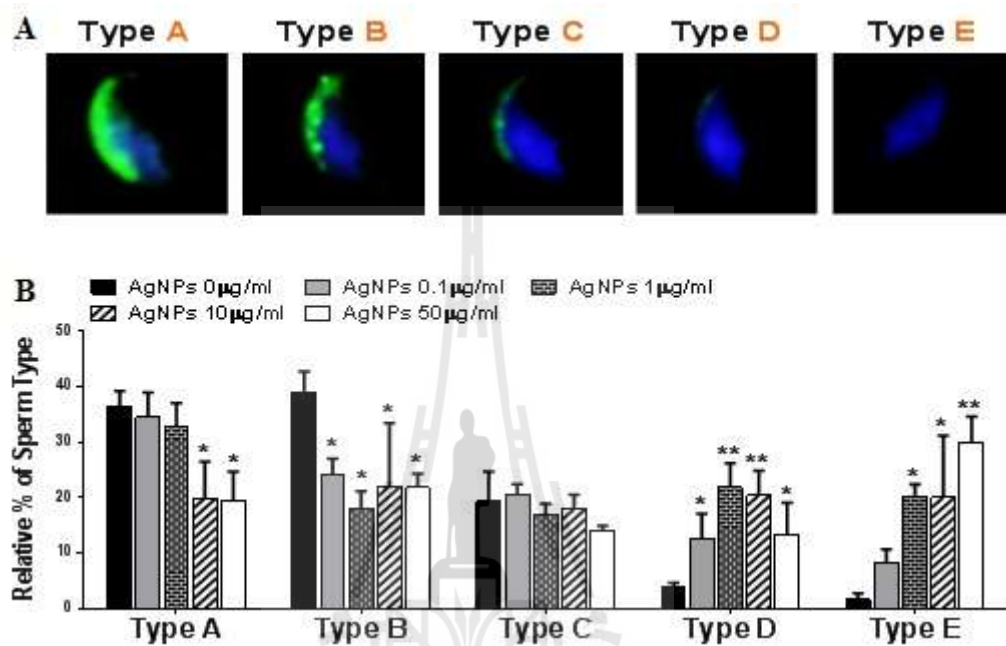


Figure 3.10 Acrosome pattern analyses according to CD46 immunofluorescent staining in sperm cells cultured in non-capacitation medium after incubation with different dosage of AgNPs. A) Representative immunofluorescent staining patterns using mouse anti-CD46 (green). Nuclei are counterstained with DAPI (blue). B) Each immunofluorescent staining pattern was analyzed by using anti-CD46 antibody after treatment with different dosage of AgNPs. * $P < 0.05$ and ** $P < 0.01$ versus the control group (Dunnett's t -tests).

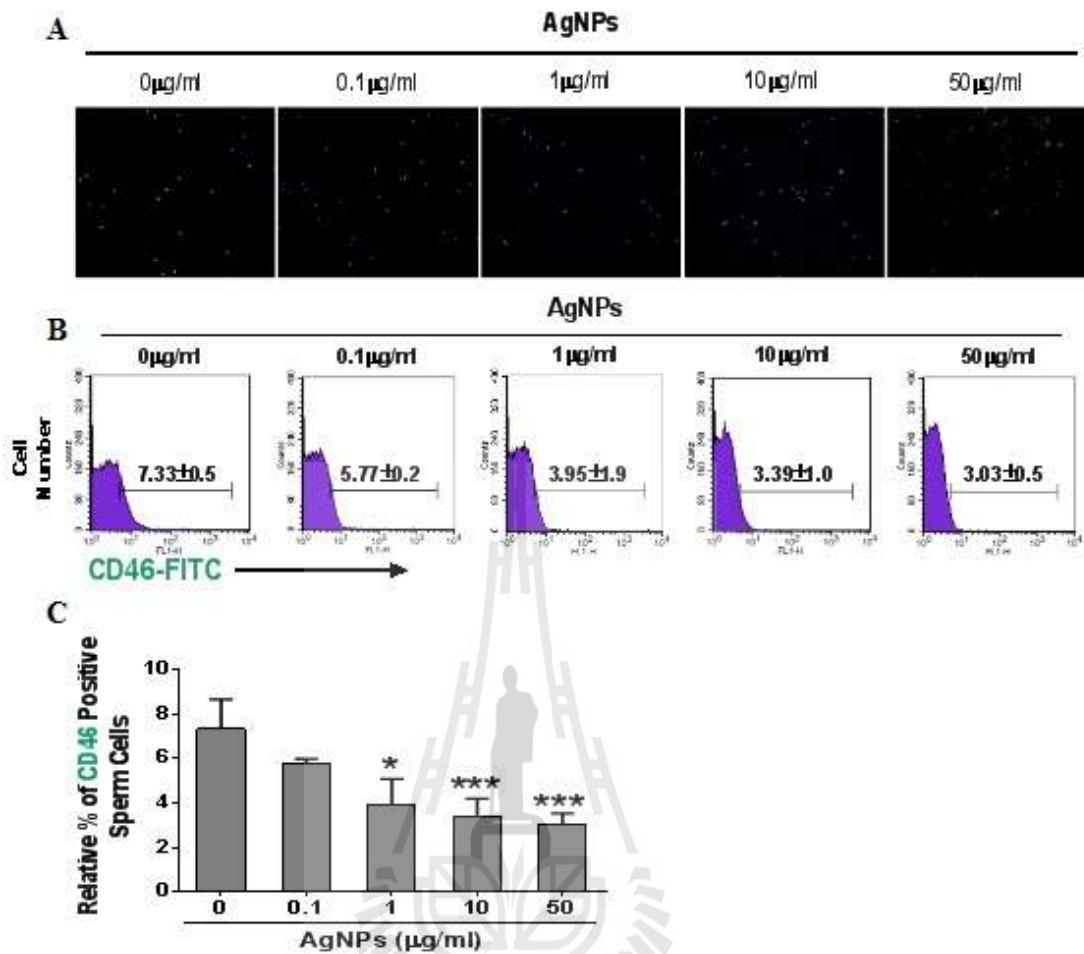


Figure 3.11 Acrosome reaction analysis in sperm cells cultured in non-capacitation medium using flow cytometry. Sperm cells were cultured in non-capacitation medium with different concentration of AgNPs for 3h. A) A representative immunofluorescent staining pattern obtained by using mouse anti-CD46 (green) antibody. Nuclei are counterstained with DAPI (blue). B) and C) Flow cytometry analysis of CD46-positive sperm populations. * $P < 0.05$, ** $P < 0.01$, *** $P < 0.001$ versus the control group (Dunnett's t Tests).

3.4.6 *In vitro* fertilization and *In vitro* culture assessment using living sperm cells after AgNP exposure and subsequent blastocyst quality analysis

Spermatozoa derived from the ampulla of male BDF1 (8–12 weeks old) mice were randomly assigned to the control or AgNP-treated groups. To examine the effect of AgNP exposure on IVF and subsequent embryonic development, spermatozoa were treated with the presence or absence of various concentrations of AgNPs for three hours before IVF. We used an IVF system to evaluate the effect of AgNP on oocyte fertilization and subsequent embryonic development. The percentage of unfertilized oocytes (44.4%, 65.2%, 77.0%) was significantly increased in spermatozoa treated with higher concentrations of AgNPs (1, 10, 50 $\mu\text{g}/\text{mL}$; $p < 0.05$) (Table 3.2). In contrast, the rate of blastocyst formation was significantly decreased by the treatment of spermatozoa with AgNPs in a dose-dependent manner ($p < 0.05$).

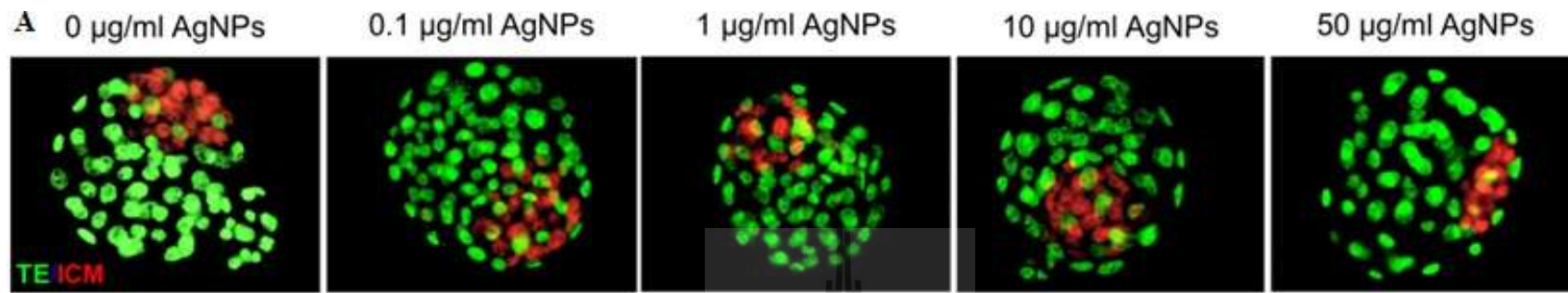
To determine the effects of AgNP-exposed spermatozoa on the quality of embryos, total number of cells, including the inner cell mass (ICM) and trophectoderm (TE) cells, in blastocysts at 96 h after *in vitro* culture (IVC) was determined by counting OCT4- and CDX2-positive signals, respectively (Figure 3.12A). At 96 h after IVC, the total number of cells, ICM, and TE cells in blastocyst stage embryos derived from 1, 10, 50 $\mu\text{g}/\text{mL}$ AgNP-treated living spermatozoa were significantly decreased ($p < 0.01$) compared to control spermatozoa (Figure 3.12B), suggesting that AgNP exposure to sperm cells could reduce both ICM and TE cell numbers. Furthermore, pluripotent marker genes such as *SOX2*, *POU5F1*, and *KLF4* in blastocysts derived from AgNP-exposed spermatozoa showed significantly lower expression with increasing AgNP dosage. Besides, TE-associated genes such as *CDX2*, *EOMES*, and *KRT8* showed significantly lower expression in spermatozoa treated with high concentrations of AgNP (10 and 50 $\mu\text{g}/\text{mL}$) compared to the control group (Figure 3.12C).

Table 3.2 Developmental competence of mouse oocytes fertilized *in vitro* after culture 96 h after insemination.

| Treatment | No. IVF | No. unfertilized (% , ±SE) | No. embryos development to (% , ±SE) | | | | | | | |
|----------------|---------|--------------------------------|--------------------------------------|----------------|----------------|----------------|-----------------|--------------------------------|---------------------------------|---------------------------------|
| | | | 2C | 4C | 8C | Mo | Early BL | BL | Hatching BL | Total BL |
| 0 µg/ml AgNP | 135 | 15 (11.1±4.8) ^c | 15 (11.1±4.0) | 0 (0.0±0.0) | 0 (0.0±0.0) | 3 (2.2±2.1) | 11 (8.1±5.4) | 42 (31.1±2.8) ^a | 49 (36.3±13.8) ^a | 102 (75.5±10.6) ^a |
| 0.1 µg/ml AgNP | 135 | 60 (44.4±10.2) ^b | 23 (17.0±11.5) | 0 (0.0±0.0) | 0 (0.0±0.0) | 3 (2.2±2.0) | 7 (5.2±3.1) | 36 (26.7±6.2) ^{ab} | 31 (23.0±14.9) ^{ab} | 74 (54.8±12.7) ^{ab} |
| 1 µg/ml AgNP | 135 | 60 (44.4±10.2) ^b | 23 (17.0±11.5) | 0 (0.0±0.0) | 2 (1.5±1.5) | 4 (3.0±2.5) | 7 (5.2±1.3) | 24 (17.8±2.4) ^b | 17 (12.6±10.9) ^{ab} | 48 (35.6±13.1) ^{bc} |
| 10 µg/ml AgNP | 135 | 88 (65.2±4.2) ^a | 25 (18.5±1.9) | 0 (0.0±0.0) | 2 (1.5±1.5) | 1 (0.7±0.6) | 8 (5.9±0.9) | 5 (3.7±1.9) ^c | 6 (4.4±4.4) ^b | 19 (14.1±5.1) ^c |
| 50 µg/ml AgNP | 135 | 104 (77.0±4.5) ^a | 17 (12.6±4.2) | 1 (0.7±1.2) | 3 (2.2±1.6) | 1 (0.7±0.4) | 7 (5.2±1.3) | 2 (1.5±1.3) ^c | 0 (0.0±0.0) ^b | 9 (6.7±2.2) ^c |

^{a,b,c} Different superscripts denote significant differences (ANOVA:Duncan's Multiple Range Test, $P<0.05$).

Mo and BL indicate molular and blastocyst, respectivel.



B

| Conc. of AgNPs ($\mu\text{g/ml}$) | No. of Blastocysts | No. of Total Cells (Mean \pm SE) | No. of ICM Cells (Mean \pm SE) | No. of TE Cells (Mean \pm SE) |
|-------------------------------------|--------------------|------------------------------------|----------------------------------|---------------------------------|
| 0 | 15 | 84.5 \pm 3.7 ^a | 20.0 \pm 1.2 ^a | 64.6 \pm 3.2 ^a |
| 0.1 | 14 | 78.7 \pm 3.6 ^{ab} | 17.3 \pm 1.1 ^a | 61.4 \pm 2.9 ^a |
| 1 | 13 | 70.7 \pm 1.9 ^{bc} | 16.5 \pm 1.0 ^{ab} | 54.2 \pm 1.3 ^{ab} |
| 10 | 13 | 60.8 \pm 2.5 ^{cd} | 13.2 \pm 1.2 ^{bc} | 47.7 \pm 1.8 ^{bc} |
| 50 | 8 | 51.6 \pm 2.5 ^d | 10.8 \pm 1.0 ^c | 40.9 \pm 2.8 ^c |

Figure 3.12 Quality analysis of blastocyst stage embryos developed *in vitro* after IVF with AgNP-treated sperm cells. A) A representative blastocyst embryo stained differentially by OCT4 and CDX2 antibodies 96 h after IVF with AgNP-treated sperm cells. OCT4-positive cells (red) are putative inner cell mass (ICM), whereas CDX2-positive cells (green) are putative trophoctoderm. B) Number of total cells, ICM, and TE cells from the blastocyst stage embryos of (A). Different superscripts denote significant differences (ANOVA: Duncan's Multiple Range Test, $P < 0.01$). C) ICM- and TE-specific mRNA

expression analysis in blastocysts developed after IVF with AgNP-treated sperm cells. The expression levels of ICM and TE associated genes were analyzed by real time RT-qPCR. The experiments were performed in triplicate; data represent the mean of three independent experiments. Error bars represent standard error of the mean (SEM). * P <0.05, ** P <0.01, *** P <0.001 versus the control group (Dunnett's t -tests).

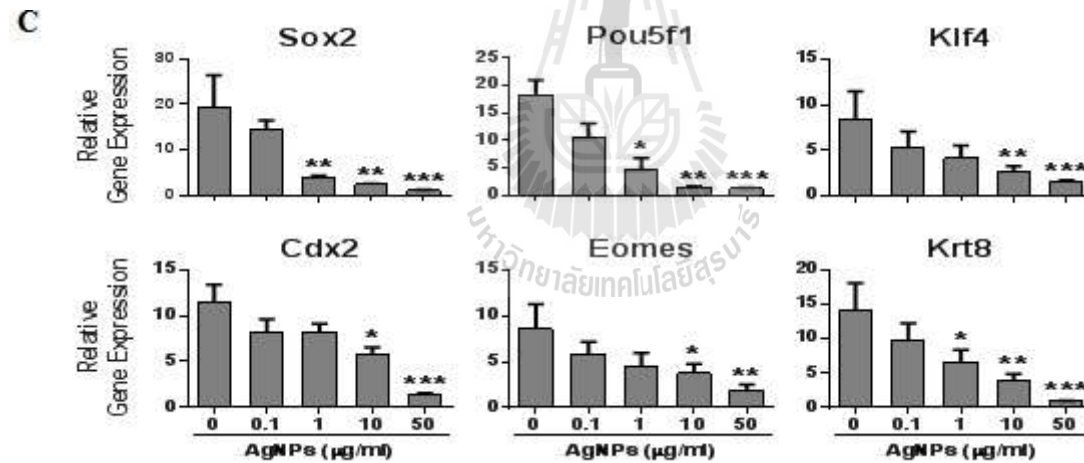


Figure 3.12 (Continued).

3.4.7 ICSI and IVC assessment using dead sperm after AgNP exposure and blastocyst quality analysis

We next compared the oocyte fertilization and subsequent blastocyst development efficiency by injecting the sperm of first grade morphology (dead sperm with normal morphology) and second grade sperm (dead sperm with detached head or coiled tails) separately. Using ICSI, spermatozoa with different morphologies were selected after treatment with different concentrations of AgNPs. Of note, the percentage of fertilized oocytes and subsequent blastocyst development following ICSI were statistically different between first- and second-morphology grade spermatozoa ($p > 0.05$) (Table 3.3). However, the rate of ICSI-derived oocyte fertilization and blastocyst formation using living sperm with normal morphology were significantly higher than those of AgNP-treated dead sperm. Therefore, our study showed that sperm grading due to morphological difference was not correlated to ICSI outcome.

Next, we examined whether dead spermatozoa with abnormal morphology after AgNP exposure would decrease embryo quality. Embryos were produced by ICSI using sperm cells with abnormal morphology after treatment with different dosages of AgNPs. At 96 hours post IVC, the total numbers of ICM and TE cells in blastocyst embryos were calculated by counting OCT4 and CDX2 positive signals, respectively (Figure 3.13A). These results showed that the dead spermatozoa with abnormal morphology (detached head, coiled tail) due to AgNP exposure significantly ($p < 0.01$) reduced both ICM and TE cell numbers (Figure 3.13B). Of note, the dead spermatozoa with normal morphology from AgNP treatment also showed a significant ($p < 0.01$) reduction in the number of ICM, TE, and total cells. Therefore, we concluded that AgNPs treatment decreased both ICM and TE cell numbers irrespective of sperm morphology.

Table 3.3 Developmental competence of mouse embryos derived from ICSI with dead AgNP-exposed sperm with different morphology after culture for 96 h.

| Treatment | No. IVF | No. undeveloped (% , ±SD) | No. embryos arrested at (% , ±SE) | | | | No. embryos development to (% , ±SE) | | | |
|-------------------------------------|---------|-------------------------------|-----------------------------------|-----------------|------------------------------|------------------|--------------------------------------|------------------|-------------------------------|-------------------------------|
| | | | 2C | 4C | 8C | Mo | Early BL | BL | Hatching BL | Total BL |
| Live sperm | 65 | 6 (9.2±1.0) ^b | 10 (15.4±3.2) | 6 (9.2±1.0) | 0 (0.0±0.0) ^b | 7 (10.8±6.5) | 9 (13.8±3.3) | 16 (24.6±6.2) | 11 (17.0±5.5) ^a | 36 (55.4±5.3) ^a |
| Dead normal morphology [*] | 65 | 9 (13.8±2.0) ^a | 14 (21.5±3.7) | 9 (13.8±4.4) | 0 (0.0±0.0) ^b | 11 (16.9±4.4) | 6 (9.2±4.2) | 13 (20.0±6.4) | 2 (3.1±2.9) ^b | 21 (32.3±4.3) ^b |
| Dead detached head [*] | 65 | 9 (13.8±1.7) ^a | 13 (20.0±5.5) | 9 (13.8±2.5) | 1 (1.5±2.0) ^{ab} | 9 (13.8±6.3) | 9 (13.8±4.3) | 12 (18.5±6.2) | 3 (4.6±5.8) ^b | 24 (36.9±7.9) ^b |
| Dead coil tail [*] | 65 | 12 (18.5±3.5) ^a | 14 (21.5±2.5) | 8 (12.3±3.1) | 3 (4.6±2.1) ^a | 9 (13.8±4.7) | 6 (9.2±3.7) | 13 (20.0±4.9) | 0 (0.0±0.0) ^b | 19 (29.2±2.9) ^b |

^{*}Dead sperm derived from AgNP exposed and different morphology. ^{a,b}Different superscripts denote significant differences (ANOVA: Duncan's Multiple Range Test, $P<0.05$). Mo and BL indicate molular and blastocyst, respectively.

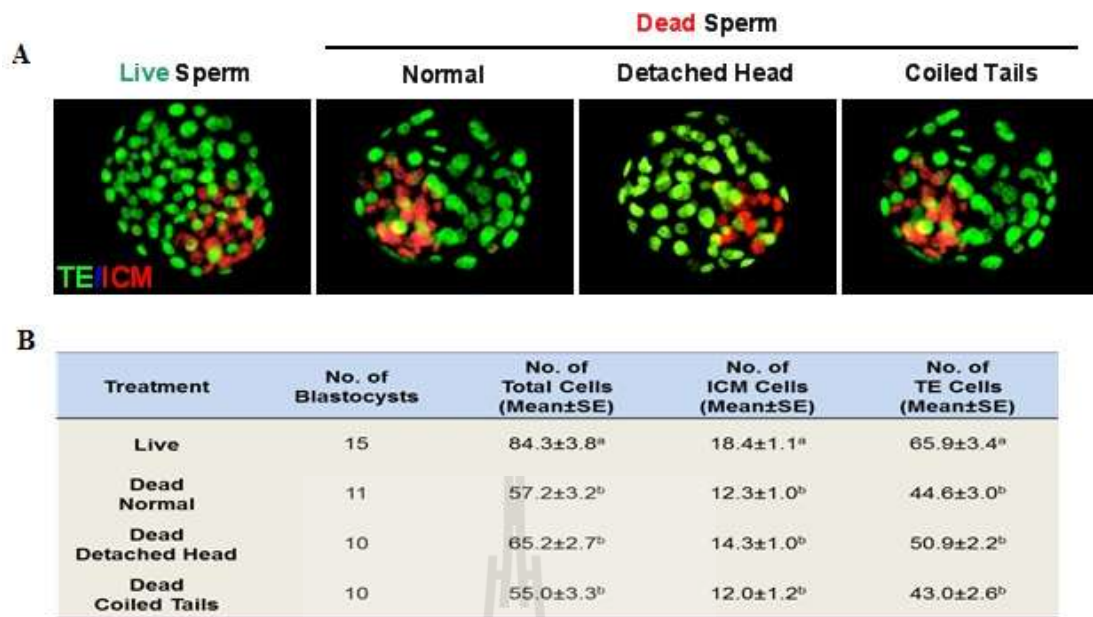


Figure 3.13 Quality analysis of blastocyst stage embryos developed *in vitro* after ICSI with AgNP-treated sperm cells with normal or abnormal morphology. A) A representative blastocyst stained differentially by OCT4 and CDX2 antibodies 96 h after ICSI with dead normal or abnormal sperm. OCT4-positive cells (red) are putative inner cell mass (ICM), whereas CDX2-positive cells (green) are putative trophectoderm. B) The number of total cells, ICM, and TE cells from the blastocyst stage embryos of (A). Different superscripts denote significant differences (ANOVA: Duncan's multiple range test, $P < 0.01$). C) ICM- and TE-specific mRNA expression analysis in blastocysts developed after ICSI with AgNP-treated normal or abnormal sperm cells. The expression levels of ICM and TE associated genes were analyzed by real time RT-qPCR. The experiments were performed in triplicate; data represent the mean of three independent experiments. Error bars represent standard error of the mean (SEM). * $P < 0.05$, ** $P < 0.01$ versus the control group (Dunnett's *t*-tests).

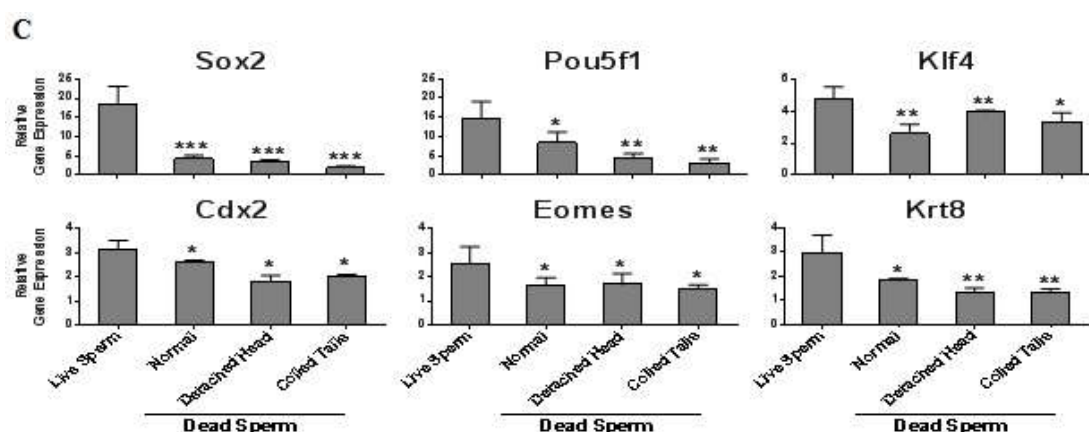


Figure 3.13 (Continued).

To confirm the effect of AgNP-exposed spermatozoa on ICM and TE-specific gene expression in ICSI-derived blastocyst embryos, embryos were produced by ICSI using dead spermatozoa with abnormal morphology due to AgNP exposure. ICM and TE-specific gene expression in blastocyst embryos was studied by RT-qPCR as shown in Figure 3.13C. These results showed that ICM- and TE-specific gene expression in blastocyst embryos produced from dead spermatozoa with abnormal morphology due to AgNP exposure was decreased relative to live spermatozoa-derived blastocyst stage embryos. However, the expression of ICM- and TE-specific genes in blastocysts derived from spermatozoa with abnormal morphology was not significantly different compared to dead sperm with normal morphology.

3.5 Discussions

In this study, we examined the cytotoxic effect of AgNPs on spermatozoa, oocyte-fertilizing capacity of sperm, and subsequent embryonic development. The average diameter of AgNPs used in our study was found to be 40 nm and 61.51 nm as measured by TEM and DLS respectively. Further, AgNPs were characterized by

ultraviolet (UV)-visible spectroscopy which showed a strong and broad surface peak located at 420 nm. The XRD results also clearly showed that the AgNPs are crystalline in nature.

Spermatozoa obtained from male BDF1 mice were treated with AgNPs at a dose of 0, 0.1, 1, 10, and 50 $\mu\text{g/mL}$ for 3 h, and the treated spermatozoa were used for IVF or ICSI of oocytes followed by embryonic culture *in vitro* for 96 h. Our results showed that AgNPs could internalize into the spermatozoa. When the AgNPs were applied at a low dosage, they mainly localized on the sperm plasma membrane. On the other hand, when applied at higher dosages, AgNPs were internalized into the head and mitochondrial region of spermatozoa. We also found that AgNP treatment could alter the normal mitochondrial architecture and increased the mtDNA copy number, thereby indicating that mitochondrial abnormalities may arise due to AgNP exposure. This was consistent with previous results that found that AgNPs could disrupt the mitochondrial respiratory chain, thereby reducing the mitochondrial activity of sperm (Asharani et al., 2008; Mathias et al., 2014).

Next, we assayed the morphological abnormalities of spermatozoa and observed that AgNP exposure significantly increased abnormal sperm morphologies, including coiled tails, roll tails, and bent tails, in a dose-dependent manner. Besides, our results showed that AgNP exposure decreased the percentage of live spermatozoa or sperm viability with increasing dose. Our findings are in agreement with several other reports that have shown that AgNP uptake in animal models decreased the total sperm count and increased abnormal sperm shape (Gromadzka-Ostrowska et al., 2012; Mangelsdorf et al., 2003). Besides, several *in vitro* studies have also demonstrated the dose-dependent adverse effects of AgNPs on sperm viability (Morette et al., 2012; Pothuraju and Kaul, 2013). In the present study, AgNPs

exposure also increased the intracellular ROS formation in sperm and pre-treatment with the ROS inhibitor NAC for 30 min significantly decreased the AgNPs-induced alterations in sperm viability and mtDNA copy number. It has been reported that AgNPs-induced ROS are responsible for sperm abnormality and reduced sperm viability (Attia, 2014; Bouwmeester et al., 2011; Cheng et al., 2013; Gaiser et al., 2013; Gromadzka-Ostrowska et al., 2012; Kruszewski et al., 2011, 2013; Mathias et al., 2014; McShan et al., 2014; Piao et al., 2011). Excess ROS can induce sperm abnormality via peroxidative damage of the sperm plasma membrane (Vernet et al., 2004). Mangelsdorf et al. (2003) and Aziz et al. (2004) showed that ROS levels were positively correlated with the proportion of spermatozoa with amorphous heads, damaged acrosomes, midpiece defects, cytoplasmic droplets, and tail defects. However, in our experiments, we could not use Ag⁺ ions as a positive control, as it formed a precipitate in modified Whitten's medium (formation of insoluble AgCl, Ag₃PO₄, etc). Therefore, AgNPs may be the main reason for the toxicity of spermatozoa. Collectively, these data suggest that AgNP-induced reduction in sperm viability and abnormal sperm morphologies appear to be closely associated with increased ROS production and mitochondrial damage.

A unique function of spermatozoa is its interaction with the oocyte for fertilization. This interaction requires several essential physiological changes in order to be competent for oocyte fertilization; this process is termed as capacitation (Liu et al., 2001). Sperm capacitation can be assayed by the sperm's ability to undergo the acrosome reaction and the detection of a membrane cofactor protein, CD46, a reliable marker of acrosome-reacted spermatozoa (Clift et al., 2009; Johnson et al., 2007). Our results showed that AgNP exposure significantly decreased the sperm acrosome reaction (CD46-negative) in a dose-dependent manner, thereby proving its negative

impact on fertility. This result is consistent with previous reports where the authors have shown that the acrosome integrity of spermatozoa from AgNP-treated animals was impaired. This is possibly due to the pro-oxidant effects of AgNPs, which increased the rate of ROS generation and affected the acrosome reaction (Braydich-Stolle et al., 2005; Chen et al., 2013; Ichikawa et al., 1999; Mathias et al., 2014; Miresmaeili et al., 2013).

In our present study, we found that AgNPs treatment had a negative effect on oocyte fertilization and subsequent embryonic development, especially late development, to expanded blastocyst and hatching blastocyst stages with increasing dose of AgNPs. This detrimental effect of AgNPs on fertilization is probably due to abnormal sperm morphology, impaired acrosome integrity and reduced sperm viability (Clift et al., 2009; Garrett et al., 1997; Menkveld et al., 1996; Park et al., 2012; Rahman et al., 2013; Suarez et al., 2008). Therefore, our results suggest that AgNPs might reduce the fertilization capacity of spermatozoa.

During normal embryogenesis, at the blastocyst stage, the TE cells from the trophoblast develop a sphere made up of epithelial cells, which surrounds the ICM and blastocoel. These TE cells are required for development of the embryonic portion of the placenta and mammalian conceptus (Cross, 2005; Kunath et al., 2004). In addition, the ICM are pluripotent cells, which give rise to the embryonic tissue that comprises the ectoderm, endoderm, and mesoderm (Marikawa and Alarcon, 2009). Li et al. (2010) suggested that AgNPs and Ag⁺ were potential cytotoxic agents for embryos that exert their effects through induction of cell apoptosis in ICM and TE cells of blastocysts, leading to decreased embryonic development and viability. Our results support this report: we showed that AgNP-treated spermatozoa significantly inhibited ICM and TE cell proliferation in blastocysts and downregulated ICM- and TE-specific gene expression that plays a crucial role in ICM and TE cell formation.

Morphological abnormality is strongly correlated with fertilization failures *in vitro* (Greco et al., 2005). With the help of ICSI, which allows oocyte fertilization irrespective of spermatozoon morphology and motility characteristics, we sought to determine the success of ICSI using spermatozoa with abnormal morphology due to AgNP exposure. We observed that dead spermatozoa with normal morphology, coiled, or bent tails obtained from AgNP treatment could reduce the fertilization rate. Our results suggested that integrity of the genomic DNA in sperm cells with abnormal morphology was not damaged by AgNPs treatment.

Moreover, dead spermatozoa with normal morphology or coiled or bent tails after exposure to AgNPs significantly inhibited ICM and TE cell proliferation in blastocysts, and also down-regulated ICM- and TE-associated genes. From our results, most of the blastocysts that were fertilized via AgNP-treated spermatozoa resulted in delayed development, as well as decreased ICM and TE cell numbers. Bos-Mikich et al. (2001) and Lundin et al. (2001) suggested that a large number of early-cleaving embryos become good quality embryos and significantly facilitate high pregnancy, implantation, and birth rates. Therefore, we expect that AgNPs may affect embryo implantation. As shown in a previous report, the critical concentration of AgNPs (5-46 nM) that resulted in embryonic abnormalities and death was found to be 1.9 nM (Lee et al., 2007). Besides, AgNPs (50 μ M) induced a high resorption rate of post-implantation embryos and a decrease in fetal weight (Li et al., 2010). Similarly, Philbrook et al. (2011) showed that administration of AgNPs to pregnant CD-1 mice resulted in reduced fetus viability.

3.6 Conclusion

AgNPs are a potential cytotoxic agent for sperm cells and exert adverse effects, possibly through the induction of oxidative stress. Furthermore, AgNP-treated sperm reduce the IVF success rate, delay subsequent blastocyst formation, and downregulate gene expression responsible for embryonic development. Our present *in vitro* study will offer further mechanistic insights into the effects of AgNPs on mammalian sperm physiology, such as the underlying mechanism or maximum size limit for AgNP internalization into sperm cells.

3.7 References

- Ahamed, M., Posgai, R., Gorey, T. J., Nielsen, M., Hussain, S. M., and Rowe, J. J. (2010). Silver nanoparticles induced heat shock protein 70, oxidative stress and apoptosis in *Drosophila melanogaster*. **Toxicol. Appl. Pharmacol.** 242: 263-269.
- Asare, N., Instanes, C., Sandberg, W. J., Refsnes, M., Schwarze, P., Kruszewski, M., Schwarze, P., Kruszewski, M., and Brunborg, G. (2012). Cytotoxic and genotoxic effects of silver nanoparticles in testicular cells. **Toxicology** 291: 65-72.
- AshaRani, P. V., Wu, Y. L., Gong, Z., and Valiyaveetil, S. (2008). Toxicity of silver nanoparticles in zebrafish models. **Nanotechnology** 19(25): 255102(8 pp).
- AshaRani, P. V., Mun, G. L. K., Hande, M. P., and Valiyaveetil, S. (2009). Cytotoxicity and Genotoxicity of Silver Nanoparticles in Human Cells. **Acs Nano.** 3: 279-290.

- Attia, A. A. (2014). Evaluation of the Testicular Alterations Induced By Silver Nanoparticles in Male Mice: Biochemical, Histological and Ultrastructural Studies. **Res. J. Pharm. Biol. Chem.** 5(4): 1558-1589.
- Aziz, T., Saleh, R. A., Sharma, R. K., Lewis-Jones, I., Esfandiari, N., Thomas, A. J., and Agarwal, A. (2004). Novel association between sperm reactive oxygen species production, sperm morphological defects, and the sperm deformity index. **Fertil. Steril.** 81: 349-354.
- Bar-Ilan, O., Albrecht, R. M., Fako, V. E., and Furgeson, D. Y. (2009). Toxicity assessments of multi-sized gold and silver nanoparticles in zebrafish embryos. **Small** 5(16): 1897-1910.
- Biggers, J. D. (1998). Reflections on the culture of the preimplantation embryo. **Int. J. Dev. Biol.** 42: 879-884.
- Bos-Mikich, A., Mattos, A., and Ferrari, A. (2001). Early cleavage of Human embryos: an effective method for predicting successful IVF/ICSI outcome. **Hum. Reprod.** 16: 2658-2661.
- Bouwmeester, H., Poortman, J., Peters, R. J., Wijma, E., Kramer, E., Makama, S., Puspitaninganindita, K., Marvin, H. J., Peijnenburg, A. A., and Hendriksen, P. J. (2011). Characterization of translocation of silver nanoparticles and effects on whole genome gene expression using an in vitro intestinal epithelium co-culture model. **ACS Nano.** 5: 4091-4103.
- Braydich-Stolle, L., Hussain, S., Schlager, J. J., and Hofmann, M. C. (2005). *In vitro* cytotoxicity of nanoparticles in mammalian germline stem cells. **Toxicol. Sci.** 88: 412-419.
- Braydich-Stolle, L. K., Lucas, B., Schrand, A., Murdock, R. C., Lee, T., Schlager, J. J., Hussain, S. M., and Hofmann, M. C. (2010). Silver nanoparticles disrupt

- GDNF/Fyn kinase signaling in spermatogonial stem cells. **Toxicol. Sci.** 116: 577-589.
- Campagnolo, L., Massimiani, M., Magrini, A., Camaioni, A., and Pietroiusti, A. (2012). Physico-chemical properties mediating reproductive and developmental toxicity of engineered nanomaterials. **Curr. Med. Chem.** 19: 4488-4494.
- Chen, S. J., Allam, J. P., Duan, Y. G., and Haidl, G. (2013). Influence of reactive oxygen species on human sperm functions and fertilizing capacity including therapeutical approaches. **Arch. Gynecol. Obstet.** 288: 191-9.
- Cheng, X., Zhang, W., Ji, Y., Meng, J., Guo, H., and Liu, J., Wu, X., and Xu, H. (2013). Revealing silver cytotoxicity using Au nanorods/Ag shell nanostructures: disrupting cell membrane and causing apoptosis through oxidative damage. **RSC Adv.** 3: 2296-305.
- Clift, L. E., Andrlíkova, P., Frolikova, M., Stopka, P., Bryja, J., Flanagan, B. F., Johnson, P. M., and Dvorakova-Hortova, K. (2009). Absence of spermatozoal CD46 protein expression and associated rapid acrosomereaction rate in striped field mice (*Apodemus agrarius*). **Reprod. Biol. Endocrinol.** 16: 7-29.
- Cross, J. C. (2005). How to make placenta: mechanisms of trophoblast cell differentiation in mice a review. **Placenta** 26: 3-9.
- Foldbjerg, R., Olesen, P., Hougaard, M., Dang, D. A., Hoffmann, H. J., and Autrup, H. (2009). PVP-coated silver nanoparticles and silver ions induce reactive oxygen species, apoptosis and necrosis in THP-1 monocytes. **Toxicol. Lett.** 190: 156-162.
- Franken, D. R., Kruger, T. F., Menkveld, R., Oehninger, S., Coddington, C. C., and Hodgen, G. D. (1990). Hemizona assay and teratozoospermia: increasing

- sperm insemination concentrations to enhance zonapellucida binding. **Fertil. Steril.** 54: 497-503.
- Gaiser, B. K., Hirn, S., Kermanizadeh, A., Kanase, N., Fytianos, K., Wenk, A., Haberl, N., Brunelli, A., Kreyling, W. G., and Stone, V. (2013). Effects of silver nanoparticles on the liver and hepatocytes in vitro. **Toxicol. Sci.** 131: 537-547.
- Gandolfi, F., and Brevini, T. A. (2010). In vitro maturation of farm animal oocytes: a useful tool for investigating the mechanisms leading to full-term development. **Reprod. Fertil. Dev.** 22: 495-507.
- Garrett, C., Liu, D. Y., and Baker, H. W. (1997). Selectivity of the human sperm-zonapellucida binding process to sperm head morphometry. **Ferti. Steril.** 67: 362-71.
- Gopalan, R. C., Osman, I. F., Amani, A., de Matas, M., and Anderson, D. (2009). The effect of zinc oxide and titanium dioxide nanoparticles in the comet assay with UVA photoactivation of human sperm and lymphocytes. **Nanotoxicology** 3: 33-39.
- Greco, E., Scarselli, F., Iacobelli, M., Rienzi, L., Ubaldi, F., Ferrero, S., Franco, G., Anniballo, N., Mendoza, C., Tesarik, J. (2005). Efficient treatment of infertility due to sperm DNA damage by ICSI with testicular spermatozoa. **Hum. Reprod.** 20(1): 226-230.
- Gromadzka-Ostrowska, J., Dziendzikowska, K., Lankoff, A., Dobrzyoska, M., Instanes, C., Brunborg, G., Gajowik, A., Radzikowska, J., Wojewódzka, M., Kruszewski, M. (2012). Silver Nanoparticles effects on epididymal sperm in rats. **Toxicol. Lett.** 214: 251-258.

- Guo, L. L., Liu, X. H., Qin, D. X., Gao, L., Zhang, H. M., Liu, J. Y., and Cui, Y. G. (2009). Effects of nanosized titanium dioxide on the reproductive system of male mice. **Zhonghua Nan Ke Xue** 15: 517-522.
- Hussain, S. M., Hess, K. L., Gearhart, J. M., Geiss, K. T., and Schlager, J. J. (2005). In vitro toxicity of nanoparticles in BRL 3A rat liver cells. **Toxicol. in Vitro** 19: 975-983.
- Ichikawa, T., Oeda, T., Ohmori, H., and Schill, W. B. (1999). Reactive oxygen species influence the acrosome reaction but not acrosin activity in human spermatozoa. **Int. J. Androl.** 22: 37-42.
- Johnson, P. M., Clift, L. E., Andriikova, P., Jursova, M., Flanagan, B. F., Cummerson, J. A., Cummerson, J. A., Stopka, P., and Dvorakova-Hortova, K. (2007). Rapid sperm acrosomereaction in the absence of acrosomal CD46 expression in promiscuous field mice (Apodemus). **Reproduction** 134: 739-747.
- Kim, Y. S., Song, M. Y., Park, J. D., Song, K. S., Ryu, H. R., Chung, Y. H., Chang, H. K., Lee, J. H., Oh, K. H., Kelman, B. J., Hwang, I. K., and Yu, I. J. (2010). Subchronic oral toxicity of silver nanoparticles. **Part Fibre Toxicol.** 7-20.
- Kruszewski, M., Brzoska, K., Brunborg, G., Asare, N., Dobrzynska, M., Duzinska, M., and Fjellsbø, L. M. (2011). Toxicity of silver nanomaterials in higher eukaryotes. **Adv. Mol. Toxicol.** 5: 179-259.
- Kruszewski, M., Gradzka, I., Bartłomiejczyk, T., Chwastowska, J., Sommer, S., Grzelak, A., Zuberek, M., Lankoff, A., Dusinska, M., and Wojewódzka M. (2013). Oxidative DNA damage corresponds to the long term survival of human cells treated with silver nanoparticles. **Toxicol. Lett.** 219: 151-159.

- Kunath, T., Strumpf, D., and Rossant, J. (2004). Early trophoblast determination and stem cell maintenance in the mouse—a review. **Placenta** 25: 32-38.
- Kvitek, L., Vanickova, M., Panacek, A., Soukupova, J., Dittrich, M., Valentova, E., Pucek, R., Bancirova, M., Milde, D., and Zboril, R. (2009). Initial Study on the Toxicity of Silver Nanoparticles (NPs) against *Paramecium caudatum*. **J. Phys. Chem C**. 113: 4296-4300.
- Kyjovska, Z. O., Boisen, A. M., Jackson, P., Wallin, H., Vogel, U., and Hougaard, K. S. (2013). Daily sperm production: application in studies of prenatal exposure to nanoparticles in mice. **Reprod. Toxicol.** 36: 88-97.
- Laban, G., Nies, L. F., Turco, R. F., Bickham, J. W., and Sepulveda, M. S. (2010). The effects of silver nanoparticles on fathead minnow (*Pimephalespromelas*) embryos. **Ecotoxicol.** 19:185-195.
- Lan, Z., and Yang, W. X. (2012). Nanoparticles and spermatogenesis: how do nanoparticles affect spermatogenesis and penetrate the blood-testis barrier. **Nanomedicine** 7: 579-96.
- Lim, D., Roh, J. Y., Eom, H. J., Choi, J. Y., Hyun, J., and Choi, J. (2012). Oxidative stress-related PMK-1 P38 MAPK activation as a mechanism for toxicity of silver nanoparticles to reproduction in the nematode *Caenorhabditiselegans*. **Environ. Toxicol. Chem.** 31: 585-592.
- Lee, K. J., Nallathamby, P. D., Browning, L. M., Osgood, C. J., and Xu, X. H. N. (2007). *In vivo* imaging of transport and biocompatibility of single silver nanoparticles in early development of zebrafish embryos. **ACS Nano**. 1: 133-143.

- Li, H., Chen, Q., Li, S., Yao, W., Li, L., Shi, X., Wang, L., Castranova, V., Vallyathen, V., Ernst, E., and Chen, C. (2001). Effect of Cr(VI) exposure on sperm quality: human and animal studies. **Ann. Occup. Hyg.** 45: 505-511.
- Li, P. W., Kuo, T. H., Chang, J. H., Yeh, J. M., and Chan, W. H. (2010). Induction of cytotoxicity and apoptosis in mouse blastocysts by silver nanoparticles. **Toxicol. Lett.** 197: 82-87.
- Liu, D. Y., Clarke, G. N., Martic, M., Garrett, C., and Baker, H. W. (2001). Frequency of disordered zona pellucida (ZP)-induced acrosome reaction in infertile men with normal semen analysis and normal spermatozoa-ZP binding. **Human. Reprod.** 16: 1185-1190.
- Lucas, B., Fields, C., and Hofmann, M. C. (2009). Signaling pathways in spermatogonial stem cells and their disruption by toxicants. **Birth Defects Res. C87**: 35-42.
- Lundin, K., Bergh, C., and Hardason, T. (2001). Early embryo cleavage is strong indicator of embryo quality in human IVF. **Hum. Reprod.** 16: 2652-2657.
- Makhluf, S. B. D., Qasem, R., Rubinstein, S., Gedanken, A., and Breitbart, H. (2006). Loading magnetic nanoparticles into sperm cells does not affect their functionality. **Langmuir.** 22: 9480-9482.
- Makhluf, S. B. D., Arnon, R., Patra, C. R., Mukhopadhyay, D., Gedanken, A., Mukherjee, P., and Breitbart, H. (2008). Labeling of Sperm Cells via the Spontaneous Penetration of Eu^{3+} Ions as Nanoparticles Complexed with PVA or PVP. **Phys. Chem. C.** 112: 12801-12807.
- Mangelsdorf, I., Buschmann, J., and Orthen, B. (2003). Some aspects relating to the evaluation of the effects of chemicals on male fertility. **Regul. Toxicol. Pharmacol.** 37: 356-369.

- Marikawa ,Y., and Alarcon, V. B. (2009). Establishment of trophectoderm and inner cell mass lineages in the mouse embryo. **Mol. Reprod. Dev.** 76: 1019-1032.
- Mathias, F. T., Romano, R. M., Kizys, M. M. L., Kasamatsu, T., Giannocco, G., and Chiamolera, M. I., Dias-da-Silva, M. R., and Romano, M. A. (2014). Daily exposure to silver nanoparticles during prepubertal development decreases adult sperm and reproductive parameters. *Nanotoxicology*. DOI: 10.3109/17435390.2014.889237.
- McShan, D., Ray, P. C., and Yu, H. (2014). Molecular toxicity mechanism of nanosilver. **J. food and drug analysis** 22: 116-127.
- Menkveld, R., Rhemrev, J. P., Franken, D. R., Vermeiden, J. P., and Kruger, T. F. (1996). Acrosomal morphology as a novel criterion for male fertility diagnosis: relation with acrosin activity, morphology (strict criteria), and fertilization in vitro. **Fertil. Steril.** 65: 637-44.
- Miresmaeili, S. M., Halvaei, I., Fesahat, F., Fallah, A., Nikonahad, A., and Taherinejad, M. (2013). Evaluating the role of silver nanoparticles on acrosomal reaction and spermatogenic cells in rat. **Iran J. Reprod.** 11(5): 423-430.
- Moretti, E., Terzuoli, G., Renieri, T., Iacoponi, F., Castellini, C., Giordano, C., and Collodel, G. (2013). In vitro effect of gold and silver nanoparticles on human spermatozoa. **Andrologia** 45(6): 392-396.
- Navarro, E., Piccapietra, F., Wagner, B., Marconi, F., Kaegi, R., Odzak, N., Sigg, L., and Behra, R. (2008). Toxicity of Silver Nanoparticles to *Chlamydomonas reinhardtii*. **Environ. Sci. Technol.** 42: 8959-8964.
- Nel, A., Xia, T., Madler, L., and Li, N. (2006). Toxic potential of materials at the nanolevel. **Science** 311: 622-627.

- Oberdörster, E. (2004). Manufactured nanomaterials (Fullerenes, C60) induce oxidative stress in the brain of juvenile largemouth bass. *Environ. Health Perspect.* 112: 1058-1062.
- Oberdörster, E., Zhu, S., Blickley, T. M., McClellan-Green, P., and Haasch, M. L. (2006). Ecotoxicology of carbon-based engineered nanoparticles: effects of fullerene (C60) on aquatic organisms. *Carbon* 44: 1112-1120.
- Oehninger, S., Toner, J. P., Muasher, S. J., Coddington, C., Acosta, A. A., Hodgen, G. D. (1992). Prediction of fertilization *in vitro* with human gametes: is there a litmus test. *Am. J. Obstet. Gynecol.* 167: 1760-1767.
- Park, E. J., Bae, E., Yi, J., Kim, Y., Choi, K., Lee, S. H., Yoon, J., Lee, B. C., and Park, K. (2010). Repeated-dose toxicity and inflammatory responses in mice by oral administration of silver nanoparticles. *Environ. Toxicol. Pharmacol.* 30: 162-168.
- Park, Y. J., and Kwon, W. S., Oh, S. A., and Pang, M. G. (2012). Fertility-related proteomic profiling bull spermatozoa separated by percoll. *J. Proteome Res.* 11: 4162-4168.
- Philbrook, N. A., Winn, L. M., Afrooz, A. R., Saleh, N. B., Walker, V. K. (2011). The effect of TiO₂ and Ag nanoparticles on reproduction and development of *Drosophila melanogaster* and CD-1 mice. *Toxicol. Appl. Pharmacol.* 257: 429-436.
- Piao, M. J., Kang, K. A., Lee, I. K., Kim, H. S., Kim, S., Choi, J. Y., Choi, J., and Hyun, J. W. (2011). Silver nanoparticles induce oxidative cell damage in human liver cells through inhibition of reduced glutathione and induction of mitochondria-involved apoptosis. *Toxicol. Lett.* 201: 92-100.

- Pothuraju, R., and Kaul, G. (2013). Effect of silver nanoparticles on functionalities of Buffalo (*BubalusBubalis*) spermatozoa. **Adv. Sci. Eng. Med.** 5: 91-95.
- Rahman, M. S., Lee, J. S., Kwon, W. S., and Pang, M. G. (2013). Sperm proteomics: road to male fertility and contraception. **Int. J. Endocrinol.** ID 360986.
- Roy, R., Kumar, S., Tripathi, A., Das, M., and Dwivedi, P. D. (2014). Interactive threats of nanoparticles to the biological system. **Immunol. Lett.** 158: 79-87.
- Sleiman, H., Romano, R. M., Oliveira, C. A., and Romano, M. A. (2013). Effects of prepubertal exposure to silver nanoparticles on reproductive parameters in adult male Wistar rats. **J. Toxicol. Environ. Health A.** 76: 1023-1032.
- Smith, C. J., Shaw, B. J., and Handy, R. D. (2007). Toxicity of single walled carbon nanotubes to rainbow trout, (*Oncorhynchusmykiss*): respiratory toxicity, organ pathologies, and other physiological effects. **Aquat. Toxicol.** 82: 94-109.
- Suarez, S. S. (2008). Control of hyperactivation in sperm. **Hum. Reprod.** 14: 647-657.
- Usenko, C. Y., Harper, S. L., and Tanguay, R. L. (2007). In vivo evaluation of carbon fullerene toxicity using embryonic zebrafish. **Carbon** 45: 1891-1898.
- Vernet, P., Aitken, R. J., and Drevet, J. R. (2004). Antioxidant strategies in the epididymis. **Mol. Cell. Endocrinol.** 216: 31-39.
- Wiwanitkit, V., Sereemasapun, A., and Rojanathanes, R. (2009). Effect of gold nanoparticles on spermatozoa: the first world report. **Fertil. Steril.** 91: e7-8.
- Xia, T., Kovoichich, M., Brant, J., Hotze, M., Sempf, J., Oberley, T., Sioutas, C., Yeh, J. I., Wiesner, M. R., and Nel, A. E. (2006). Comparison of the abilities of ambient and manufactured nanoparticles to induce cellular toxicity according to an oxidative stress paradigm. **Nano. Lett.** 6: 1794–1807.

Zakhidov, S. T., Pavliuchenkova, S. M., Marshak, T. L., Rudoi, V. M., Dement'eva, O. V., Zelenina, I. A., Skuridin, S. G., Makarov, A. A., Khokhlov, A. N., and Evdokimov, Iu. M. (2012). Effect of gold nanoparticles on mouse spermatogenesis. **Izv. Akad. Nauk. Ser. Biol.** 3: 279-87.

Zhu, S., Oberdorster, E., and Haasch, M. L. (2006). Toxicity of an engineered nanoparticle (fullerene, C60) in two aquatic species, daphnia and fathead minnow. **Mar. Environ. Res.** 62: S5-S9.



CHAPTER IV

EFFECT OF HEXAVALENT CHROMIUM-TREATED SPERM ON *IN VITRO* FERTILIZATION AND EMBRYO DEVELOPMENT

4.1 Abstract

Hexavalent chromium, Cr(VI), is an environmental contaminant that is associated with reproductive abnormalities in both humans and animals. In the present study, we evaluated the cytotoxic effect of Cr(VI) on sperm function and subsequent embryo development after *in vitro* fertilization (IVF). Sperm obtained from BDF1 male mice were treated with $K_2Cr_2O_7$ (0, 3.125, 6.25, 12.5, 25, or 50 μ M) for 3 h. Cr(VI) significantly decreased sperm viability and acrosome reaction with increasing dose. These Cr(VI)-treated sperm were further used for IVF of oocytes obtained from BDF1 female mice. Results showed that Cr(VI)-treated sperm caused a significant reduction in IVF success, higher developmental arrest at the 2-cell stage of embryos, and delayed blastocyst formation with increasing dose. In particular, most blastocysts from the Cr(VI)-treated sperm resulted in hatching failure as well as decreased inner cell mass and trophectoderm. Furthermore, blastocysts obtained from Cr(VI)-treated sperms showed lower expression of not only trophectoderm-associated genes (*eomes*, *cdx2*, and *krt8*) but also pluripotent marker genes (*sox2*, *pou5f1*, and *klf4*) that are responsible for further embryo development of blastocyst embryos. The results of our current study showed that Cr(VI)-treated sperm had negative effects on oocyte fertilization and subsequent embryo development.

4.2 Introduction

Chromium (Cr) is a naturally occurring element that is mostly found in rocks, volcanic dust and gases, soils, as well as in animals and plants. It is extensively used in pigment and stainless steel production; leather tannery; wood processing; welding; cement manufacturing; chrome plating, textile, ceramic, glass, and photography industries; catalytic converters for automobiles; and cooling plant (Stohs et al., 2001); disposal of these kinds of industrial waste creates severe environmental pollution. In addition to occupational exposure of workers (via inhalation and skin contact), people are also exposed to Cr when it contaminates ground and surface water, agricultural land, and aquatic life. Cr can exist in a variety of oxidative states ranging from -2 to +6, among which the trivalent (III) and hexavalent (VI) forms have biological importance (Stoecker, 2004). Hexavalent Cr, Cr(VI), can readily cross cellular membranes via nonspecific anion transporters, whereas the trivalent form, Cr(III), is poorly transported across membranes. Therefore, Cr toxicity is mainly attributed to Cr(VI).

Cr(VI) has been reported to cause allergic dermatitis as well as cytotoxic, genotoxic, immunotoxic, and carcinogenic effects in both humans and laboratory animals (Stohs et al., 2001; Li et al., 2011). Moreover, Cr(VI) exposure has also been reported to induce reproductive toxicity in both humans and laboratory animals (Danadevi et al., 2003; Li et al., 2001; Subramanian et al., 2006). In welding industries and chromate factories, workers exposed to Cr suffer from increased risk of reduced semen quality and sperm abnormalities that ultimately lead to infertility (Danadevi et al., 2003; Kumar et al., 2005). Additionally, decreased sperm count and increased numbers of abnormal spermatozoa have been reported in Cr-treated/exposed mice, rats, rabbits, and bonnet monkeys (Acharya et al., 2006; Li et al., 2001;

Subramanian et al., 2006; Yousef et al., 2006). Women working in Cr industries or living around Cr-contaminated areas, who have high levels of Cr in blood and urine experience irregular menses and complications during pregnancy and childbirth (Shmitova, 1980; Zhang et al., 1992; Greene et al., 2010). In addition, toxic effects on embryos and fetuses in laboratory animals exposed to Cr(VI) have also been reported (Junaid et al., 1996; Marouani et al., 2011). However, only limited number of extensive *in vitro* studies has evaluated the effects of Cr(VI) on sperm parameters and sperm fertilizing ability during *in vitro* fertilization (IVF) of oocytes as well as subsequent development of embryos.

Therefore, the objectives of the present study were to (i) determine the cytotoxic effect of Cr(VI) on sperm obtained from mice; (ii) evaluate the effect of Cr(VI) on sperm capacitation; (iii) assess the effect of Cr(VI) on sperm fertilizing ability during IVF of oocytes and embryo development; (iv) understand the role of Cr(VI) on cell proliferation in blastocysts; and (v) explore the effect of Cr(VI) on inner cell mass (ICM) and trophectoderm (TE) cell-specific gene expression in blastocysts.

4.3 Materials and methods

4.3.1 Materials

$K_2Cr_2O_7$ (molecular weight, 294.18) was purchased from Duksan Company (South Korea). NaCl, KCl, KH_2PO_4 , $CaCl_2$, $MgSO_4$, $NaHCO_3$, glucose, and BSA were purchased from Sigma-Aldrich (St. Louis, MO, USA).

4.3.2 Animal

Male BDF1 (8-12 weeks old) mice were housed in wire cages at $22 \pm 1^\circ\text{C}$ with 70% humidity under a 12/12 h light-dark cycle. Mice had access to food *ad libitum*. All experiments were performed with approval from the Institutional Animal Care and Use Committee at Konkuk University (IACUC approval no. KU11035), Seoul, Korea.

4.3.3 Sperm preparation and treatments

The cauda of the epididymis of male BDF1 mice (8-12 weeks old) were cut and squeezed; the collected fluid was then suspended in 200 μL of modified Whitten's medium (118.5 mM NaCl, 4.7 mM KCl, 1.18 mM KH_2PO_4 , 2.54 mM CaCl_2 , 1.18 mM MgSO_4 , 24.9 mM NaHCO_3 , 5.56 mM glucose, and 3 mg/mL BSA). Subsequently, the suspension was incubated at 37°C in a humidified atmosphere of 5% CO_2 for 30 min. The sperm suspension was placed in the bottom of a 5 mL snap tube containing 1 mL of modified Whitten's medium and incubated at 37°C in 5% CO_2 for 30 min to allow live spermatozoa to swim up. The sperm suspension was collected from the top of the tube and centrifuged at 3000 rpm for 5 min. The pellets were re-suspended in modified Whitten's medium. $\text{K}_2\text{Cr}_2\text{O}_7$ was dissolved in deionized water to prepare 1 mM stock solution. Approximately 2×10^5 sperm were treated with different concentrations of $\text{K}_2\text{Cr}_2\text{O}_7$ (0, 3.125, 6.25, 12.5, 25, or 50 μM) and incubated for 3 h at 37°C in a humidified atmosphere of 5% CO_2 .

4.3.4 Live/dead sperm detection by fluorescence microscopy and flow cytometry

Sperm viability was assessed using a LIVE/DEAD Sperm Viability Kit (Molecular Probes, Inc., Eugene, OR, USA). Briefly, the samples were incubated with 100 nM of SYBR 14 dye at 37°C for 10 min in the dark and then incubated with 12 µM of propidium iodide (PI) for 5 min at 37°C. The stained sperm were placed on a microscope slide coated with 0.1% poly-D-lysine (Sigma-Aldrich, St. Louis, MO, USA) and covered with a cover glass. The sperm that showed bright green fluorescence were considered alive, whereas sperm that fluoresced red were considered dead. Sperm viability was calculated by the following formula: sperm viability = (number of live sperm × 100) / total sperm count. For flow cytometry analysis, 10,000 sperm per sample were analyzed for the log of their green fluorescence passing through a 525-nm band pass filter (FL1) and red fluorescence passing through 575-nm band-pass filters (FL2). The generated data were then analyzed to determine the relative fluorescence of the FL1 and FL2 using the Coulter Histogram Analysis program (Coulter Corporation, Miami, FL, USA).

4.3.5 Sperm acrosome reaction analysis by fluorescence microscopy and flow cytometry

The samples were centrifuged at 3000 rpm for 5 min, fixed with 2% paraformaldehyde for 10 min at room temperature, and then washed twice. Afterward, the samples were blocked with 1% BSA in PBS overnight followed by washing with PBS. The pellet was re-suspended in PBS and divided into two aliquots. The first aliquot was diluted 1:50 with FITC-CD46 and incubated at 4°C for 30 min in the dark, followed by washing with PBS twice. Then, the sample was incubated with

1:200 diluted secondary antibody for 30 min. After washing, sperm were placed on a microscope slide coated with 0.1% poly-D-lysine, covered with a cover glass, and then observed by fluorescence microscope. The second aliquot samples were then analyzed by flow cytometry by taking the log of the green fluorescence passing through a 525-nm band pass filter (FL1).

4.3.6 *In vitro* fertilization (IVF)

Female BDF1 mice (6–8 weeks old) were superovulated by intraperitoneal injection of pregnant mare's serum gonadotropin (PMSG; 10 units). After 48 h, they were injected by human chorionic gonadotropin (hCG; 10 units). Metaphase II oocytes with cumulus cells were collected from the oviductal ampulla after 12–14 h of hCG injection and then suspended in 50 μ L of modified Whitten's medium. Sperm from each Cr(VI) treatment were washed twice by centrifugation at 3000 rpm for 5 min. Then, sperm pellets were re-suspended in 50 μ L of modified Whitten's medium and mixed with 50 μ L of the above drop of modified Whitten's medium containing the oocytes. The sperm and oocytes were then co-incubated for 6 h at 37°C in a humidified atmosphere of 5% CO₂. Subsequently, embryos were washed and cultured *in vitro* (IVC) in KSOM medium (GlobalStem, Rockville, MD, USA) for 96 h. IVF rate and embryo development were checked by light microscopic analysis.

4.3.7 Inner cell mass (ICM) and trophectoderm cell (TE) analysis

After 96 h IVC, the blastocysts were collected and washed twice with PBS containing 1% BSA. The blastocysts were then fixed in 4% paraformaldehyde for 40 min at room temperature. Subsequently, embryos were washed twice and incubated with 1% BSA and 0.1% Triton-X 100 in PBS overnight at 4°C. The embryos were

again washed twice (15 min each time) and incubated with mouse anti-CDX2 (1:50) and rabbit anti-OCT4 (1:100) antibodies for 1 h at room temperature. After incubation with primary antibody, embryos were washed three times (15 min each time). Then, embryos were incubated with secondary antibody (1:200) in the dark for 1 h at room temperature. After incubation, embryos were washed three times, mounted on slides, and observed with a fluorescent microscope. Immunostaining with anti-OCT4 and anti-CDX2 antibodies in blastocysts was performed to determine the amount of ICM and TE cells, respectively.

4.3.8 Gene expression analysis

Fifteen blastocysts per treatment were collected 96 h after fertilization and kept at -80°C. For total mRNA extraction, the mRNA from collected blastocysts was extracted by freezing in LN₂ and thawing in 37°C water for five times. cDNA was synthesized by Reverse Transcription Kit (Roche, Mannheim, Germany) in a final volume of 20 µL according to the manufacturer's instructions. The quantification of all gene transcripts (*sox2*, *pou5f1*, *klf4*, *eomes*, *cdx2*, and *krt8*) was approved out in three replicates by real-time quantitative reverse transcription (qRT-PCR) on a Lightcycler using Lightcycler® FastStart DNA Master SYBR Green I via an Applied Biosystems machine. The primer sequences for each gene are shown in Table 4.1. The relative quantification of gene expression was analyzed by the 2-ddCt method. In all experiments, GAPDH mRNA was used as an internal standard.

Table 4.1 Primers and conditions used for real-time qRT-PCR.

| Primer name | Primer sequence |
|---------------|--|
| <i>GAPDH</i> | F: AGGTCGGTGTGAACGGATTTG R: TGTAGACCATGTAGTTGAGGTCA |
| <i>Pou5f1</i> | F: CTCCTACAGCAGATCACTCACA R: AACCATACTCGAACCACATCCT |
| <i>Sox2</i> | F: CACAACCTCGGAGATCAGCAA R: CTCCGGGAAGCGTGTACTTA |
| <i>Klf4</i> | F: CTGAACAGCAGGGACTGTCA R: GTGTGGGTGGCTGTTCTTTT |
| <i>Cdx2</i> | F: AGACAAATACCGGGTGGTGTA R: CCAGCTCACTTTTCCTCCTGA |
| <i>Eomes</i> | F: GAGCTTCAACATAAACGGACTCAA R: CGGCCAGAACCACTTCCA |
| <i>Krt8</i> | F: ATCGAGATCACCACTACCG R: TGAAGCCAGGGCTAGTGAGT |

4.3.9 Statistical analysis

Each experiment was performed at least three times and was subjected to statistical analysis. For statistical analysis, one-way analysis of variance (ANOVA) was performed to determine whether there were differences within the groups ($P < 0.01$) and Dunnett's *t* test was performed to determine significance between treatment and control groups. A *P*-value was considered significant as shown in figure. Statistical tests were performed using StatView version 5.0 (SAS Institute, Cary, NC, USA).

4.4 Results

4.4.1 Cytotoxic effect of Cr(VI) on spermatozoa

To determine the cytotoxic effect of Cr(VI) on sperm, sperm were exposed to 0, 3.125, 6.25, 12.5, 25, or 50 μM Cr(VI) for 3 h. Figure 4.1A shows a fluorescence microscopic image of living (stained with SYBR-14), dead (stained with PI), and moribund (stained with both SYBR-14 and PI) sperm are shown in green, red, and yellow, fluorescence respectively. The number of dead and live sperm was calculated by counting the red and green fluorescence, respectively. These results (Figure 4.1B) showed that Cr(VI) exposure significantly ($P < 0.001$) increased the percentage of dead sperm and decreased the percentage of live sperm with increasing Cr(VI) concentration compared with non-treated sperm. Flow cytometry analysis (Figure 4.1C) also showed that the percentage of dead sperm progressively increased compared with non-treated sperm when sperm were exposed to increasing concentrations of Cr(VI).

4.4.2 Impact of Cr(VI) exposure on sperm acrosome reaction

Sperm acrosome reaction was determined by evaluating the sperm's ability to undergo the acrosome reaction via CD46 immunofluorescence staining and flow cytometry (Figure 4.2). Cr(VI) exposure decreased sperm acrosome reaction, as evidenced by decreased CD46 immunofluorescence intensity with increasing Cr(VI) concentrations (Figure 4.2A). Flow cytometry analysis also indicated that Cr(VI) significantly reduced the percentage of acrosome-reacted (CD46-positive) spermatozoa in groups treated with 12.5 μM or more of Cr(VI) compared with the non-treated group (Figure 4.2B-C).

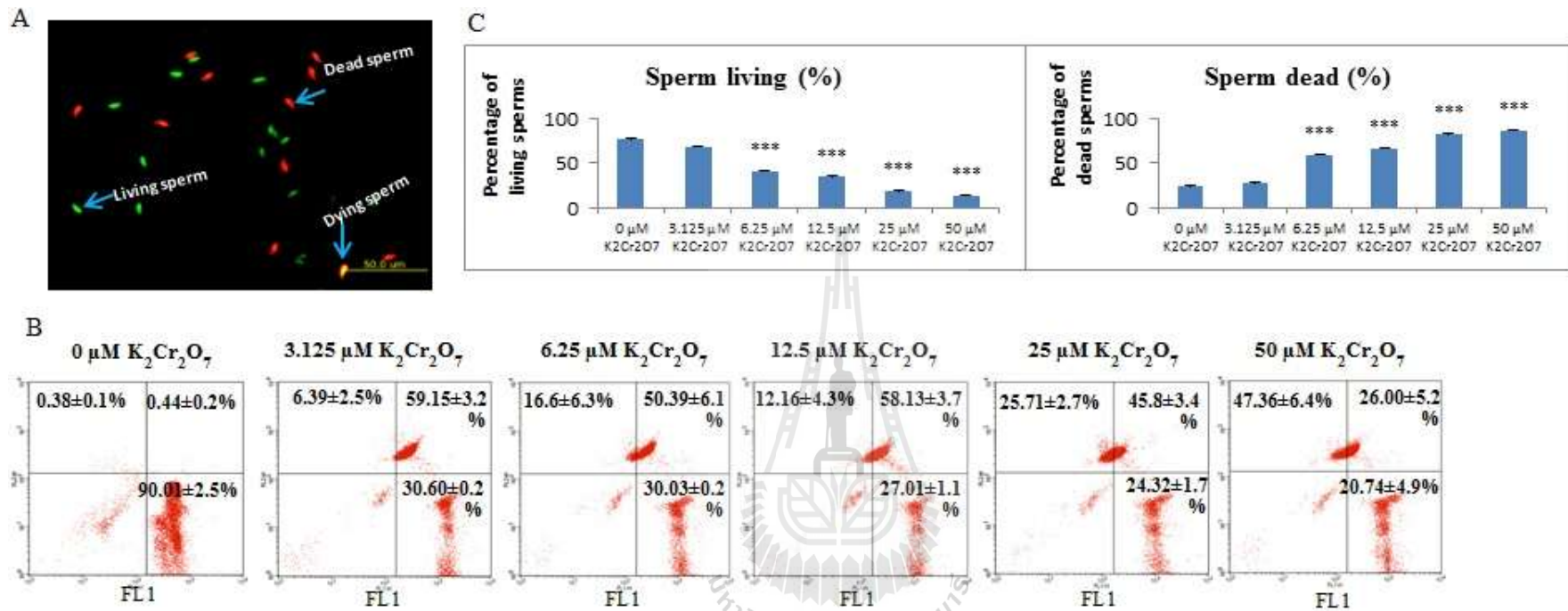


Figure 4.1 Sperm viability under Cr(VI) exposure. Sperm were treated with 0, 3.125, 6.25, 12.5, 25, or 50 μM Cr(VI). A) A fluorescence microscopic image depicting live sperm stained with SYBR 14 dye (green fluorescence) and dead sperm stained with PI (red fluorescence). The red box depicts the magnified image. B) Sperm viability was calculated by the following formula: (number of live sperm \times 100)/total sperm count. Each treatment was conducted in triplicate. C) Sperm viability was measured by flow cytometer: FL1 represents green (living sperm), FL2 represents red (dead sperm), and moribund sperm fluoresced both green and red. *** $P < 0.001$ versus the control group (Dunnnett's t -tests).

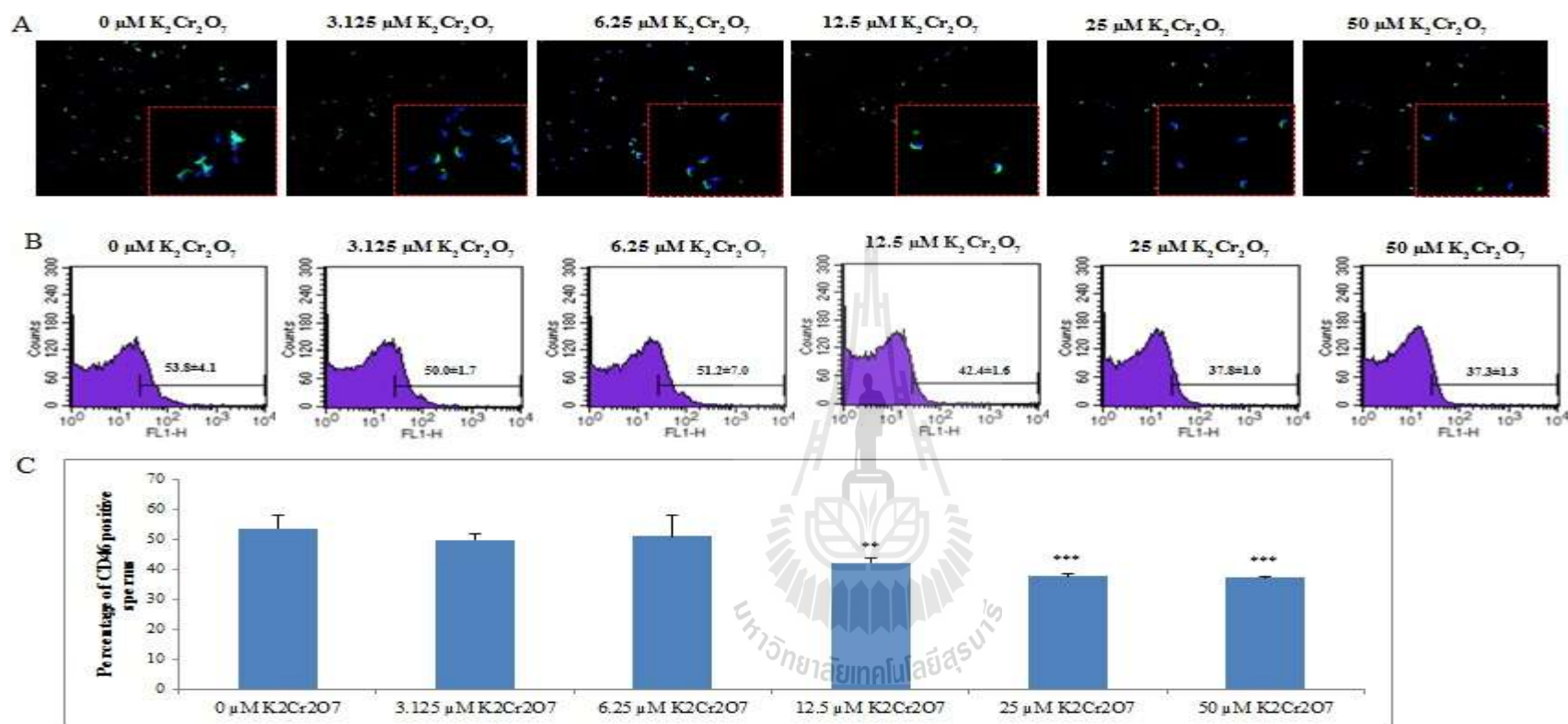


Figure 4.2 Acrosome reaction analyses by using CD46 immunofluorescence staining and flow cytometry. Sperm cells were treated with different concentrations of $\text{K}_2\text{Cr}_2\text{O}_7$ for 3 h. A) Immunofluorescence staining with mouse anti-CD46 (green). Nuclei are counterstained with DAPI (blue). The red box depicts magnified image, 40x magnification. B) The flow cytometer analysis of CD46-positive sperm populations. C) The percentage of CD46-positive sperm populations determined by flow cytometry. ** $P < 0.01$ and *** $P < 0.001$ versus the control group (Dunnett's t -tests).

4.4.3 Effect of Cr(VI) exposure on sperm function and embryo development

To understand the effect of Cr(VI) exposure on sperm function and embryo development, sperm were treated with various concentrations of Cr(VI) (0, 3.125, 6.25, 12.5, 25, or 50 μ M) for 3 h before IVF, and the results at 96 h after IVC are shown in Table 4.2. These results demonstrate that the percentage of unfertilized oocytes in the Cr(VI)-treated sperm groups significantly ($P<0.01$) increased with increasing dose of Cr(VI) (26.4%, 32.0%, 36.0%, 50.4%, and 57.6%, respectively) compared with the non-treated group (19.2%). Interestingly, the percentage in the 2-cell stage of the Cr(VI)-treated sperm was significantly ($P<0.01$) higher (25.6%–34.4%) compared with non-treated sperm (9.3%). Importantly, embryos derived from Cr(VI)-treated sperm were later developed to expanded blastocyst stage and hatching blastocyst stage. In this study, the results showed that Cr(VI) treatment reduced sperm fertilizing ability and had a negative effect on embryo development up to the blastocyst stage with increasing Cr(VI) dose.

4.4.4 Effect of Cr(VI)-exposed sperm on cell proliferation in blastocysts

To further determine the effects of Cr(VI)-exposed sperm on proliferation of embryos, differential staining followed by cell counting was performed to assess cell proliferation in blastocysts, at 96 h after IVC. Immunostaining with anti-oct4 and anti-cdx2 antibodies was performed in blastocysts to determine ICM (red) and TE (green) cells, respectively (Figure 4.3). The results showed that Cr(VI)-exposed sperm were able to block the proliferation of cells in the blastocyst stage of embryos compared with non-treated sperm (Table 4.3). Blastocysts derived from 6.25, 12.5, and 25 μ M of Cr(VI)-exposed sperm groups caused a significant ($P<0.01$) reduction of both ICM and TE cell proliferation compared with non-treated sperm (Table 4.3). In addition, a significant reduction in total number of cells was observed in Cr(VI)-exposed groups compared with the non-treated group.

Table 4.2 Developmental competence of mouse oocytes 96 h after IVF.

| Treatment | No. IVF | No. unfertilized (% , ±SE) | No. embryos development to (% , ±SE) | | | | | | | |
|---|---------|--------------------------------|--------------------------------------|----------------|----------------|------------------|-----------------|--------------------------------|-------------------------------|--------------------------------|
| | | | 2C | 4C | 8C | Mo | Early BL | Expanded BL | Hatching BL | Total BL |
| 0 μM K ₂ Cr ₂ O ₇ | 125 | 24 (19.2±2.7) ^c | 12 (9.3±1.3) ^b | 2 (1.6±1.1) | 0 (0.0±0.0) | 2 (4.8±2.7) | 6 (4.8±2.7) | 53 (42.4±5.0) ^a | 26 (20.8±4.8) ^a | 85 (68.0±4.4) ^a |
| 3.125 μM K ₂ Cr ₂ O ₇ | 125 | 33 (26.4±3.6) ^{bc} | 32 (25.6±6.4) ^a | 3 (2.4±1.0) | 2 (1.6±0.9) | 3 (2.4±1.6) | 7 (5.6±2.7) | 36 (28.8±5.5) ^b | 9 (7.2±2.5) ^b | 45 (36.0±6.2) ^b |
| 6.25 μM K ₂ Cr ₂ O ₇ | 125 | 40 (32.0±1.9) ^b | 32 (25.6±4.3) ^a | 3 (2.4±1.7) | 1 (0.8±0.8) | 10 (8.0±2.4) | 10 (8.0±3.5) | 26 (20.8±5.5) ^{bc} | 3 (2.4±1.0) ^{bc} | 29 (23.2±5.5) ^{bc} |
| 12.5 μM K ₂ Cr ₂ O ₇ | 125 | 45 (36.0±3.8) ^b | 37 (29.6±4.9) ^a | 2 (1.6±1.1) | 2 (1.6±1.1) | 15 (12.0±4.2) | 11 (8.8±5.5) | 13 (10.4±5.4) ^{cd} | 0 (0.0±0.0) ^c | 13 (10.4±5.9) ^{cd} |
| 25 μM K ₂ Cr ₂ O ₇ | 125 | 63 (50.4±6.0) ^a | 37 (29.6±4.4) ^a | 3 (2.4±1.0) | 3 (2.4±1.4) | 11 (8.8±5.4) | 6 (4.8±4.8) | 2 (1.6±1.1) ^d | 0 (0.0±0.0) ^c | 8 (6.4±4.5) ^{de} |
| 50 μM K ₂ Cr ₂ O ₇ | 125 | 72 (57.6±5.0) ^a | 43 (34.4±4.3) ^a | 0 (0.0±0.0) | 0 (0.0±0.0) | 7 (5.6±4.1) | 2 (1.6±1.1) | 1 (0.8±0.6) ^d | 0 (0.0±0.0) ^c | 3 (2.4±1.5) ^e |

^{a,b,c,d,e} Different superscripts denote significant differences (ANOVA: Duncan's Multiple Range Test, $P < 0.01$)

Table 4.3 TE and ICM cell counts in blastocysts at 96 h after IVC via oct4 and cdx2 expression analysis.

| Treatment | No. of Blastocysts | No. of total cells (Mean±SE) | No. of TE cells (Mean±SE) | No. of ICM cells (Mean±SE) |
|---|--------------------|------------------------------|---------------------------|----------------------------|
| 0 μM $\text{K}_2\text{Cr}_2\text{O}_7$ | 15 | 87.9±3.0 ^a | 68.5±2.6 ^a | 19.4±2.4 ^a |
| 3.125 μM $\text{K}_2\text{Cr}_2\text{O}_7$ | 15 | 78.7±3.1 ^a | 62.1±3.2 ^{ab} | 16.5±2.4 ^{ab} |
| 6.25 μM $\text{K}_2\text{Cr}_2\text{O}_7$ | 15 | 68.3±3.2 ^b | 53.8±2.9 ^{bc} | 14.5±3.1 ^{bc} |
| 12.5 μM $\text{K}_2\text{Cr}_2\text{O}_7$ | 14 | 63.3±2.2 ^b | 49.9±2.0 ^{cd} | 13.4±3.6 ^c |
| 25 μM $\text{K}_2\text{Cr}_2\text{O}_7$ | 10 | 49.4±2.9 ^c | 38.4±2.7 ^d | 11.0±2.5 ^d |

^{a,b,c,d} Different superscripts denote significant differences (ANOVA: Duncan's Multiple Range Test, $P < 0.01$)

4.4.5 Effect of Cr(VI)-exposed sperm on ICM- and TE-specific gene expression

In this study, the effects of Cr(VI)-exposed sperm on TE/ICM-specific gene expression in blastocysts were examined by qRT-PCR as shown in Fig. 4.3B. In this study, the pluripotent marker genes (*sox2*, *pou5f1*, and *klf4*) in blastocysts from Cr(VI)-exposed sperm showed significant down-regulation with increasing Cr(VI) dose. Additionally, TE-associated genes, such as *Cdx2*, showed significant down-regulation in both 12.5 and 25 μM Cr(VI)-exposed groups. Other TE-associated genes, such as *eomes* and *krt8*, only showed significant down-regulation in the 25 μM Cr(VI)-exposed group. Thus, our study clearly demonstrated that Cr(VI) not only decreased the expression of pluripotency genes but also that of TE-associated genes with high doses of Cr(VI) exposure.

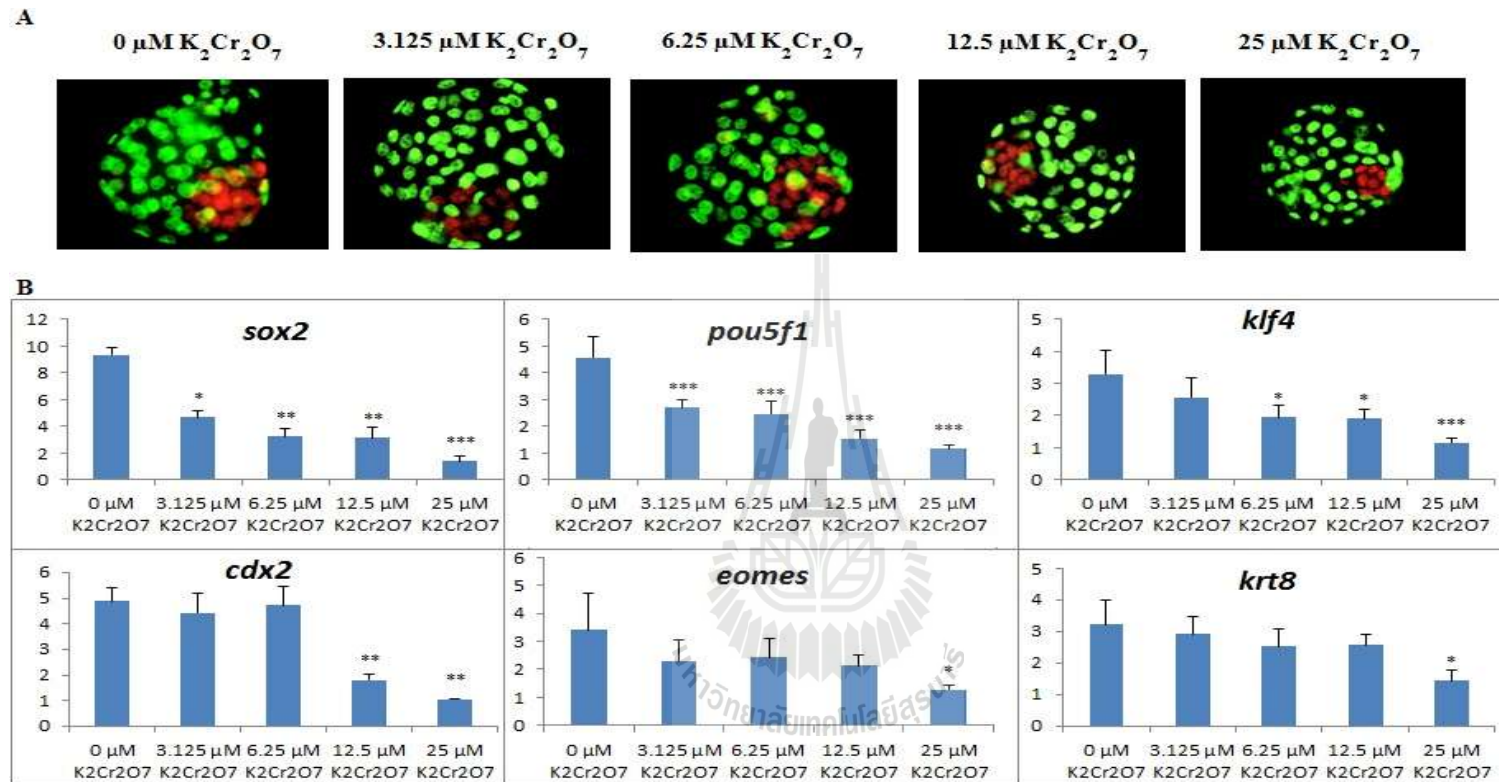


Figure 4.3 Blastocyst quality analyses. A) Immunostaining of blastocysts after IVC for 96 h with anti-oct4 and anti-cdx2 antibodies. The ICM and TE cells appeared red and green, respectively. B) Expression profiles of ICM and TE associated genes. The expression levels of ICM- and TE-associated genes were analyzed by qRT-PCR. The experiments were performed in triplicate; data represent the mean of three independent experiments. Error bars represent standard error of the mean (SEM). * $P < 0.05$, ** $P < 0.01$ versus the control group (Dunnett's t -tests).

4.5 Discussions

This study was undertaken to determine *in vitro* cytotoxic effects of Cr (VI) on sperm viability and function, sperm fertilizing ability during IVF of oocytes, and subsequent embryo development. To achieve this, sperm obtained from male BDF1 (8–12 weeks old) mice were treated with Cr(VI) at a dose of 3.125, 6.25, 12.5, 25, or 50 μ M for 3 h, and the treated sperm were then co-incubated with oocytes obtained from female BDF1 mice (6–8 weeks old) for 6 h followed by embryo IVC for 96 h.

Our results showed that Cr(VI) exposure significantly decreased the percentage of live sperm and sperm viability with increasing dose, thereby confirming its cytotoxic effects. These results are also supported by previous reports in which authors have shown that occupational exposure to Cr(VI) led to reduction in sperm count in workers (Li et al., 2001). Additionally, $K_2Cr_2O_7$ exposure also significantly reduced the epididymal sperm count in laboratory animals (Chandra et al., 2007; Marouani et al., 2012).

After mammalian sperm are removed from the epididymis, they undergo several essential physiological changes to be able to fertilize an oocyte; this process is called capacitation. Capacitation helps the sperm to gain the ability to (i) develop hyperactivated motility, (ii) bind to the zona pellucida (ZP), (iii) undergo the acrosome reaction, and (iv) fuse with the oolemma and fertilize the egg (Rodriguez et al., 2005; Rahman et al., 2014a, 2014b). Capacitation can be inferred by the sperm's ability to undergo the acrosome reaction, and the detection of membrane cofactor protein (CD46) is a reliable marker of acrosome-reacted spermatozoa (Johnson et al., 2007; Clift et al., 2009). Our results showed that Cr(VI) exposure significantly decreased sperm acrosome reaction (CD46-negative) with increasing dose, thereby demonstrating its negative impact on fertility.

In IVF, sperm must bind to the ZP, undergo the acrosome reaction, penetrate the ZP, and then fuse with the oolemma. Therefore, the fertilization rate is correlated with the number of sperm bound to the ZP. Among the several aspects of sperm that facilitate the sperm-ZP interaction, normal sperm morphology and increased sperm concentration, motility, and viability are most important (Suarez, 2008; Park et al., 2012; Rahman et al., 2013). It has been reported that $K_2Cr_2O_7$ exposure significantly decreased the epididymal sperm count/viability and motility as well as increased sperm abnormality in laboratory animals (Chandra et al., 2007; Marouani et al., 2012; Devi et al., 2012). In the present study, we evaluated the IVF rate and blastocyst development of oocytes fertilized by Cr(VI)-treated sperm after IVC. We observed that Cr(VI) treatment of sperm had a negative effect on oocyte fertilization and subsequent embryo development, as evidenced by the increased 2-cell population as well as late development to expanded blastocyst and hatching blastocyst stages with increasing Cr(VI) concentrations.

The TE cells arising from the trophoblast at the blastocyst stage develops a sphere of epithelial cells surrounding the ICM and blastocoel. These TE cells are required for the development of embryonic portion of the placenta and mammalian conceptus (Kunath et al., 2004; Cross, 2005). Moreover, the ICM is a group of pluripotent cells that gives rise to the embryonic tissue that comprises the ectoderm, endoderm, and mesoderm (Marikawa and Alarcon, 2009). Our results showed that Cr(VI)-exposed sperm not only significantly inhibited the ICM/TE cell proliferation in blastocysts but also downregulated the ICM/TE-associated genes, which play crucial roles in ICM and TE cell formation, reflecting a negative effect on embryo development.

From our results, we suspect that Cr(VI) affects embryo implantation. In particular, most of the blastocysts that were formed with Cr(VI)-treated sperm resulted in hatching failure as well as decreased inner cell mass and trophoctoderm development. Lundin et al. (2001) and Bos-Mikich et al. (2001) suggested that a high number of early-cleaving embryos become good quality embryos and significantly facilitate high pregnancy, implantation, and birth rates. Several studies have previously administered Cr(VI) to rats and mice via drinking water and found effects on the placental and fetal development, leading to implantation failure. (Junaid et al., 1995; Junaid et al., 1996; Kanojia et al., 1998; Elsaieed and Nada, 2002).

Cr(VI)-induced oxidative stress has been established to be a major factor that leads to male infertility (Acharya et al., 2004; Aruldas et al., 2005; Chandra et al., 2007). Under physiological conditions, after entering into the cell, Cr(VI) is reduced by hydrogen peroxide, glutathione (GSH) reductase, ascorbic acid, and GSH to produce reactive intermediates, including Cr(V), Cr(IV), reactive oxygen species (ROS), and ultimately Cr(III). Any of these species can attack intracellular macromolecules, including DNA, proteins, and membrane lipids, thereby disrupting cellular integrity and inducing toxic as well as mutagenic effects (Mattia et al., 2004).

4.6 Conclusion

Cr(VI) is a potential cytotoxic agent for sperm and exerts adverse effects, possibly through the induction of oxidative stress and DNA damage. Furthermore, Cr(VI)-treated sperm reduce the IVF success rate, delays subsequent blastocyst formation, and down-regulates the genes responsible for embryo development. Our current *in vitro* study will provide further mechanistic insights into the effects of Cr(VI) on mammalian sperm function.

4.7 References

- Acharya, U. R., Mishra, M., Tripathy, R. R., and Mishra, I. (2006). Testicular dysfunction and antioxidative defense system of Swiss mice after chromic acid exposure. **Reprod. Toxicol.** 22: 87-91.
- Acharya, U. R. Mishra, M., Mishra, I., and Tripathy, R. R. (2004). Potential role of vitamins in chromium induced spermatogenesis in Swiss mice. **Environ. Toxicol. Pharmacol.** 15: 53-59.
- Aruldas, M. M., Subramanian, S., Sekar, P., Vengatesh, G., Chandrahasan, G., Govindarajulu, P., and Akbarsha, M. A. (2005). Chronic chromium exposure induced changes in testicular histoarchitecture are associated with oxidative stress: study in a non-human primate (*Macaca radiata* Geoffroy). **Hum. Reprod.** 20: 2801-2813.
- Bos-Mikich, A., Mattos, A., and Ferrari, A. (2001). Early cleavage of Human embryos: an effective method for predicting successful IVF/ICSI outcome. **Hum. Reprod.** 16: 2658-2661.
- Chandra, A. K., Chatterjee, A., Ghosha, R., and Sarkar, M. (2007). Effect of curcumin on chromium-induced oxidative damage in male reproductive system. **Environ. Toxicol. Pharmacol.** 24: 160-166.
- Clift, L. E., Andrlíkova, P., Frolikova, M., Stopka, P., Bryja, J., Flanagan, B. F., Johnson, P. M., Dvorakova-Hortova, K. (2009). Absence of spermatozoal CD46 protein expression and associated rapid acrosome reaction rate in striped field mice (*Apodemus agrarius*). **Reprod. Biol. Endocrinol.** 16: 7-29.
- Cross, J. C. (2005). How to make placenta: mechanisms of trophoblast cell differentiation in mice-a review. **Placenta** 26: 3-9.

- Danadevi, K., Rozati, R., Reddy, P. P., and Grover, P. (2003). Semen quality of Indian welders occupationally exposed to nickel and chromium. **Reprod. Toxicol.** 17: 451-456.
- Devi, K. R., Mosheraju, M., and Reddy, K. D. (2012). Curcumin prevents chromium induced sperm characteristics in mice. **IOSR J. Pharmacy** 2: 312-316.
- Elsaieed, E. M., and Nada, S. A. (2002). Teratogenicity of hexavalent chromium in rats and the beneficial role of ginseng. **Bull Environ. Contam. Toxicol.** 68: 361-8.
- Greene, L. E., Riederer, A. M., Marcus, M., and Lkhasuren, O. (2010). Associations of fertility and pregnancy outcomes with leather tannery work in Mongolia: a pilot study. **Int. J. Occup. Environ. Health** 16: 60-68.
- Johnson, P. M., Clift, L. E., Andriikova, P., Jursova, M., Flanagan, B. F., Cummerson, J. A., Stopka, P., and Dvorakova-Hortova, K. (2007). Rapid sperm acrosome reaction in the absence of acrosomal CD46 expression in promiscuous field mice (*Apodemus*). **Reproduction** 134: 739-47.
- Junaid, M., Murthy, R. C., and Saxena, D. K. (1995). Chromium fetotoxicity in mice during late pregnancy. **Vet. Hum. Toxicol.** 37: 320-323.
- Junaid, M., Murthy, R. C., and Saxena, D. K. (1996). Embryo-toxicity of orally administered chromium in mice: exposure during the period of organogenesis. **Toxicol. Lett.** 84: 143-148.
- Kanojia, R. K., Junaid, M., and Murthy, R. C. (1998). Embryo and fetotoxicity of hexavalent chromium: a long-term study. **Toxicol. Lett.** 95: 165-172.
- Kumar, S., Sathwara, N. G., Gautam, A. K., Agarwal, K., Shah, B., Kulkarni, P. K., Patel, K., Patel, A., Dave, L. M., Parikh, D. J., and Saiyed, H. N. (2005).

- Semen quality of industrial workers occupationally exposed to chromium. **J. Occup. Health** 47: 424-430.
- Kunath, T., Strumpf, D., and Rossant, J. (2004). Early trophoblast determination and stem cell maintenance in the mouse-a review. **Placenta** 25: 32-38.
- Li, Z. H., Li, P., and Randak, T. (2011). Evaluating the toxicity of environmental concentrations of waterborne chromium (VI) to a model teleost, *oncorhynchus mykiss*: a comparative study of in vivo and in vitro. **Comp. Biochem. Physiol C**. 153: 402-407.
- Li, H., Chen, Q., Li, S., Yao, W., Li, L., Shi, X., Wang, L., Castranova, V., Vallyathen, V., Ernst, E., and Chen, C. (2001). Effect of Cr(VI) exposure on sperm quality: human and animal studies. **Ann. Occup. Hyg.** 45: 505-511.
- Lundin, K., Bergh, C., and Hardason, T. (2001). Early embryo cleavage is strong indicator of embryo quality in human IVF. **Hum. Reprod.** 16: 2652-2657.
- Marikawa, Y., and Alarcon. V. B., 2009. Establishment of trophectoderm and inner cell mass lineages in the mouse embryo. **Mol. Reprod. Dev.** 76: 1019-1032.
- Marouani, N., Tebourbi, O., Mahjoub, S., Yacoubi, M. T., Sakly, M., Benkhalifa, M., and Rhouma, K. B. (2012). Effects of hexavalent chromium on reproductive functions of male adult rats. **Reprod. Biol.** 12: 119-133.
- Marouani, N., Tebourbi, O., Mokni, M., Yacoubi, M. T., Sakly, M., Benkhalifa, M., and Ben Rhouma, K. (2011). Embryotoxicity and fetotoxicity following intraperitoneal administrations of hexavalent chromium to pregnant rats. **Zygote** 19: 229-235.
- Mattia, G. D., Bravi, M. C., Laurenti, O., Luca, O. D., Palmeri, A., Sabatucci, A., Mendico, G., and Ghiselli, A. (2004). Impairment of cell and plasma redox

- state in subjects professionally exposed to chromium. **Am. J. Ind. Med.** 46: 120-125.
- Park, Y. J., Kwon, W. S., Oh, S. A., and Pang, M. G. (2012). Fertility-related proteomic profiling bull spermatozoa separated by percoll. **J. Proteome. Res.** 11: 4162-4168.
- Rahman, M. S., Kwon, W. S., and Pang, M. G. (2014a). Calcium influx and male fertility in the context of the sperm proteome: an update. **Biomed. Res. Int.** 84: 161-5.
- Rahman, M. S., Kwon, W. S., Lee, J. S., Kim, J., Yoon, S. J., Park, Y. J., You, Y. A., Hwang, S., and Pang, M. G. (2014b). Sodium nitroprusside suppresses male fertility in vitro. **Andrology** doi: 10.1111/j.2047-2927.2014.00273.x.
- Rahman, M. S., Lee, J. S., Kwon, W. S., and Pang, M. G. (2013). Sperm proteomics: road to male fertility and contraception. **Int. J. Endocrinol.** 360986.
- Rodriguez, P. C., O'Flaherty, C. M., Beconi, M. T., and Beorlegui, N. B. (2005). Nitric oxide induces acrosome reaction in cryopreserved bovine spermatozoa. **Andrologia** 37: 166-172.
- Shmitova, L. (1980). Content of hexavalent chromium in the biological substrates of pregnant women and women in the immediate postnatal period engaged in the manufacture of chromium compounds. **Gig. Trud. Prof. Zabol.** 2: 32-35.
- Stohs, J. S., Bagchi, D., Hassoun, E., and Bagchi, M. (2001). Oxidative mechanism in the toxicity of chromium and cadmium ions. **J. Environ. Pathol. Toxicol. Oncol.** 20: 77-88.
- Stoecker, J. B. (2004). Chromium in elements and their compounds in the environment 2nd edition, pp 709-729. Eds Merian E, Anke M, Ihnat M, Stoepler M. Copyright, Weinheim, Germany.

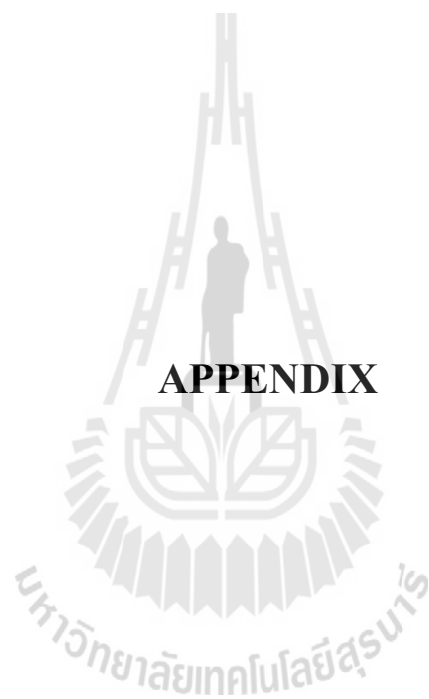
- Suarez, S. S. (2008). Control of hyperactivation in sperm. **Hum. Reprod. Update** 14: 647-657.
- Subramanian, S., Rajendiran, G., and Sekhar, P. (2006). Reproductive toxicity of chromium in adult bonnet monkeys (*Macaca radiata* Geoffrey). Reversible oxidative stress in the semen. **Toxicol. Appl. Pharmacol.** 215: 237-249.
- Yousef, M. I., El-Demerdash, F. M., Kamil, K. I., and Elswad, F. A. M. (2006). Ameliorating effect of folic acid on chromium (VI)-induced changes in reproductive performance and seminal plasma biochemistry in male rabbits. **Reprod. Toxicol.** 21: 322-328.
- Zhang, J., Cai, W. W., and Lee, D. J. (1992). Occupational hazards and pregnancy outcomes. **Am. J. Ind. Med.** 21: 397-40.

CHAPTER V

CONCLUSION

Although the increased use of silver nanoparticles (AgNPs) or Cr(VI) have gained much interest regarding their adverse effects on human health, the underlying their mechanism of action on spermatozoa and subsequent embryonic development are poorly understood. This study can conclude that AgNPs are a potential cytotoxic agent for sperm cells and exert adverse effects, possibly through the induction of oxidative stress. Furthermore, AgNPs-treated sperm reduce the IVF success rate, delay subsequent blastocyst formation, and downregulate gene expression responsible for embryonic development. Our present *in vitro* study will offer further mechanistic insights into the effects of AgNPs on mammalian sperm physiology, such as the underlying mechanism or maximum size limit for AgNPs internalization into sperm cells.

Cr(VI) is a potential cytotoxic agent for sperm and exerts adverse effects, possibly through the induction of oxidative stress. Furthermore, Cr(VI)-treated sperm reduce the IVF success rate, delays subsequent blastocyst formation, and down-regulates the genes responsible for embryo development. Our current *in vitro* study will provide further mechanistic insights into the effects of Cr(VI) on mammalian sperm function.



APPENDIX

BUFFERS AND MEDIA

1. Buffered formal saline solution

| | Final conc. |
|----------------------------------|-------------|
| Na ₂ HPO ₄ | 34.72 mM |
| KH ₂ PO ₄ | 18.68 mM |
| NaCl | 92.4 mM |
| Formaldehyde | 4% (v/v) |

2. CZB-HEPES (pH 7.3)

| | Final conc. (mM) | g/100ml |
|--------------------------------------|------------------|---------|
| NaCl | 81.62 | 0.4770 |
| KCl | 4.83 | 0.0360 |
| KH ₂ PO ₄ | 1.18 | 0.01605 |
| MgSO ₄ ·7H ₂ O | 1.18 | 0.0291 |
| Na Lactate | 31.30 | 520 µl |
| Na Pyruvate | 0.27 | 0.0030 |
| EDTA 2Na | 0.11 | 0.0041 |
| Glutamine | 1.00 | 0.0146 |
| CaCl ₂ ·2H ₂ O | 1.70 | 0.0250 |
| NaHCO ₃ | 25.12 | 0.1250 |
| HEPES free acid | - | 0.5960 |
| Phenol red (0.5%) | - | 70 µl |

3. mDPBS

| | |
|--------------------------------------|----------|
| NaCl | 4 g |
| KCl | 0.1000 g |
| KH ₂ PO ₄ | 0.1000 g |
| Na ₂ HPO ₄ | 0.5750 g |
| Glucose | 0.5000 g |
| Pyruvic acid | 0.0180 g |
| CaCl ₂ ·2H ₂ O | 0.0687 g |
| MgCl ₂ ·6H ₂ O | 0.0500 g |
| P-S (stock 100x) | 500 µl |
| Ultra pure water | 500 µl |

4. PBS (-)

| | |
|----------------------------------|----------|
| NaCl | 10 g |
| KCl | 0.2500 g |
| Na ₂ HPO ₄ | 1.4400 g |
| KH ₂ PO ₄ | 0.2500 g |
| Ultra pure water | 1 L |

5. Modified Whitten's medium

| | Final conc. |
|---------------------------------|-------------|
| NaCl | 118.5 mM |
| KCl | 4.7 mM |
| KH ₂ PO ₄ | 1.18 mM |
| CaCl ₂ | 2.54 mM |
| MgSO ₄ | 1.18 mM |
| NaHCO ₃ | 24.9 mM |
| Glucose | 5.56 mM |
| BSA | 3 mg/ml |

6. Non capacitation medium

| | Final conc. |
|---------------------------------|-------------|
| NaCl | 118.5 mM |
| KCl | 4.7 mM |
| KH ₂ PO ₄ | 1.18 mM |
| CaCl ₂ | 2.54 mM |
| MgSO ₄ | 1.18 mM |
| NaHCO ₃ | 24.9 mM |
| Glucose | 5.56 mM |

BIOGRAPHY

Mr. Ton Yoisungnern was born in Bangkok, Thailand on Thursday September 17th, 1985. He finished his high school at Wapipathum School in Mahasarakham. In 2007, he received Bachelor's Degree (B.Sc.) in Animal Production Technology from Institute of Agricultural Technology, Suranaree University of Technology. Then, he pursued his Ph.D. study in Animal Biotechnology at School of Biotechnology, Institute of Agricultural Technology. During this time, he has chances to practice skill the field of animal biotechnology including animal cloning, *in vitro* fertilization, ICSI, molecular biology techniques. While study, he also received a scholarship from Royal Golden Jubilee (RGJ) Ph.D. Program of Thailand Research Fund. In 2013, he has good chance to research in part of his thesis in South Korea with Professor Jin Hoi Kim for 10 months. His Ph.D. thesis title was "Effect of silver nanoparticles and hexavalent chromium on mouse spermatozoa functions and embryo development". First part of this work was published in Scientific reports journal on June 8, 2015 (DOI: 10.1038/srep11170). Second part of this work was published in Toxicology and Industrial Health journal on April 2015 (DOI:10.1177/0748233715579805) and presented as poster presentation in the RGJ-Ph.D. Congress XVI on June 11-13, 2015 at Jomtien Palm Beach Hotel and Resort, Pattaya, Chonburi, Thailand.